THE NATURE AND ORIGIN OF GOLD MINERALIZATION IN THE TUGELA VALLEY: NATAL STRUCTURAL AND METAMORPHIC PROVINCE

THESIS

Submitted in Partial Fulfilment of the
Requirements for the Degree of
MASTER OF SCIENCE (EXPLORATION GEOLOGY)
at Rhodes University
Grahamstown

By

Ian Duncan de Klerk

September 1990

DECLARATION

All work in this thesis is that of the writer except where specific reference is made to the work of others.

Signed: .....

28/9/90

ABSTRACT

The project area is situated within the Tugela Valley, located in the Northern Marginal Zone of the Natal Structural and Metamorphic Province, and this work outlines the different styles of gold mineralization found in the Tugela Valley. Two different styles have been recognized and both have economic significance:-

1) Epigenetic shear zone-hosted gold occurs in late-stage relatively undeformed thin quartz veins confined to shear zones, and is present in both the greenschist facies Natal Thrust Belt and the amphibolite facies Natal Nappe Complex. However the vast majority of these occurrences are concentrated within the thrust front (i.e. the Natal Thrust Belt). The gold grades (up to 7 g/t) and the hydrothermal alteration assemblages associated with the epigenetic deposits have been documented.

2) An as yet unrecognized occurrence of syngenetic gold mineralization is found associated with the sediment-hosted exhalative massive, to semi-massive, sulphides of the iThuma prospect, located within the amphibolite facies Natal Nappe Complex. Here gold (up to 3 g/t) is concentrated together with the main sulphide ore, as well as some gold enrichment (230ppb) in the hydrothermally altered footwall feeder pipe.

It is proposed that the epigenetic mineralization was formed as a consequence of the northward directed obduction of the major thrust slices of the Natal Nappe Complex. This increased the permeability of the rocks and provided channelways for the focussing of fluids. Deposition took place at the thrust front where metamorphic hydrothermal fluids interacted with meteoric water.

CONTENTS

CONTENTS (cont.)

LIST OF FIGURES

LIST OF FIGURES (cont.)

LIST OF PLATES

LIST OF PLATES (cont.)

ACKNOWLEDGEMENTS

First and foremost I would like to thank Professor Franco Pirajno for his continuous interest, help and enthusiasm throughout the project. Without his support and ideas this work would probably not have taken place. I also wish to thank him for his input into the modular component of the Exploration Geology course - this was was of great inspiration to me.

Thanks are also due to the other staff members of the geology department at Rhodes University, particularly Professor Roger Jacob, for their support and patience over the years, and also to my student colleagues on the Exploration Geology course.

I acknowledge Professor A. E. Schoch of the University of the Orange Free State for his assistance with fluid inclusion studies, and Gold Fields of South Africa for their assistance in the field and their financial help with XRF analyses.

Last, but certainly not least, I wish to thank my wife, Susan, and my parents for their solid support through some tough times. For all this I am extremely grateful.

1. INTRODUCTION

The aim of this study is to outline the different styles of gold mineralization encountered in the Tugela Valley in northern Natal. The area is located in the northern-most part of the Natal Structural and Metamorphic Province and is the site of numerous gold occurrences and old workings which were operative around the turn of the century. The study involves regional and detailed mapping, and geochemical investigations in an attempt to define hydrothermal alteration assemblages and identify styles of mineralization. Fluid inclusion studies also formed part of the exercise.

The terrain is characterized by a rugged topography, abundant vegetation cover and generally poor rock outcrop. The best exposures are usually confined to river beds and along the tops of spurs. Hill slopes mostly show a thick soil cover. All areas considered in this study are located within the borders of KwaZulu and the local chiefs must be consulted when entering the area. All major access routes traversing the Tugela Valley are usually in fair condition, but travelling on secondary roads should not be attempted without a four wheel drive vehicle, especially in the wet season.

2. NATAL STRUCTURAL AND METAMORPHIC PROVINCE

2.1 Overview and Regional Geology

The Natal Province occurs as inliers of Proterozoic terrane exposed in eastern Natal with Phanerozoic, Natal Group and Karoo Sequence, sediments obscuring the western, southern and most of the eastern margins of the Province. **Fig. 2** shows the extent of the Natal Province and indicates the major subdivisions based on structural and metamorphic criteria. The metamorphic grade increases from low-grade greenschist facies in the north to high-grade granulite facies metamorphism in the south, and it is suggested by Tankard et al. (1982) that the gneiss terrane may extend westwards beneath cover rocks, skirting the southern margin of the Kaapvaal Craton, to link up with the high-grade Namaqua Province in the west (see **Fig. 1**).

Radiometric dating of samples from several widely spaced localities, covering the whole Natal Province, provide mineral separate and whole rock Rb/Sr ages, as well as U/Pb zircon ages, in the range 950-1194 Ma (Nicolaysen and Burger, 1965; Burger and Coertze, 1975-76). The ages are interpreted as dating the prominent ~1000 Ma Namaqua-Natal tectonic and metamorphic event and do not represent formation ages for the rocks concerned, although younger ages tend to occur in the south. However Eglington and Harmer (1984) produced Rb/Sr whole rock data, from the Central and Southern Zones, to indicate that significant volumes of granitoid melt were still being introduced as recently as 860 Ma ago. This will be considered further under Tectonic Evolution in chapter 2.2.

There is a marked contrast between the intensely deformed metamorphic rocks of the Northern Marginal Zone and the cratonic foreland to the north of the thrust front. The cratonic foreland comprises a crystalline granitoid basement which is unconformably overlain by a thick (~6000m), relatively undeformed and unmetamorphosed, volcano-sedimentary package which constitutes the Nsuze Group of the Pongola Sequence. Rb/Sr whole rock and U/Pb zircon age determinations from Nsuze lavas yield an age in the range 3090-3150 Ma (Burger and

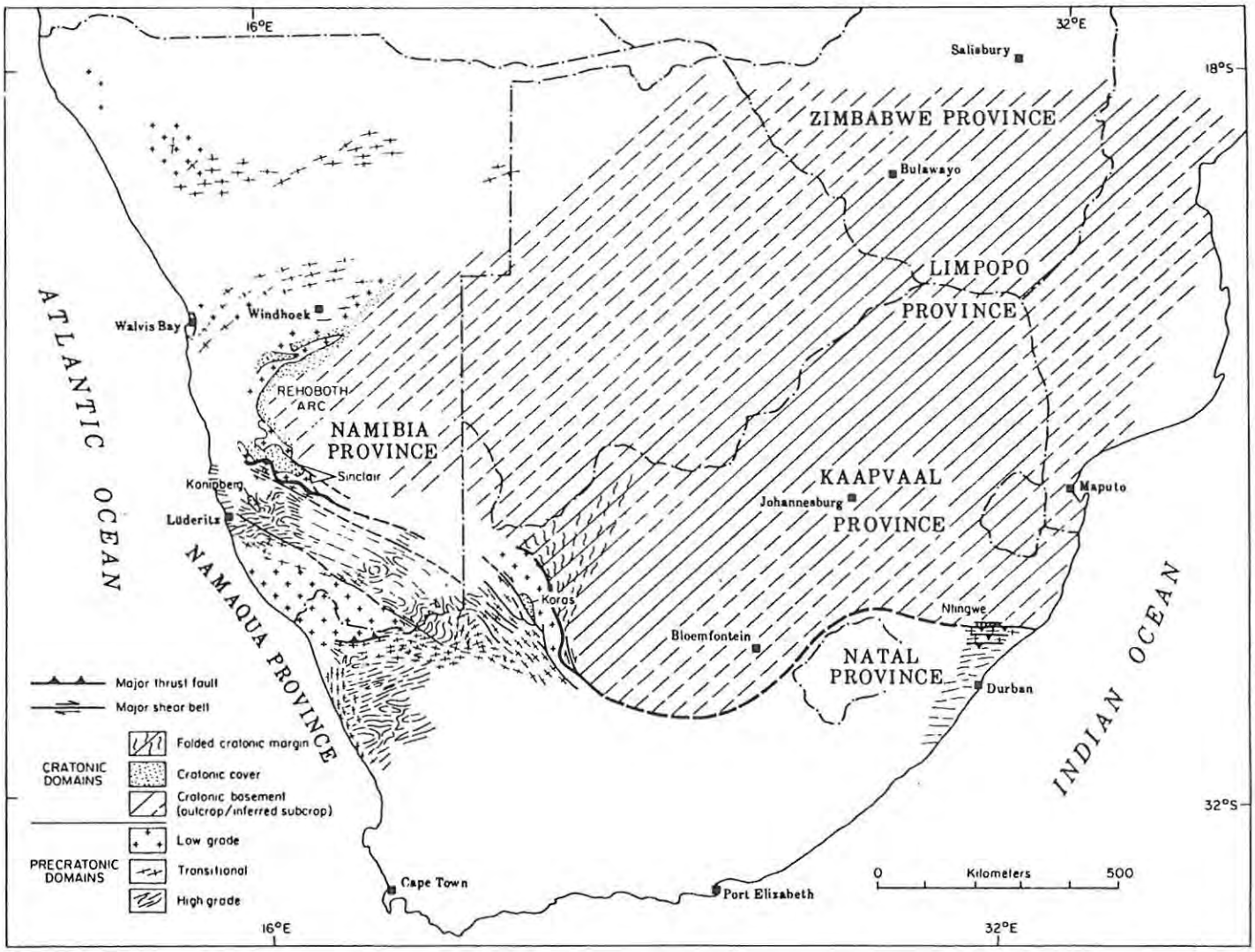

FIGURE 1. Map showing the regional setting of the Natal Province in relation to Proterozoic orogenies from 2100Ma to 1000Ma. (After Tankard et al., 1982).

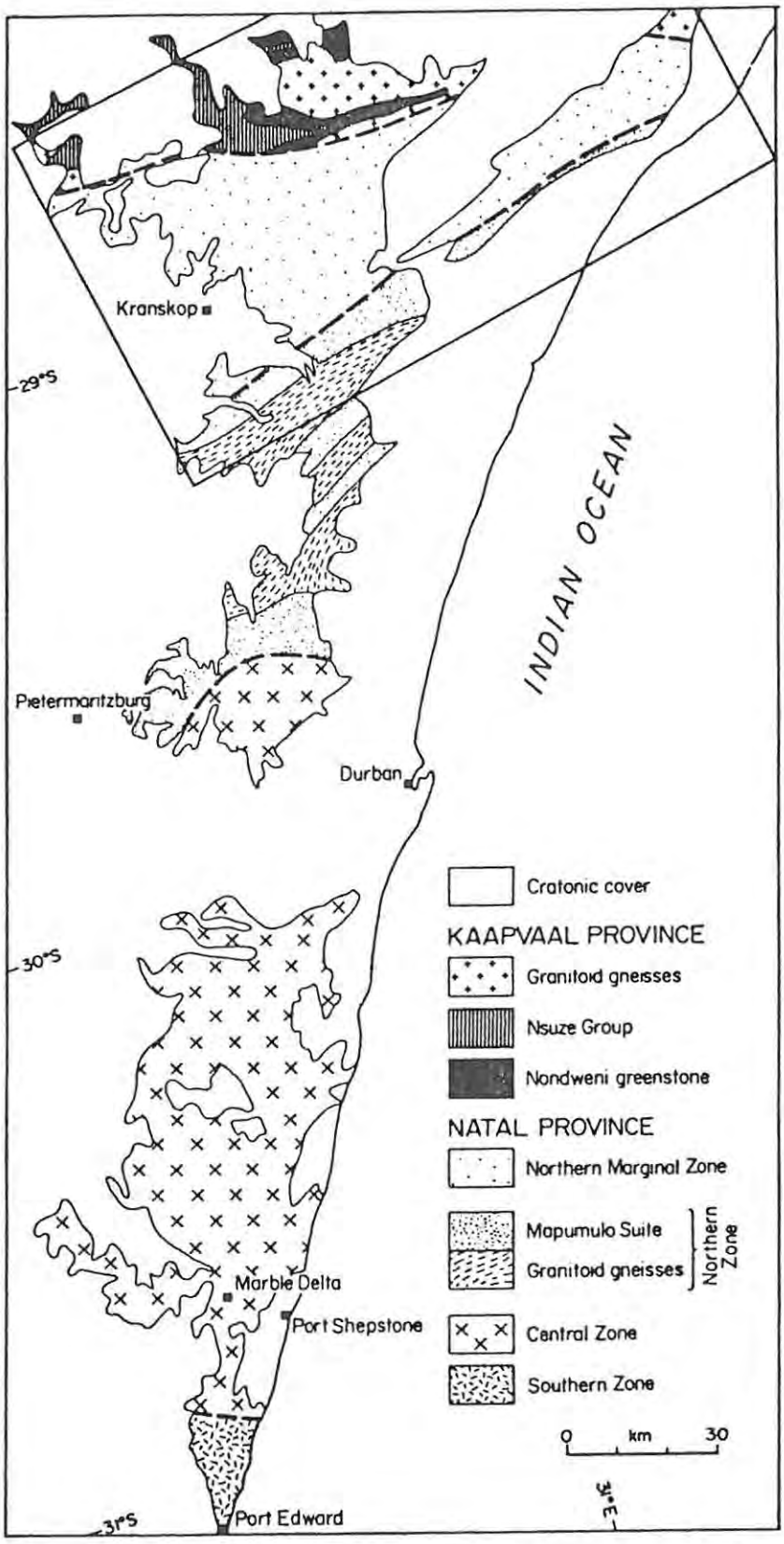

FIGURE 2. Locality map showing the extent of the Natal Province. The rectangle shows the location of the area depicted in Fig. 3. (After Tankard et al., 1982).

Coertze, 1973). The basement rocks consist of uniform megacrystic potassium-rich granite which shows intrusive contacts against narrow, widely spaced synformal greenstone belts of the Nondweni Group.

The following is a brief review of the regional geology within the various zonal subdivisions of the Natal Province (see Fig. 2), and is essentially a summary of the work presented by Matthews (1981a).

2.1.1 Northern Marginal Zone

The Northern Marginal Zone (Fig. 3) comprises a region of northward directed overthrust structures onto the southern flank of the Kaapvaal Craton and can be divided into two zones with contrasting lithological and metamorphic features. (1) The northern zone is the Natal Thrust Belt; a 2-5km wide southerly dipping, imbricate complex of low-grade metamorphic rocks, that defines the structural and metamorphic front of the mobile belt. (2) The southern zone is the Natal Nappe Complex; a 15-45km wide zone comprising four extensive thrust sheets composed mainly of amphibolitic schists and gneisses with some infolded granitic and sedimentary elements. The thrust sheets pass southward into a highly deformed steep to vertical belt, known as the Steep or Slide Zone, which is interpreted by Matthews (1981a) as representing the downwarped root-zone of the nappe complex. These features are better illustrated in Fig. 4, which shows the regional geology of the Northern Marginal Zone and the cratonic foreland to the north at a scale of 1:250 000.

(1) The Natal Thrust Belt:

The east-west trending thrust belt consists of imbricate slices of two unconformable supracrustal sequences metamorphosed to greenschist facies. The younger Ntingwe Group occurs as para-autochthonous slices that represent a transgressive sequence deposited unconformably on a stable shelf represented by the Archaean cratonic foreland, and consists of a basal conglomerate followed by grits, shales and dolomitic limestones. The Ntingwe Group is overridden from the south by allochthonous thrust nappes of the older Mfongosi Group, consisting of argillite and mafic lavas with relict pillow structures and

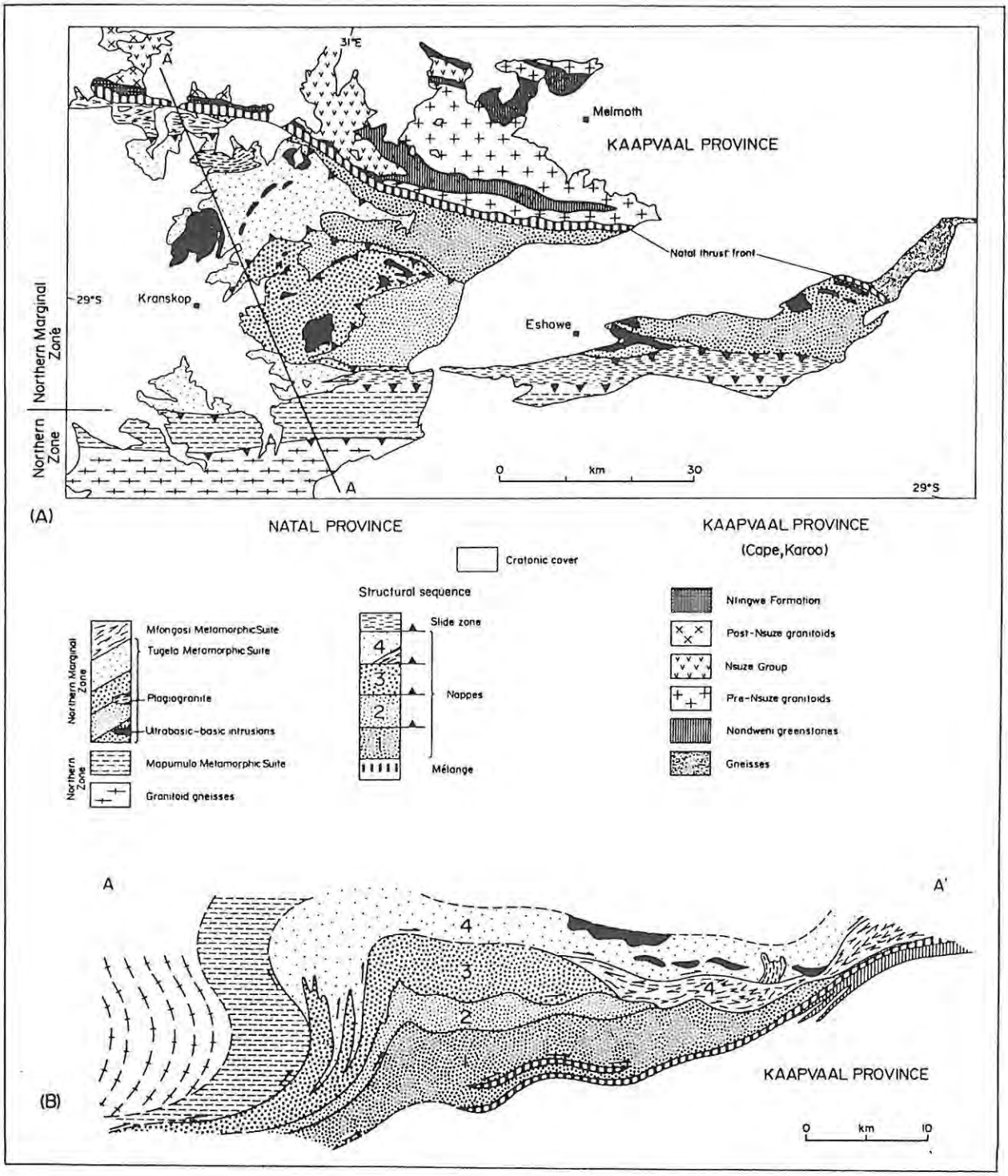

FIGURE 3. (A) Geological map of the Northern Marginal Zone and adjoining parts of the Kaapvaal Craton. (B) Structural profile through the Northern Marginal Zone showing the structural sequence of nappes and overthrusting onto the cratonic foreland. 1 = Nkomo Nappe, 2 = Madidima Nappe, 3 = Mandleni Nappe, 4 = Tugela Nappe. (After Matthews, 1981a).

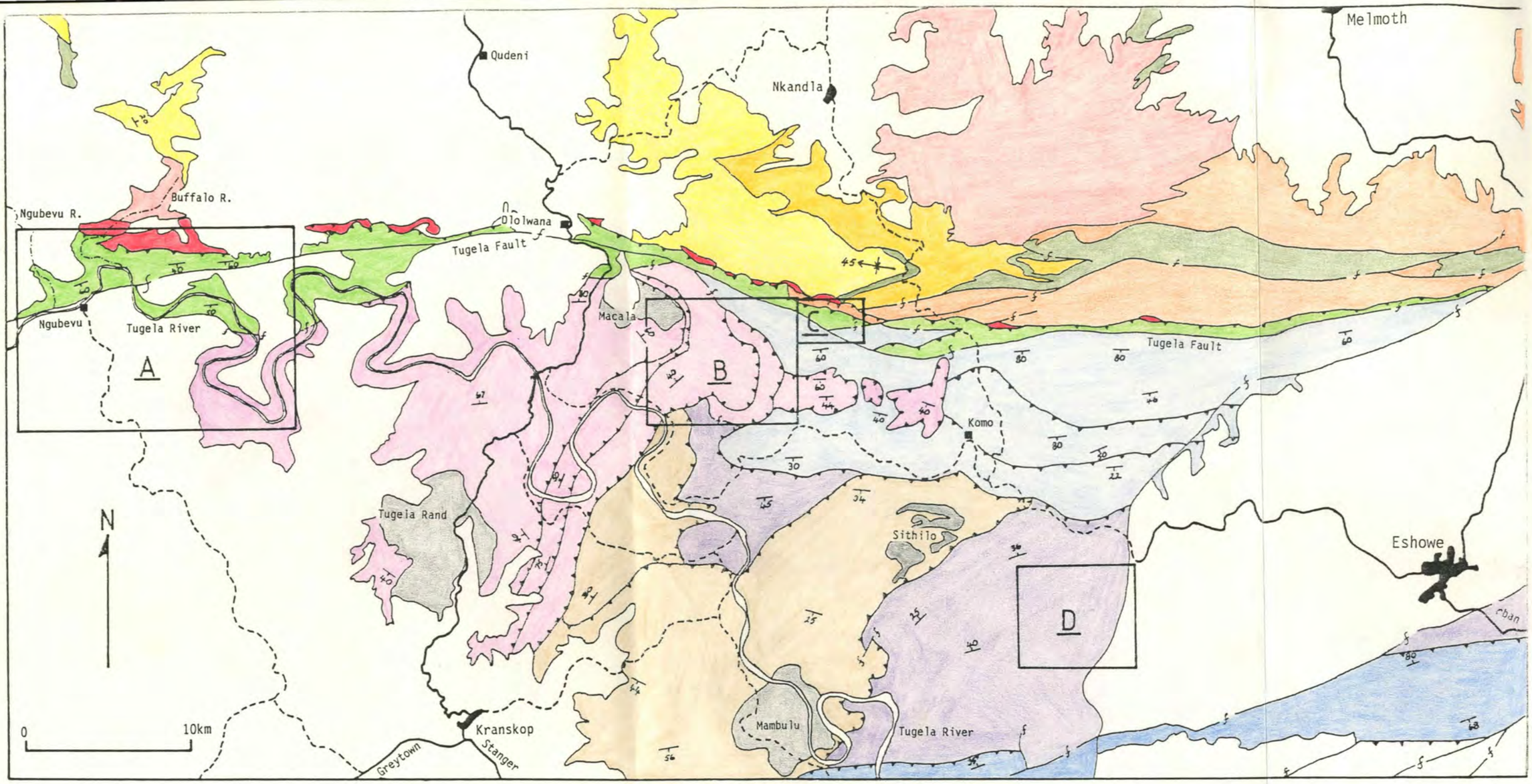

Figure 4 Regional geological map of the Northern Marginal Zone showing the major structural features and the localities of study areas. (Compiled from Geological Survey sheet 2830 DUNDEE).

Scale 1:250 000

KAAPVAAL CRATON
ARCHAEAN

Group

Nsuze — Quartzite, conglomerate, mafic volcanics
Granite
Granite gneiss

Nondweni — Quartzite, conglomerate, sericite schist
Chlorite schist, chert, iron-formation

NATAL STRUCTURAL AND METAMORPHIC PROVINCE
LATE PROTEROZOIC (~1000 Ma)
Structural sequence in ascending order, from bottom to top

Group

Matigulu — Steep Zone

Tugela — Tugela Nappe
Mandleni Nappe
Madidima Nappe
Nkomo Nappe

Mfongosi
Ntingwe
Natal Thrust Belt

Younger cover rocks (Natal Group & Karoo Sequence)

Intrusive Mafic/Ultramafic Complexes

60 Dip and strike of foliation
Thrust fault
Fault
Major roads
Minor roads
Rivers

amygdales, and thin intercalations of limestone and arenaceous sediments (see **Figs. 3** and **4**). In the western sector of the Natal Thrust Belt, the major thrusts dip to the south at angles of 10 to 20°. When traced eastwards, the southerly dip increases to angles between 45 and 60°, and Matthews and Charlesworth (1981) attribute this to a late differential downwarping of the thrust front. This southward monoclinal warping is associated with normal faults with downthrow to the south. These relationships are illustrated by the series of sections depicted in **Fig. 5**, and show the progressive downwarping of the thrust belt from west to east.

The northward tectonic displacement of the Ntingwe and Mfongosi Groups from the southern margin of the Kaapvaal Craton was accompanied by intense deformation and imbrication within the thrust belt, which is overridden from the south by the Natal Nappe Complex.

(2) The Natal Nappe Complex:

The complex consists of four, essentially flat-lying, major thrust sheets which have been metamorphosed to amphibolite facies and tectonically displaced northward onto the southern margin of the Kaapvaal Craton (see **Fig. 3B**). Due to a regional structural plunge to the west, the nappes outcrop in ascending structural order from east to west, and collectively they comprise the Tugela Group (see **Fig. 4** for the structural sequence). Extensive, but discontinuous, sheets of talc schist with pods of serpentinite occur along the basal slides of all major thrust sheets. The Tugela Group comprises mafic metalavas represented by amphibolites and migmatitic hornblende gneisses, and subordinate clastic and chemical sediments represented by metapelitic schists, quartzo-feldspathic gneiss and marble. The lower thrust sheets also contain tectonic slices and infolded elements of granitic gneiss which, in places, has undergone remobilization so that the associated Tugela formations usually contain networks of deformed granitic, aplitic and pegmatitic sheets and veins. Ultramafic intrusions occur in the upper thrust sheets and serpentinite bodies may contain segregations of podiform chromite, e.g. the Tugela Rand and Sithilo intrusions (see **Fig. 4**).

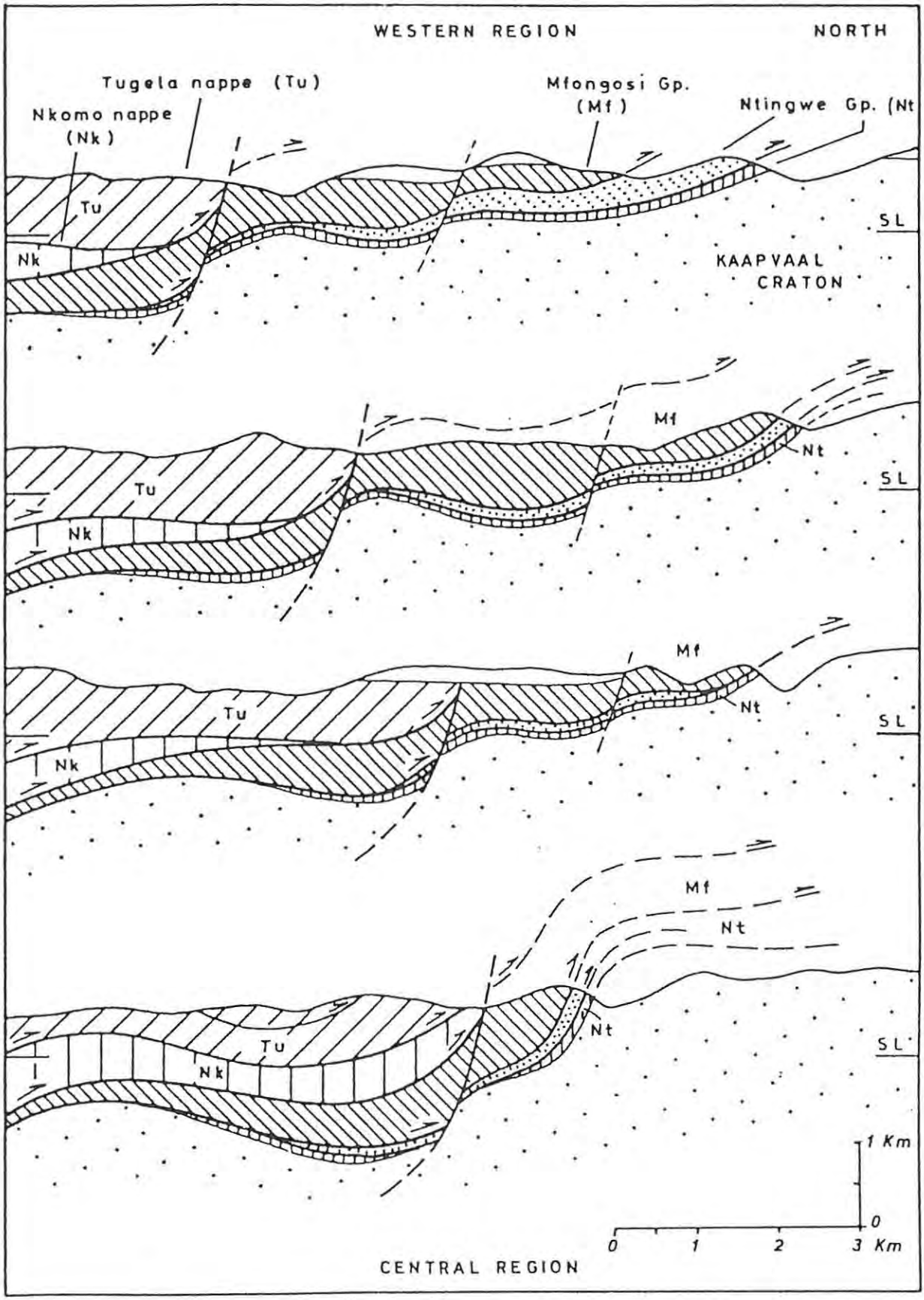

FIGURE 5. Series of sections showing the progressive monoclinal warping and normal faulting downthrown to the south along strike of the Natal Thrust Belt from west to east. (After Matthews and Charlesworth, 1981).

With regard to metamorphism and deformation, it is clear that the upper amphibolite facies migmatitic gneisses of the Tugela Group have been thrust northwards over the greenschists of the Mfongosi Group, and the polymetamorphic nappe complex rocks have undergone at least three phases of deformation. The first deformational phase (D_1) is represented by large- to small-scale isoclinal folding and a dominant phase of foliation generally parallel to the lithological layering. This deformation occurred under upper amphibolite facies conditions of metamorphism, demonstrated by the development of sillimamite + garnet cordierite in metapelitic schists, and clinopyroxene in some amphibolites. It was also accompanied by extensive migmatisation, and local remobilization of infolded granitic gneisses with the resulting emplacement of granitic sheets and veins.

The second phase of deformation (D_2) is represented by a regional episode of lateral ductile shearing with a major component of northward rotation. This phase was accompanied by a slight change in metamorphic conditions to higher pressure, producing kyanite in metapelites.

The D_3 deformational event, or nappe-forming event, was accompanied by widespread disharmonic folding with a consistent sense of asymmetry indicative of overthrusting to the north. Amphibolite facies metamorphic conditions prevailed, with some retrogressive effects along the boundary with the Natal Thrust Belt.

Matthews (1981a) calculates that the total northward tectonic displacement involved in the emplacement of the Natal Nappe Complex and the development of the imbricate zone in the Natal Thrust Belt was not less than 100km. This is estimated from a down-plunge structural profile, on the assumption that the various nappes were originally adjacent parts of the same crustal segment.

All of the mineralized occurrences considered during this investigation are located within the Northern Marginal Zone and the various study areas are shown in **Fig. 4.** The geology of these areas will be considered in detail at a later stage.

2.1.2 Northern Zone

The extent of this approximately 60km wide zone is shown in Fig. 2 and consists of four major ENE trending belts of highly deformed, steeply dipping migmatitic gneisses, with intervening belts of well foliated granitoid rocks which contain extensive units of porphyroblastic and augen gneiss. The migmatitic gneisses, which make up the Mapumulo Metamorphic Suite, occur in two main associations: (1) a group of predominantly quartzo-feldspathic gneisses; and (2) a group of uniform banded hornblende-biotite gneisses with some interlayered amphibolites, which together possibly represent a meta-greywacke - volcanic sequence. The four major belts of Mapumulo rocks represent synformal relicts separated by anticlinoria of intrusive granitoid rocks, now preserved as well foliated augen gneisses, which have been partially remobilized and are charnokitic in places.

Cain (1975) suggested that these granitoid gneisses may represent a high-grade granulite facies basement that was deformed and metamorphosed before deposition of the Mapumulo Metamorphic Suite. However Tankard et al. (1982) point out that the structural and metamorphic relations between the so-called 'basement' granitoid gneisses and the Mapumulo supracrustals bear a striking resemblance to those between the 2.7Ga Bulai granitoid gneiss and the >3.2Ga cover of the Bietbridge sequence in the Limpopo Province. They conclude that the 'basement', according to Cain (1975), represents granitoids intruded syntectonically after the paragneissic Mapumulo Suite had accumulated. Furthermore, Eglington et al. (1986), after a geochemical and isotopic investigation of the Natal Province, stress that nowhere has a basement to these supracrustal gneisses been identified.

2.1.3 Central Zone

This essentially granitic zone is about 120km wide with a general east-west structural trend and is characterized by extensive bodies of massive to foliated biotite or hornblende granitoids which are commonly megacrystic. The batholithic granitoid masses are separated

by augen gneisses and charnokitic (orthopyroxene-bearing) intrusions which crosscut the granitoids in places. Metamorphic assemblages generally indicate that upper amphibolite facies metamorphism prevailed, with local development of granulite facies at high temperatures and low pressures. Thick bodies of dolomitic marble, quartz-graphite schist and metaquartzite as well as amphibolitic dykes and lavas occur at Marble Delta (Fig. 2).

2.1.4 Southern Zone

The Southern Zone is characterized by a more extensive development of charnokite and granulite facies rocks than in the Central Zone, although the boundary between the two zones is somewhat arbitrary. In this zone granites from the Central Zone intrude metasediments which consist mainly of banded hypersthene-garnet granulites with thin quartzite bands that show isoclinal folding overturned towards the north. The granites and granulites are intruded by an extensive suite of charnokitic rocks that range in composition from dioritic to granitic. These intrusions contain xenoliths of the metasedimentary granulites and have a minimum age of 990Ma (Nicolaysen and Burger, 1965). McIver (1966) attributes the charnokitic character of these rocks to crystallization of a normal granitic suite under oxygen deficient conditions.

2.2 Tectonic Evolution

The crustal evolution and tectonic history of the Natal Province is indeed complex and the topic suffers from a conspicuous absence from the literature, with the exceptions of published contributions by Matthews (1959; 1972; 1981a; 1981b), Matthews and Charlesworth (1981), and more recent papers by Eglinton et al. (1986a; 1986b; 1988) that relate mainly to geochemical and isotopic studies. This dearth in the literature may possibly be attributed to the lack of known, economically viable, mineral deposits within the Province. Had a greater economic importance been associated with the area, as is the case in the Namaqua Province, there would probably have been a greater emphasis on research into the crustal evolution of the Natal Province.

Matthews (1972) offered the first attempt at a tectonic model in which he proposed a collision setting involving northward obduction of oceanic crust onto the cratonic foreland. As one moves from north to south, three different tectono-stratigraphic domains are encountered which show contrasting lithological, structural and metamorphic features. These are, from north to south; (1) the Natal Thrust Belt, (2) the Natal Nappe Complex, and (3) the Mapumulo migmatitic gneisses and granitoid intrusives, and Matthews (op. cit.) incorporates these different terrane characteristics in his model.

He points out the three layer structure of oceanic crust, i.e. a thin upper layer of deep sea sediments - argillite, chert and pelagic limestone, followed by a layer of pillowed basalts and sheeted dykes, followed by the lower most layer of massive to layered plutonic mafic and ultramafic rocks, and draws similarities between this and the Natal Nappe Complex. The amphibolite gneisses of the nappe complex are interpreted as representing segments of obducted oceanic crust. The recognision of these rocks as a typical ophiolite suite is obscured by the widespread effects of migmatization and recrystallization, however some suggestive features still remain. At a few localities, deformed relict pillow structures can still be seen in the amphibolites of the Tugela Nappe Complex and metasedimentary horizons present in the upper nappes include psammitic to pelitic schists and gneisses, magnetite quartzites and limestone bands. These features are consistent with the upper part of an ophiolite suite. The migmatization of the Tugela Group involved partial anatexis which produced a compositional banding consisting of thin leucocratic layers of quartz and plagioclase alternating with thicker dark hornblende-rich layers. However, Matthews (1972) states that the rocks from which the Tugela Group migmatites have been derived were of basaltic to andesitic composition and probably represent the upper part of an ocean crust. Furthermore, the Tugela Group contains several isolated and deformed masses of intrusive ultramafic rocks consisting of serpentinites with podiform chromitite bodies, pyroxenites and peridotites, e.g. Sithilo Complex - **Fig. 4.** These bodies are thought to represent parts of the lower mafic to ultramafic layer of an

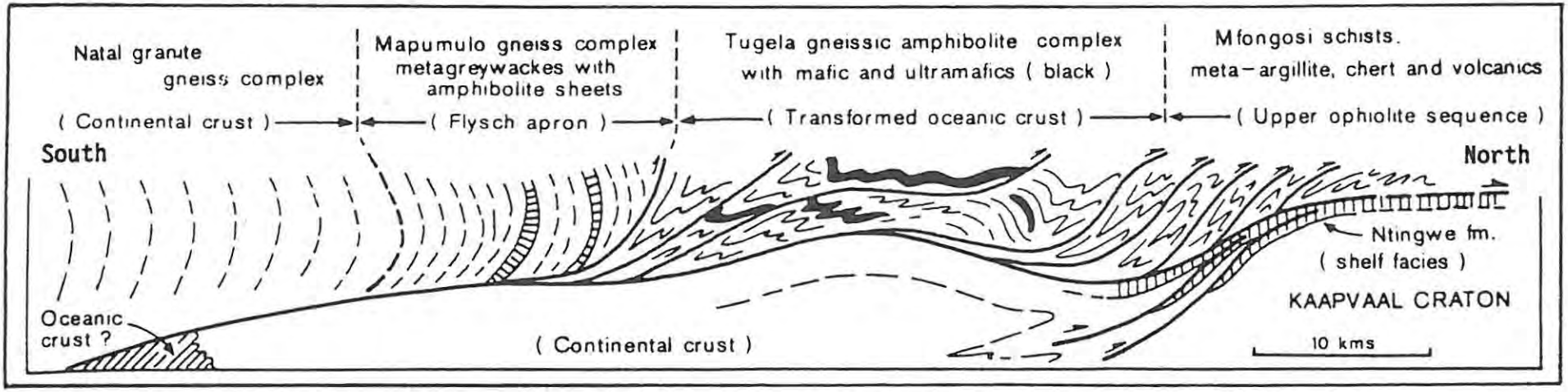

FIGURE 6. Section showing a structural and geological interpretation of the northern frontal region of the Natal Province. (After Matthews, 1972).

ophiolite suite, which is also characterized by the presence of podiform chromitite bodies.

The Ntingwe Group clastic and chemical sediments were interpreted by Matthews (1972) as a shallow water shelf facies that formed a southward thickening sedimentary wedge along the southern margin of the craton and acted as a ramp during the northward emplacement of the nappe complex. Fig. 5 shows a schematic cross-section which depicts the structural and geological interpretation of the Natal Province by Matthews (1972).

The para-gneissic Mapumulo Metamorphic suite is interpreted by Matthews (1972) as a predominantly meta-greywacke sequence welded onto the leading edge of a continental plate above a subduction zone. He believes that the continental plate in question is represented by the extensive granitoid gneiss terrane to the south, i.e. the Central and Southern Zones (Fig. 6), and that northward obduction of ocean crust resulted as a consequence of convergence and collision between this continental plate and the Kaapvaal Craton.

After further work in the Northern Marginal Zone, Matthews (1981a) recognized and delineated the occurrence of four major thrust nappes that make up the Natal Nappe Complex, and produced a down-plunge structural profile through the Zone (see Fig. 3B). The structural sequence of the major nappe structures is shown in Fig. 4. He also recognized that the migmatitic amphibolites of the nappe complex have been thrust northwards over the greenschist facies Mfongosi Group of the Natal Thrust Belt. Thus the increase in metamorphic grade encountered when moving from north to south across the Northern Marginal Zone does not represent a progressive change, as the two metamorphic domains are separated by a major thrust fault. This thrust contact between the Natal Thrust Belt and the Natal Nappe Complex is largely obscured by the post-thrust, possibly Karoo age, southerly dipping Tugela Fault (see Fig. 4). This major, east-west trending, normal fault has downthrown the Tugela Group rocks against the low-grade rocks of the Natal Thrust Belt and the thrust contact is preserved below the present level of erosion. It should be pointed out

here that the allochthonous Mfongosi and Tugela Groups need not necessarily represent originally adjacent parts of the same oceanic crustal segment. This has strong implications for the assumptions made by Matthews (1981a) when he calculated a 100km northward tectonic displacement for the Northern Marginal Zone (chapter 2.1.1), and displacements could in fact have been much greater.

Matthews (1981b) modified his original single-stage obduction model, outlined above, and presented a new two-stage obduction model. Evidence for the new model was based on; (1) structural relationships between the thrust units of the Natal Nappe Complex, (2) lithological associations within the thrust units, and (3) the metamorphic and deformational history of the Tugela Group.

Essentially, the model involves a first stage of southward obduction of the ophiolitic Tugela Group onto a platform of extensive granitoid plutonic components of an island arc complex, now represented by the Mapumulo Metamorphic Suite and granitoid gneisses. During the second stage, the obducted ophiolitic assemblage and underlying components of the island arc complex moved northwards above a southerly dipping subduction zone, and collided with the southern margin of the Kaapvaal Craton. This collision event resulted in thrust slices of island arc complex and overlying ophiolitic rocks being driven northwards across a volcano-sedimentary prism along the southern margin of the craton. Remnants of this prism are preserved in the Natal Thrust Belt and are represented by the essentially mafic volcanic Mfongosi Group and the sedimentary Ntingwe Group.

Eglington et al. (1986a; 1986b; 1988) provide geochemical and isotope data on a variety of lithologies from the Natal Province with the aim of better constraining the ideas of Proterozoic crustal development in Natal. Their work is concentrated on the metasedimentary gneiss and intrusive granitoid terrane of the Northern, Central and Southern Zones, and nowhere have they been able to identify a basement to the metasedimentary supracrustal gneisses - the oldest recognizable lithologies. In light of this, Eglington et al. (1986a) point out that the nature of the substrate onto which the pre-metamorphic sediments

were deposited can only be constrained by geochronological studies of the metasediments themselves and geochemical and geochronological studies of the intrusive granitoids, which must have been derived, at least in part, from a previously thickened crust. These authors distinguish two types of intrusive granitoid in southern-central Natal; (1) a megacrystic A-type, often charnokitic, suite characterized by a high FeO/(FeO + MgO) ratio and high concentrations of High Field Strength elements such as Nb, Zr and Y, and (2) a syn- to late-tectonic suite which typically shows more calc-alkaline characteristics. The A-type granitoids range in age from 1089Ma to 859Ma and field relationships suggest that some of these granitoids pre-date the major regional metamorphic and tectonic event (~1000Ma), while others clearly post-date it. It would therefore appear that conditions were favourable for the formation of A-type granitoids throughout much of the history of the Natal Province.

Kroner (1976) suggests that the supracrustal gneisses and intrusive granitoids of the Natal Province represent reworked Archaean material, but isotope data presented by Eglington et al. (1986b) indicate that this is not the case and it is unlikely that there was any significant involvement of Archaean crust. $^{87}Sr/^{86}Sr$ initial ratios of the intrusive granitoids range from 0.702 to 0.710, with most samples tending towards the lower end of the range. The low ratios suggest that the protolith to these units could not have formed much before 1400Ma (Eglington et al., 1986b). The lack of evidence for the participation of older material in the formation of the intrusive granitoids argues against a continental margin magmatic arc environment being involved. Also, the A-type character of many of the intrusives is not compatible with a subduction zone environment, but rather indicates a 'within-plate' setting. It is conceivable that the supracrustal gneisses could have been partially melted to produce the granitoid intrusions but, here too, the isotopic signatures of the gneisses are not consistent with the low $^{87}Sr/^{86}Sr$ initial ratios of the granitoids.

In addition, Eglington et al. (1986a) point out that carbonates precipitated from aqueous solution will be in isotopic equilibrium

with the parent solution, and the $^{87}Sr/^{86}Sr$ ratio in marine waters is a function of the proportion of Sr derived from oceanic (i.e. mantle) or continental sources. Thus limestones may provide a window to the conditions prevailing during deposition of the sediments. Where a continental source is old, its $^{87}Sr/^{86}Sr$ ratio will be higher than for a source which has only recently differentiated from the mantle. Therefore limestones formed near a continental margin, or in an intra-continental basin, will have higher $^{87}Sr/^{86}Sr$ ratios than those formed further away from the continental source. Limestones investigated in the Natal Province show that the $^{87}Sr/^{86}Sr$ ratios are <u>low</u>, suggesting that no old, radiogenic continental source was likely to have been close to the site of deposition of the Proterozoic sediments.

To summarize then, isotopic evidence indicates that the intrusive granitoids of central-southern Natal were not derived by partial melting of the supracrustal paragneisses, nor were they derived from the reworking of continental material similar to that of the Kaapvaal Craton. Furthermore, isotope data obtained from limestone units suggest that the deposition site of pre-metamorphic sediments was far removed from any old continental source, and therefore the sediments themselves could not have been derived from the Kaapvaal Craton. However the presence of such a high proportion of intrusive granitoid material in central-southern Natal indicates the existence of a previously thickened crust. Although granitoids of the composition and abundance observed could not have been derived directly from the mantle, the mantle may have provided an important contribution to their chemical composition (Eglington et al., 1986a).

The only available evidence as to the nature of lower crust below the Natal Province is the presence of granulite xenoliths brought to the surface by Cretaceous kimberlites in Lesotho (Eglington et al., 1986b). Rare earth element data from seven of these xenolith samples indicates that they represent melts derived from the mantle that were trapped and crystallized in the lower crust, and a Sm-Nd age of 1400Ma was obtained for the samples. It is therefore possible that the entrapment of these mantle derived melts gave rise to a thickened crust, as well as providing a suitable source for the granitoid

intrusives observed in Natal and, due to the large volume of granitic material produced, this protolith would have to have been essentially intermediate in composition. It is also possible that the early mafic to intermediate crustal thickening event took place in an island arc type environment, and this would be consistent with the two-stage obduction model proposed by Matthews (1981b). However, as pointed out above, the presence of large volumes of A-type granitoids is more characteristic of a 'within-plate' setting than a subduction setting.

The following summarizes the major features that need to be explained when considering any model for the Proterozoic crustal evolution in Natal (Eglington et al., 1988):-

(i) The bimodal distribution of lithologies within the Natal Province, i.e. predominantly mafic in the north and felsic in the south.

(ii) The apparent absence of a pre-existing sialic crust.

(iii) Uniform, extremely low $^{87}Sr/^{86}Sr$ initial ratios in the carbonate sediments - indicating deposition far removed from the Archaean Kaapvaal Craton.

(iv) Limited exposures of calc-alkaline, magmatic arc type plutons.

(v) A predominance of A-type granitoids throughout central-southern Natal.

(vi) No noticeable bulk geochemical change with time.

(vii) Geochemical and petrological characteristics in some of the granitoids which require the existence of a previously thickened crust.

(viii) Early isotopic initial ratios which approximate to depleted mantle values.

(ix) An apparent absence of reworking of significantly older material.

(x) Mafic orthocumulates, possibly formed by underplating, which are approximately contemporaneous with, or slightly older than, the exposed granitoids.

3. INTRODUCTION TO THE PROJECT AREA AND STUDY PROCEDURES

The locations of study areas, within a regional context, are shown in **Fig. 4** and labelled A, B, C and D respectively, and each area contains one or more mineralized occurrences. Geological maps of the individual study areas are provided at a scale of 1:50 000 in order to highlight the local geology and accurately locate mineralized horizons. The 1:50 000 maps were compiled by the South African Development Trust Corporation (STK) during the 'Tugela Mapping Project', in which the author was involved. This comprised a compilation of previous work in conjunction with ongoing STK projects to produce a comprehensive lithological and mineral occurrence map of the Tugela Valley.

The emphasis of the project is concentrated on a petrographic and geochemical investigation with the aim of defining the nature of the mineralization and discussing some ideas on its possible genesis. This involved the examination of thin sections and the collection and interpretation of whole rock major, trace and precious metal analyses (whole rock analyses are given in **Appendix A** and their rock descriptions in **Appendix B**), together with a study of fluid inclusions from quartz vein material associated with the mineralization. During the course of the investigation it became clear that two distinct styles of mineralization can be identified in the Northern Marginal Zone of the Natal Structural and Metamorphic Province. The first style consists of syngenetic, stratabound massive, to semi-massive, sulphides of exhalative origin, and is confined to the amphibolite facies Natal Nappe Complex. The massive sulphide horizons consist predominantly of pyrite, together with very minor galena and sphalerite, and exhibit enhanced gold and silver values. Study area B (**Fig. 4**) is devoted to a study of this style of mineralization, which occurs within the Tugela Nappe. The second style consists of epigenetic quartz vein hosted gold mineralization occurring in shear zones in both the greenschist facies rocks of the Natal Thrust Belt and the amphibolite facies rocks of the Natal Nappe Complex. Study areas A and C deal with the development of this style of mineralization in the Mfongosi Group schists of the Natal Thrust Belt,

while area D deals with the same style occurring in the Madidima Nappe of the Natal Nappe Complex.

The gold occurrences in the Tugela Valley, which essentially exposes the Northern Marginal Zone, were extensively explored by early prospectors at around the turn of the century. These early prospectors concentrated on gold hosted in quartz veins and all old workings and exploratory adits are located in zones of shearing. Early records of the small-scale mining operations are almost non-existant, although Hatch (1910) reports that the Phoenix Mine (**Fig. 7**) produced 1kg of gold from 100 tons of ore in 1907.

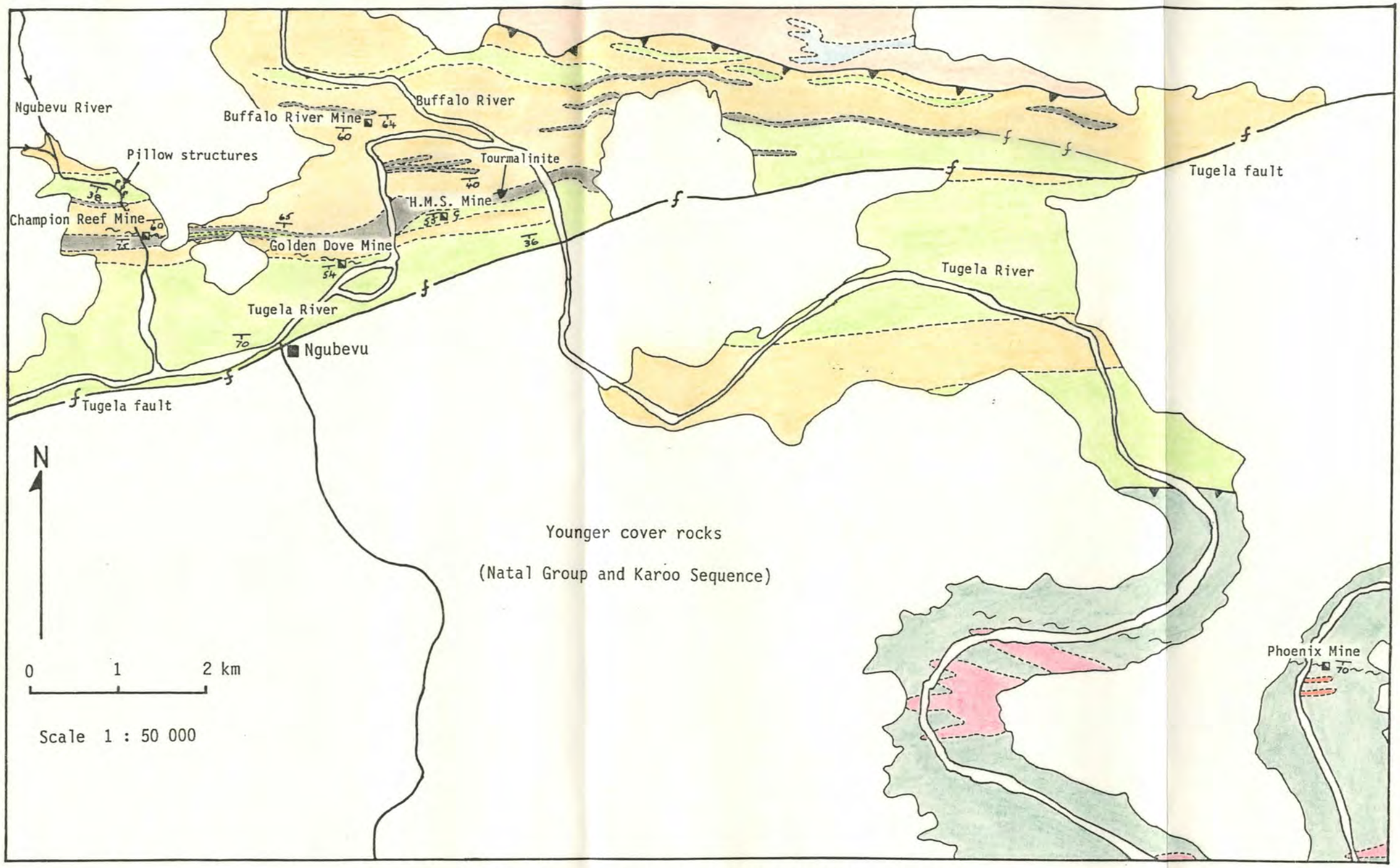

FIGURE 7. Geological map of study area A showing lithologies and the locations of old workings situated on gold occurrences.

NATAL THRUST BELT	NATAL NAPPE COMPLEX	
Group	Group	60 Dip and strike of foliation
Ntingwe: mudstone & shale; red and white limestone	aplite	Thrust fault
Mfongosi: graphite schist; phyllite & quartz-sericite schist; chlorite, quartz-chlorite schist	Kotongweni tonalite I-type	Fault
	Tugela (Tugela Nappe): amphibolite	Shear zone
		G Gossan
		Old working
		Road

4. STUDY AREA A

The local geology of study area A, together with the locations of old workings, is shown in **Fig. 7**. The gold occurrences are all located within shear zones in the Mfongosi Group schists, with the exception of the Phoenix Mine (southeast corner of **Fig. 7**) which occurs in Tugela Group rocks of the Natal Nappe Complex. To the best of the author's knowledge there are no gold occurrences located within the Ntingwe Group sediments, and it has become evident that all gold mineralization in the Tugela Valley, both epigenetic and syngenetic, is either hosted by, or closely associated with, mafic volcanics.

The Mofongosi Group schists represent intensely folded imbricate slices thrust northwards over the younger Ntingwe Group sediments and display a strongly developed foliation which dips at 40 to 70° to the south. An example of the intense isoclinal folding which accompanied the northward tectonic displacement is shown in **Plate 1** and gives an idea of the complex structural nature of the area. Two major lithological varieties dominate the succession (described below) - these are schistose mafic metalavas metamorphosed to greenschist facies, and meta-argillites now represenred by phyllites and mica schists. In addition, several fairly thin, but persistent, graphitic schist horizons are developed, and these usually show pervasive carbonate alteration.

4.1 Petrography and Local Geology

NOTE The convention used in this work for the purpose of naming rocks is as follows:- The mineral occurring in greatest abundance is placed first in the list of minerals preceeding the rock name (e.g. chlorite-epidote-carbonate schist - the order of abundance of minerals is chlorite > epidote > carbonate).

PLATE 1. Isoclinal folding and boudinaged early qartz veins in mafic metalavas of the Mfongosi Group. These highly deformed veins contain no calcite and are barren of mineralization.

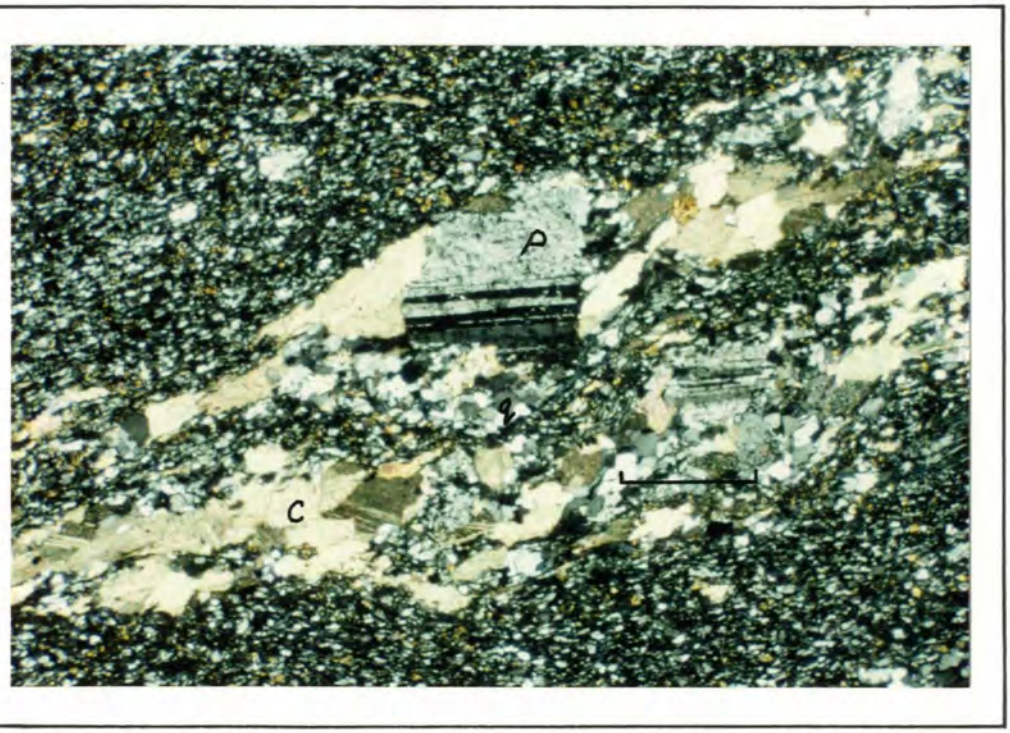

PLATE 2. Photomicrograph illustrating the nature of late-stage carbonate alteration (C = calcite). Note the increase in abundance and grain size of quartz grains (q) associated with the carbonate. The plagioclase crystal (P) illustrates the feldspathization described by Matthews (1959). The rock matrix consists of fine-grained quartz, chlorite, epidote and muscovite. (Bar scale = 1mm).

4.1.1 Mfongosi Group

Mafic Metalavas:

These light green to greyish green rocks characteristically display the typical greenschist mineral assemblage of chlorite-epidote-sericite-albite, and also contain varying amounts of quartz, carbonate, clinozoisite and biotite. In thin section the metalavas are fine grained and show a well developed schistose fabric defined by chlorite and sericite. Chlorite is the dominant mineral, usually constituting between 40 and 60% of the rock, and disseminated epidote is present in varying amounts up to about 15%. Where epidote is more abundant the green colour of the rock is enhanced. Undeformed amygdales can be recognized in certain thin sections and consist of a granular core of epidote surrounded by a rim of granular quartz and calcite. Fine grained quartz grains are generally abundant and in places these have recrystallized into coarser grained aggregates and are often associated with carbonate alteration.

Carbonate alteration is evident in varying intensities in all metalava samples examined and shows a full spectrum of intensity from weak to very intense and pervasive. It is most strongly developed in zones of intense shearing and is ubiquitously associated with mineralized occurrences. This alteration is late in the paragenetic sequence and occurs as patches of undeformed fine- to medium-grained carbonate developed along foliation planes. In places, thin (1/2 to 1mm thick) carbonate veins cross-cut the foliation and in areas of intense carbonate veining a general increase in the abundance and grain size of quartz was also noted. These features are illustrated in **Plate 2.** Carbonate is also present in late-stage quartz veins **that** vary in thickness from 1 to 10cm and are essentially undeformed. These veins generally occur parallel to the foliation but in places cross-cut it, generally at a shallow angle. An earlier generation of quartz veining is also present within the metalavas and show isoclinal folding and boudinaging into discontinuous lenses paralleling the foliation. There is no carbonate associated with this early phase of quartz veining.

Feldspathization of the greenschists is common and, as first pointed

out by Matthews (1959), the degree of feldspathization increases towards the south, i.e. towards the Natal Nappe Complex. Porphyroblasts of polysynthetically twinned plagioclase range in size from 0.1 to 2mm and often show sutured outlines and well developed sieve textures, enclosing grains of quartz, sericite and chlorite. Matthews (1959) notes that the majority of porphyroblasts are almost pure albite in composition and suggests that feldspathization took place subsequent to the maximum metamorphism.

Pillow structures, shown in **Plate 3**, are exposed in the Ngubevu River (**Fig 7**) in a relatively undeformed state and it is possible to determine a way-up for the sequence at this locality. It is clear that the rocks are the right-way-up and are dipping to the south at about 35°. Immediately overlying the pillow structures is a 2m thick horizon of spatter material, comprising an unsorted assemblage of different sized, oval shaped, fragments up to about 10cm in length (**Plate 4**). These are interpreted as **volcanic** fragments erupted explosively, possibley as a result of interaction with water, and form a layer overlying the pillow structures.

Phyllite and Quartz-Sericite Schist:

The grey to pale-green coloured, finely laminated, micaceous phyllites consist dominantly of sericite, together with varying amounts of quartz, chlorite and albite. The phyllites grade into brown quartz-sericite schists as the amount of quartz increases and these rocks are more abundant than the phyllitic variety. Matthews (1981a) suggests that the phyllites and quartz-sericite schists represent metamorphosed and deformed argillaceous sediments. Minor amounts of chlorite and epidote present in the schists may indicate the incorporation of mafic tuffaceous material within the sedimentary package.

Feldspathization within these rocks is generally better developed than in the metalavas and albite porphyroblasts may reach as large as 1cm in length. Quartz veining and carbonate alteration is also present and parallels the foliation as in the case of the metalavas.

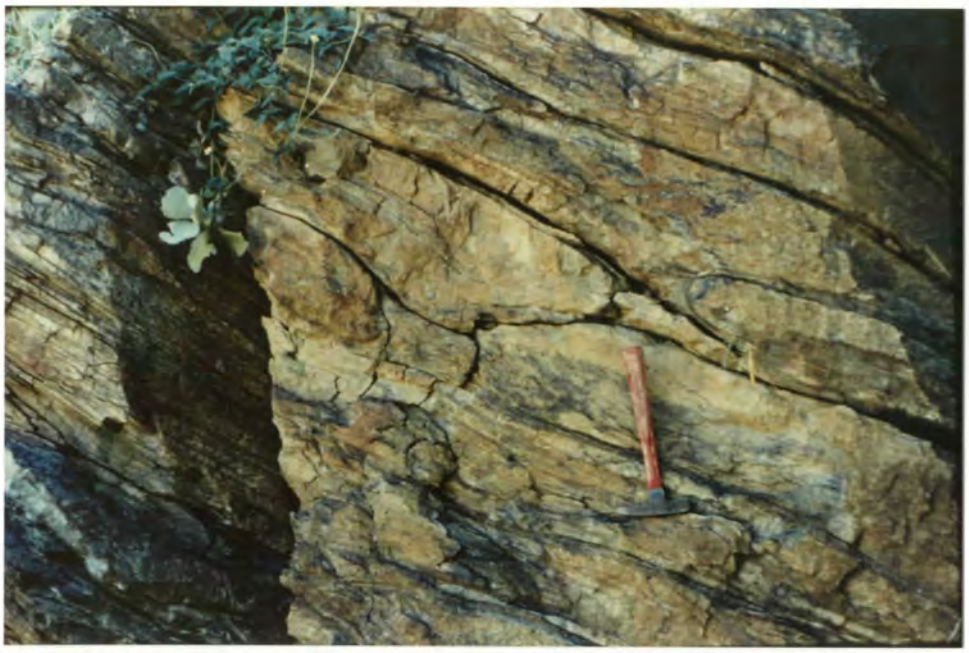

PLATE 3. Deformed pillow lavas exposed in the Ngubevu River (see Fig. 7). The pillow structures indicate that the rock sequence in this area is the right-way-up.

PLATE 4. Volcanic spatter debris immediately overlying the pillow lavas shown in Plate 3. This consists of an assortment of poorly sorted fragments showing a large variation in size and is approximately 3m in thickness.

PLATE 5. Shows a well exposed strongly foliated graphitic schist horizon developed approximately 800m east of H.M.S. Mine. Thin tourmalinite zones were identified within this graphitic horizon.

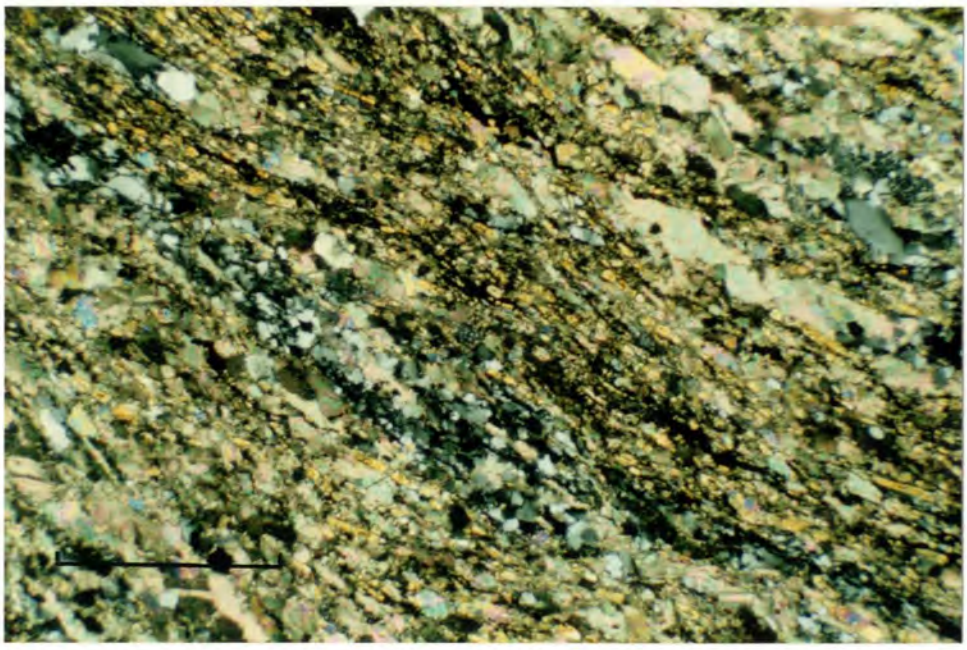

PLATE 6. Photomicrograph showing a typical tourmalinite zone. The rock consists of fine-grained tourmaline (yellow needles), quartz and graphite, as well as coarser-grained carbonate alteration. The tourmaline-rich nature of the rock cannot be recognized in the field due to the fine grain size. (Bar scale = 0.5mm).

Graphitic Schist:

Several horizons of graphitic schist have been mapped in study area A (**Fig 7**) and usually occur along the contacts between the metalavas and meta-sediments now represented by quartz-sericite schists and phyllites. However some graphitic horizons occur enclosed within the metasediments. **Plate 5** shows the nature of a graphitic schist horizon, in close up, from a locality 800m to the east of H.M.S. Mine and the dark graphite is almost always associated with a secondary ferruginous staining, probably goethite.

A thin section examination of the graphitic horizon at the above locality shows that it has been intensely carbonated and fine-grained tourmaline is abundant, often constituting >20% of the slide, with varying amounts of quartz and sericite also present. The width of the tourmaline-rich zone within the graphitic horizon is poorly defined but does not appear to be wider than several metres, although tourmaline-enrichment is fairly persisent along strike. Due to the fine-grained nature of tourmaline the enriched zones cannot be mapped in the field and their definition is confined to thin section studies. **Plate 6**, from the same locality as **Plate 5**, shows an example of a tourmaline-rich graphitic zone in thin section, and the rock may be described as a tourmalinite according to the definition by Slack (1982). He defines tourmalinites to be stratabound lithological units broadly concordant with their enclosing host rocks and containing 15 to 20% or more tourmaline by volume. Slack et al. (1984) note the common occurrence of carbonaceous material or graphite with many tourmalinites and together with the stratigraphic continuity of these units they suggest deposition under reducing conditions, perhaps in a dense brine pool, with boron ultimately being derived from volcanic and/or hydrothermal activity. The above authors also describe the formation of tourmalinites under evaporitic conditions, but this mechanism is rejected here since there is no evidence for evaporitic sequences within the Mfongosi Group.

The recognition of tourmaline-rich horizons can be important from a mineral deposit and exploration point of view, and this is discussed by Slack (1982). He points out the increasingly realized spatial

association of tourmalinites with stratabound base metal sulphide, gold, tin and tungsten mineralization and suggests that tourmalinites may be intimately linked to the genesis of these deposits. At several base metal deposits in the Appalachian-Caledonide orogen underground observations suggest that tourmalinites may be local facies equivalents of stratabound sulphides. Slack (1982) also notes that many stratabound tourmaline concentrations not of obvious plutonic or evaporitic origin were probably formed by submarine exhalative processes. Where tourmalinites are abundant, boron was an important component of the hydrothermal fluid, and these rocks may indicate a proximal environment in which boron- and metal-bearing fluids discharged from fumarolic vents and were deposited locally as chemical precipitates. However, regardless of the exact genetic relationship, a close spatial association exists between tourmalinites and stratabound mineral deposits, and the location of these tourmaline-rich rocks should be considered as a potential prospecting tool.

In the case of the study area it was found that the tourmalinite shown in **Plate 6** is significantly enriched in gold and returned a value of 350ppb Au. This zone is confined within the graphitic schist horizon that runs along strike between the H.M.S., Golden Dove and Champion Reef mines and the possibility of further tourmalinite zones occurring in other graphitic horizons cannot be discounted as this has not been tested. It is therefore possible that the epigenetic mineralization observed at the above mine workings were derived, at least in part, from an, as yet unrecognized, syngenetic stratabound exhalative protore related to the deposition of tourmalinite. This would seem to be substantiated by the close spatial association between the epigenetic deposits and the potential protore.

Plimer (1987) describes tourmalinite-hosted scheelite deposits from Zimbabwe and Australia, and although no tungsten analyses are available from the study area, the presence of scheelite was detected, by UV lamp, in a late cross-cutting quartz vein from the outcrop shown in **Plate 5**. This further suggests that an early syngenetic mineralizing event was associated with tourmalinite deposition.

4.1.2 Tugela Group

The Phoenix Mine, situated in the southeastern corner of Fig 7, is located within amphibolites of the Tugela Nappe which constitutes part of the Tugela Group. The amphibolites are fine- to medium-grained with foliated to massive textures and contain more or less equal proportions of hornblende and plagioclase as the dominant minerals. Chlorite occurs in varying proportions, probably as a retrograde product of hornblende, and where its abundance is significant the rock takes on a schistose fabric. Minor amounts of quartz and biotite are also present.

The Phoenix Mine itself is hosted by a sheared metagabbro that is intrusive into the amphibolite sequence. The unsheared metagabbro consists of medium- to coarse grained sericitized plagioclase and altered pyroxene crystals. Clinozoisite and actinolite are abundant and less common chlorite and muscovite flakes occur in random orientations. In some thin sections minor amounts of fresh secondary feldspar can be observed and accessory amounts of zircon are also present.

4.2 Nature of Mineralization and Geochemistry

4.2.1 Overview

The old workings, shown in Fig. 7 were investigated with a view to determining the mode of occurrence of gold and the type of alteration, if any, associated with the mineralization. The samples collected (see Appendix A and B) may be categorized as follows:-

Quartz vein material:

1) Strongly deformed veins not associated with shearing.
2) Relatively undeformed, carbonate-bearing, veins not associated with shearing.
3) Veins from within shear zones.

Whole rocks:

1) Shear zone material. 2) Rock immediately adjacent to shear zones and likely to show effects of alteration. 3) Host rock significantly removed from zones of shearing, mineralization and alteration.

Other:

Lithological horizons of potential interest, e.g. graphitic schist/ tourmalinite.

The resulting analyses show quite conclusively that gold enrichment is confined to shear zones and that the highest values are derived from quartz veins within these zones. Shear zone material may show an enrichment, but this is insignificant when compared to gold values obtained from the quartz veins they host. Zones of alteration can be distinguished adjacent to shear zones but gold values here are no different to the values obtained from unaltered host rocks, where values do not exceed 10ppb Au.

Another important consideration is to determine which phase of quartz veining was responsible for the gold mineralization. Analytical results show that the earliest recognized quartz veins, those that have been isoclinally folded along with their host schists, do not carry any gold values (<10ppb Au). It is likely that these veins were emplaced at some stage during the metamorphic history of the area prior to the deformational event resulting in isoclinal folding and prior to the northward thrusting event, which is recorded by Matthews (1981a) as the last major deformation affecting the Northern Marginal Zone.

It is the thin, often discontinuous, quartz veins and stringers that vary from fine veinlets to veins about 3cm in width and occur within shear zones, parallel to the shear foliation, that are mineralized, with 7100ppb Au being the highest value recorded during this study. However much higher values are quoted in exploration company reports, and Hatch (1910) reports values of 15 g/t Au over a width of 1.7m and strike length of 19m and 7.3 g/t Au over a width of 1.1m and strike

length of 20m from the Golden Dove Mine. Unfortunately the mineralization appears to be patchy and discontinuous. The mineralized veins generally display a 'rusty' colour and thin section examinations reveal that carbonate is absent, indicating that they pre-date the late-stage carbonate alteration. The veins are broken in places, thus showing signs of limited deformation which may be ascribed to subsequent movement along the shears, but there is no evidence of the folding and intense deformation observed in the earliest phase of quartz veining. It is therefore postulated that mineralizing fluids were channeled through the shear zones and deposited gold in quartz veins during an event that post-dates the last major deformation. Shearing and mineralization could have been more or less contemporaneous and the gold-bearing quartz veins may have been modified slightly by subsequent shear movements.

A final phase of veining is related to the late-stage influx of CO_2-rich fluids resulting in extensive carbonate alteration. This gave rise to undeformed quartz veins, containing substantial amounts of carbonate, and cross-cut the foliation in places. Gold values in these veins, whether they are located in shear zones or not, may be enhanced but seldom exceed 20ppb Au. It is therefore considered that this phase of fluid activity was unimportant from a mineralization point of veiw.

4.2.2 H.M.S. Mine

The H.M.S. Mine consists of two inclined shafts and three vertical shafts, with limited underground development. The old workings are located in a zone of intensely deformed and strongly schistose metalavas and it is practically impossible to identify individual shear zones. An example of the strongly schistose appearance of the metalavas is shown in **Plate 7**.

A possible indicator for the detection of fluid channelways (shear zones) during surface exploration is provided by the gossan outcrop, shown in **Plate 8**, and marked on **Fig 7**.

PLATE 7. Illustrates the intensely deformed and strongly foliated nature of the metalavas in the vicinity of the H.M.S. Mine.

PLATE 8. Gossan outcrop developed approximately 200m to the east of H.M.S. Mine. Note the poorly developed foliation when compared to **Plate 7.** This could be due to the passage of large volumes of fluid which have obliterated the rock fabric.

The gossan is developed about 200m along strike to the east of H.M.S. Mine, and it is clear from Plate 8 that the schistosity, although still present, has been largely obliterated. If it is assumed that the sulphide mineralization at this locality is a result of fluids moving through a shear zone, then it is logical that interaction with the passage of large volumes of fluid has resulted in obliteration of the rock fabric. If this is the case, then the identification of zones showing a subdued fabric along strike may be useful in locating fluid channelways and hence potential targets for mineralization. Unfortunately, analyses of the gossan returned very low precious and base metal values, although sulphur is high (sample NH/2, Appendix A). It should also be pointed out that the phenomenon of fabric obliteration in fluid channelways is confined to the vicinity of H.M.S. Mine. The other mineral occurrences are developed in easily identifyable shear zones.

In underground exposures at H.M.S. Mine, where the rock is less weathered, it is possible to detect changes in the fabric more easily, and a silicified shear zone was identified, striking 084° and dipping 63°S. The mineralization occurs as thin, gold-bearing, quartz veinlets, varying up to 1cm in width and confined to the shear.

The chemical changes observed in a traverse from the mineralized H.M.S. shear zone to the unaltered host rock are shown in Fig 8. It is not possible to ascertain the true width of the shear from underground exposures, but the zone appears to be a minimum of 3m in width. The zone of shearing is represented by a quartz-sericite rock, containing very minor carbonate, and there is little evidence of a foliation, both in handspeciman and in thin section. Gold-bearing quartz veinlets from within this zone returned a value of 5200ppb Au and minor amounts of finely disseminated pyrite are visible within the quartz-sericite rock. It is clear from thin section examinations that the zone has been strongly silicified, thus resulting in obliteration of the shear fabric. This is of interest since the other mineralized localities within the Mfongosi Group (Figs. 9 and 10) show a silica depletion in shear zones. The silica depletion phenomenon indicates that silica has been leached from the shear, and surrounding alteration zone, and

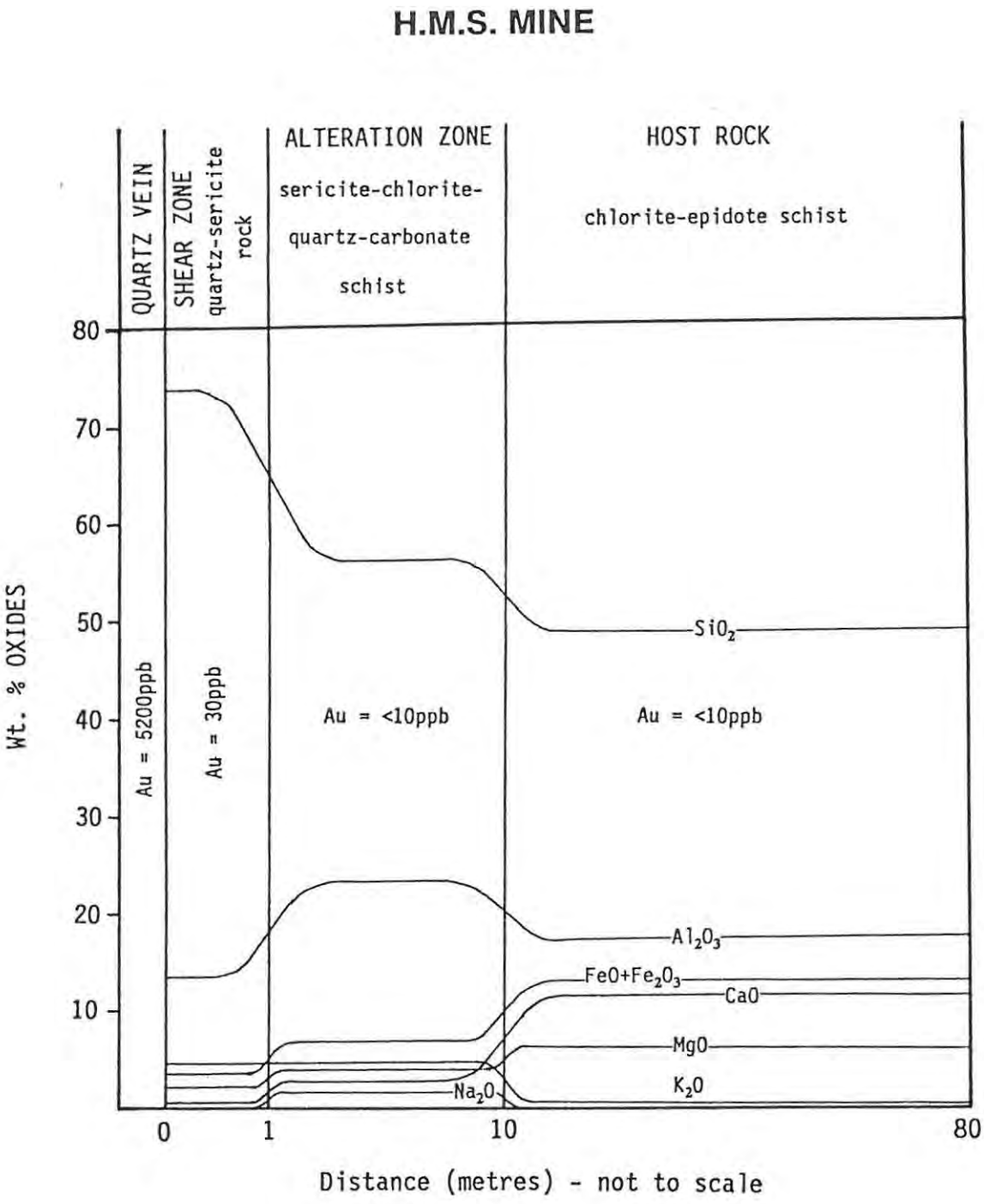

FIGURE 8. Chemical changes associated with the mineralization at H.M.S. Mine. The diagram represents a geochemical traverse from shear zone to host rock and is orientated perpendicular to strike.

redeposited as quartz veins within the shear zone. It is therefore not certain whether the silicification observed at H.M.S. Mine was coeval with mineralization, or whether it was introduced at a later stage. A possible explanation for the lack of carbonate alteration in the H.M.S. shear zone may lie in the impermeable nature of the silicified horizon to late CO_2-bearing fluids. This also implies that if silicification post-dates mineralization, it must pre-date the late-stage CO_2-rich fluid activity.

The movement of fluids through the shear zone have also affected alteration of the adjacent host rocks and in thin section the dominant minerals are sericite, chlorite and quartz. Relatively unaltered secondary plagioclase crystals are also abundant, together with minor biotite and disseminated pyrite. Carbonate is abundant, but appears late in the paragenetic sequence and is probably unrelated to the initial alteration by mineralizing fluids. When compared to the unaffected host rock, consisting dominantly of fine-grained chlorite and epidote, the altered rock represents a zone of addition of silica, aluminium, potassium and sodium, and a subtraction of iron, calcium and magnesium. This is characteristic of sericitic alteration, where sericite, quartz and pyrite (QSP) form the diagnostic mineral assemblage, and occurs as a result of the leaching of Ca^{2+}, Mg^{2+}, $+/-Na^{+}$ and the introduction of K^{+}. The observed enrichment in iron in the alteration zone may have been derived from the original mafic minerals and combines with sulphur, introduced by fluids, to produce pyrite.

4.2.3 Champion Reef Mine

The Champion Reef Mine is located on a 4m wide shear zone, striking 095° and dipping 60°S, hosted by sericite-quartz schists and occurs in close proximity to a graphitic schist horizon (**Fig. 7**). **Plate 9** shows part of the strongly developed shear zone exposed above the entrance to an adit. It was not possible to enter the mine to collect samples of quartz vein material along strike of the shear, and analyses of quartz veins exposed in the shear at the entrance to the adit returned no enhanced gold values. However, Hatch (1910) reported a value of 5.4

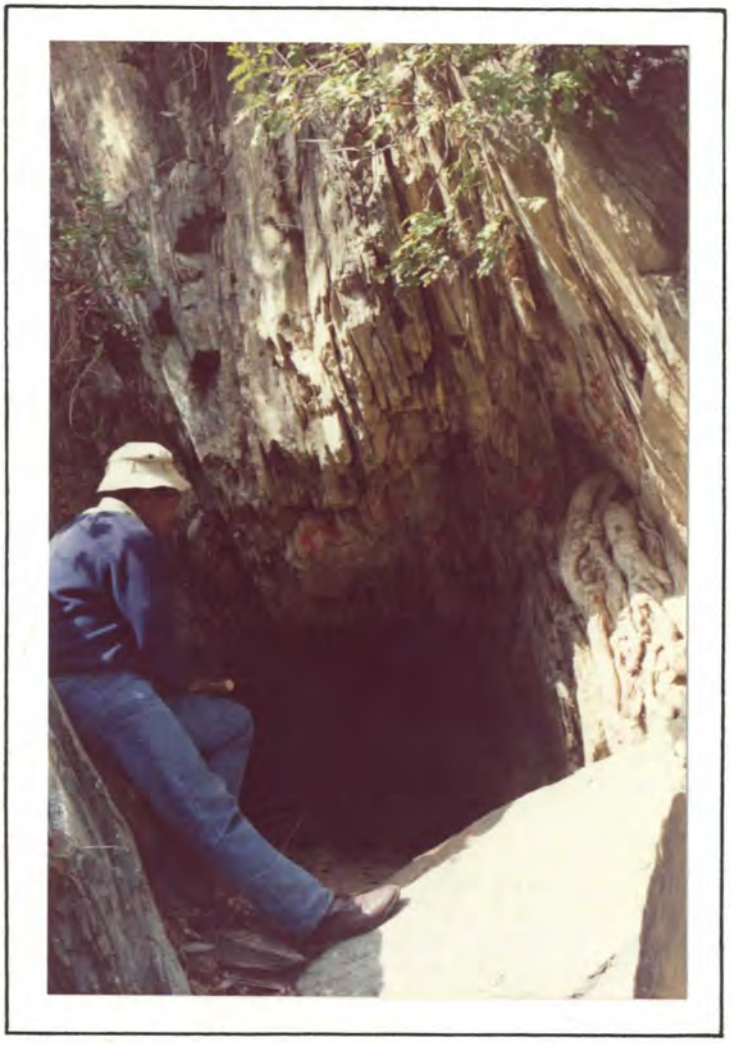

PLATE 9. Shear zone clearly developed above the entrance to an adit at the Champion Reef Mine. The thin, relatively undeformed, quartz veins seen paralleling the shear (top left corner) are typical in appear ance to those carrying the mineralization, although in this instance they are barren.

PLATE 10. Illustrates the sharp contact between sericite-carbonate alteration (left - lighter) and epidote-chlorite alteration (right - darker), with the contact at the hammer head. These colour changes in the field may serve as a useful exploration guide.

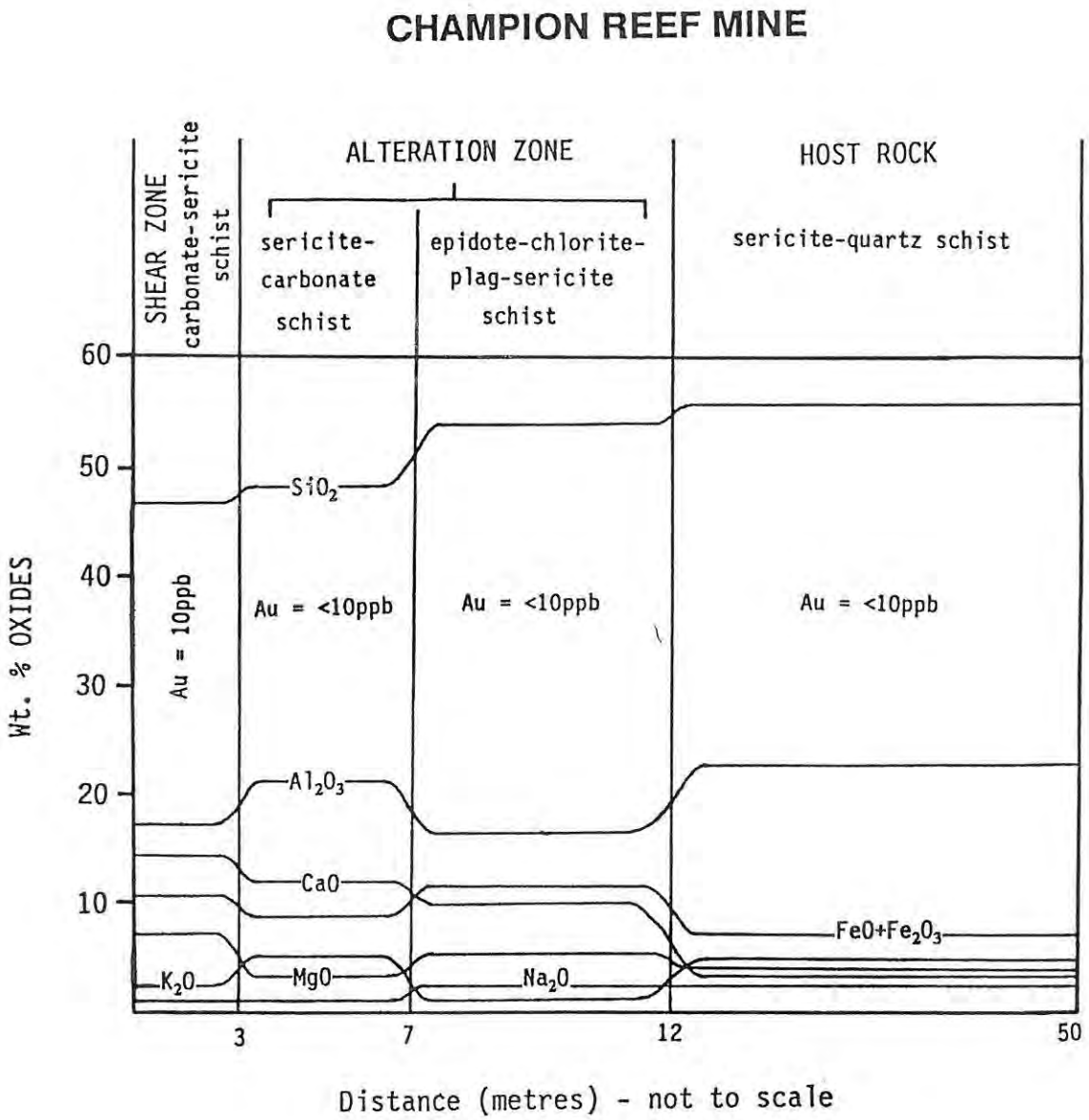

FIGURE 9. Chemical changes across strike at the Champion Reef Mine. Note that no gold values are available from mineralized quartz veins within the shear.

g/t Au over a width of 1.24m.

The alteration associated with the passage of fluids through the shear zone is well developed and best defined at Champion Reef Mine, and the chemical changes observed in a traverse from the shear zone to unaltered host rock are shown in Fig. 9. Thin section investigations of the shear zone material show that the rock is strongly foliated and consists dominantly of carbonate and sericite, with sericite being subordinate to carbonate. Biotite is also present in varying proportions but is generally minor, as is finely disseminated pyrite. There are no quartz grains present and the shear zone shows a marked depletion in silica, indicating that silica has been mobilized from the altered rock and probably redeposited as thin quartz veins within the shear. Sericite is the dominant alteration mineral and again carbonate appears late in the paragenetic sequence, probably resulting from 'flushing' of the shear zone by late-stage CO_2-rich fluids. Gold concentrations in the shear zone material are low, in the region of 10ppb Au.

Immediately adjacent to the shear margins is a well developed 5m wide zone of sericite-carbonate alteration. Here carbonate is subordinate to sericite, indicating the reduced permeability of the wall rocks, relative to the shear, with respect to the late CO_2-rich fluids. The sericitic alteration within this zone, although pervasive, is less intense than that observed in the shear. Fine-grained secondary plagioclase crystals are abundant and minor quartz and disseminated pyrite are also present.

The serictic alteration described above gives way sharply to an approximately 5m wide outer halo of epidote-chlorite alteration which may be described as an equivalent to the propylitic zone observed in porphyry systems. The sharp contact between the two different alteration types is illustrated in Plate 10 and also demonstrates the colour contrast between the two types. The mineralogy within the propylitic zone is characterized by the assemblage epidote-chlorite-plagioclase-sericite, with the dominant mineral, epidote, comprising about 50% of the rock. Chlorite is extremely fine-grained and sericite

PLATE 11. Plates 11 A, B and C are a series of photomicrographs illustrating the changes in alteration assemblages and rock texture as one moves away from the shear zone, towards host rocks unaffected by the hydrothermal alteration.

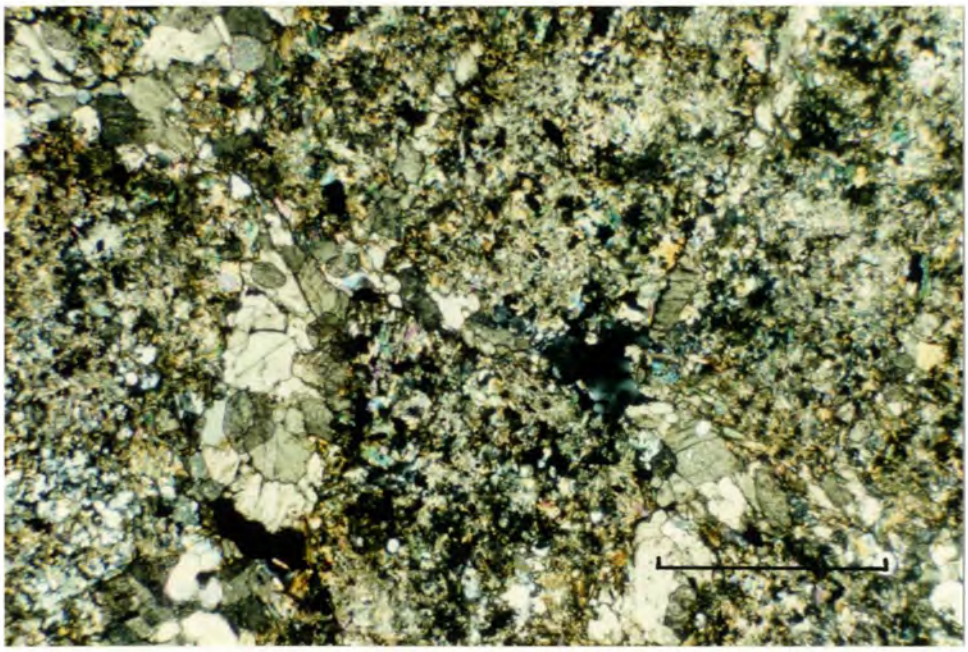

PLATE 11A. Sericite-carbonate alteration zone:- The rock consists essentially of sericite together with minor amounts of fine-grained muscovite and chlorite. Coarser late-stage carbonate veinlets are also common. (Bar scale = 0.5mm).

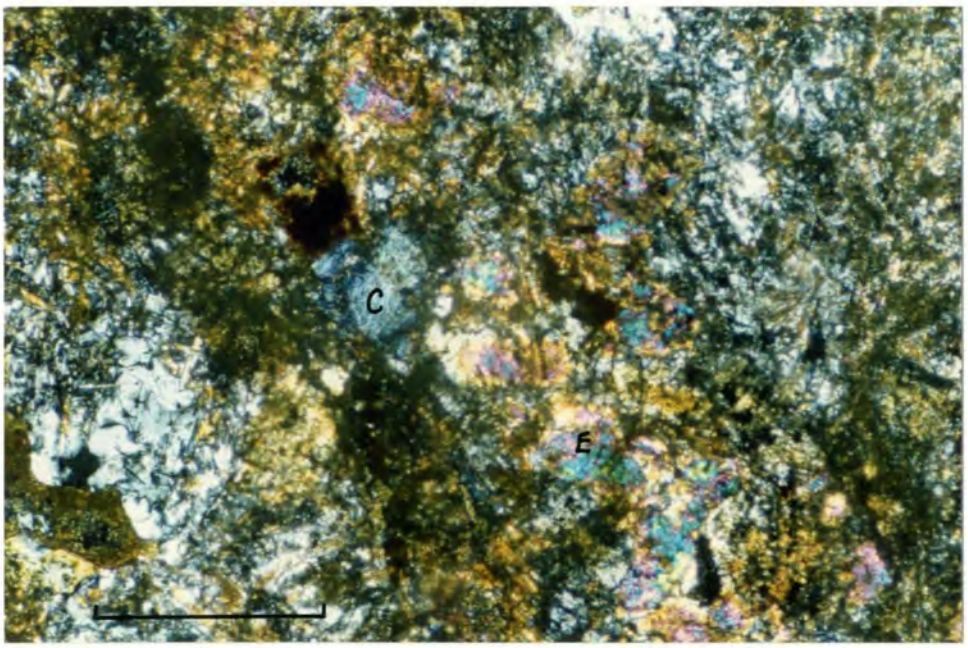

PLATE 11B. Epidote-chlorite alteration zone:- The rock typically shows a ferruginous staining and is dominated by the minerals epidote (E) and chlorite (C), together with lesser amounts of plagioclase and sericite. (Bar scale = 0.5mm).

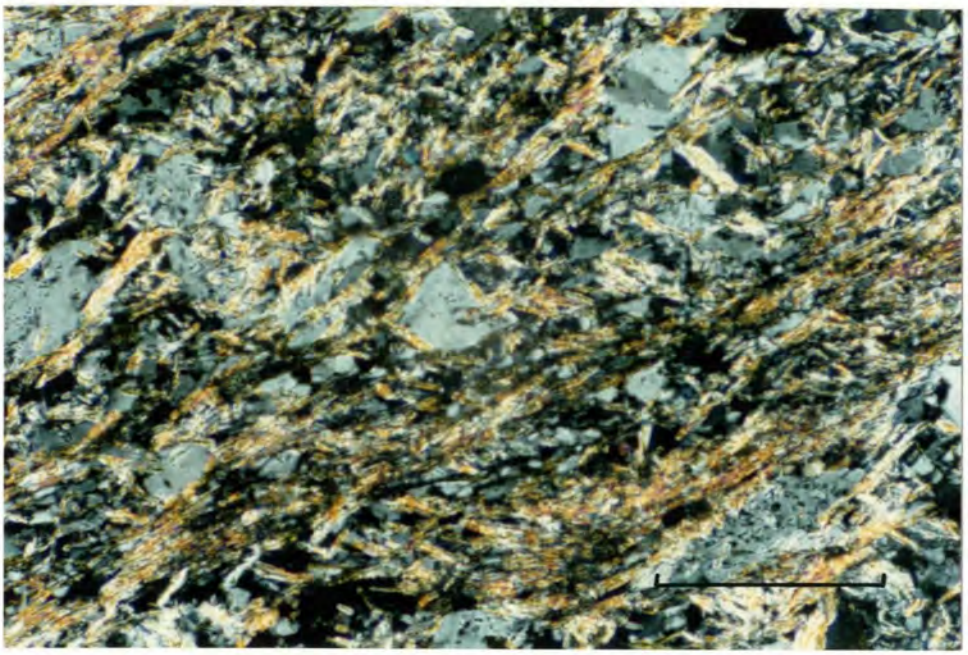

PLATE 11C. Unaltered host rock:- This is a sericite-quartz schist containing minor amounts of plagioclase, and is located approximately 50m away from the shear zone. (Bar scale = 0.5mm).

is much less abundant than in the sericitic zone. Fine-grained quartz is abundant, while carbonate occurs as a very minor constituent only, and this is reflected by a drop in the calcium content across the sericitic - propylitic boundary (**Fig. 9**). Geochemically, the propylitic zone is characterized by an enrichment in iron and magnesium relative to the unaffected host rock, while the strongest potassium enrichment is seen in the sericitic zone. The host rocks far removed from the shear zone, and unaffected by the shear associated alteration, comprise sericite-quartz schists and probably represent original argillaceous sediments. Feldspathization of the sericite-quartz schists is generally strongly developed and feldspar porphyroblasts may reach 1cm in length.

Plate 11 shows a series of three photomicrographs that illustrate examples of the sericitic alteration, propylitic alteration and unaffected host rock respectively. This gives an indication of the change in mineral assemblages and rock texture as one moves through the alteration zone into unaltered host rock.

4.2.4 Golden Dove Mine

The Golden Dove Mine is located on a well defined shear zone, striking 095° and dipping 55°S, hosted by schistose metalavas. Gold mineralization occurs in fine quartz stringers and veinlets within the shear zone and these returned a value of 7100ppb Au. Chemical changes associated with the shear related alteration are shown in **Fig. 10**. The shear zone material is strongly foliated and dominated by an assemblage of chlorite-carbonate-sericite-pyrite, with carbonate appearing as a late phase. Analysis of this material (excluding quartz veins) returned a value of 450ppb Au, and represents the highest gold value obtained from a shear zone hosting mineralized quartz veins. This is attributed to the fact that disseminated pyrite is particularly abundant in the Golden Dove shear (up to 5%) and probably hosts the gold recorded by the above analysis.

The alteration zone affecting the host rocks adjacent to the shear is poorly defined in this case and is recognized as a zone dominated by

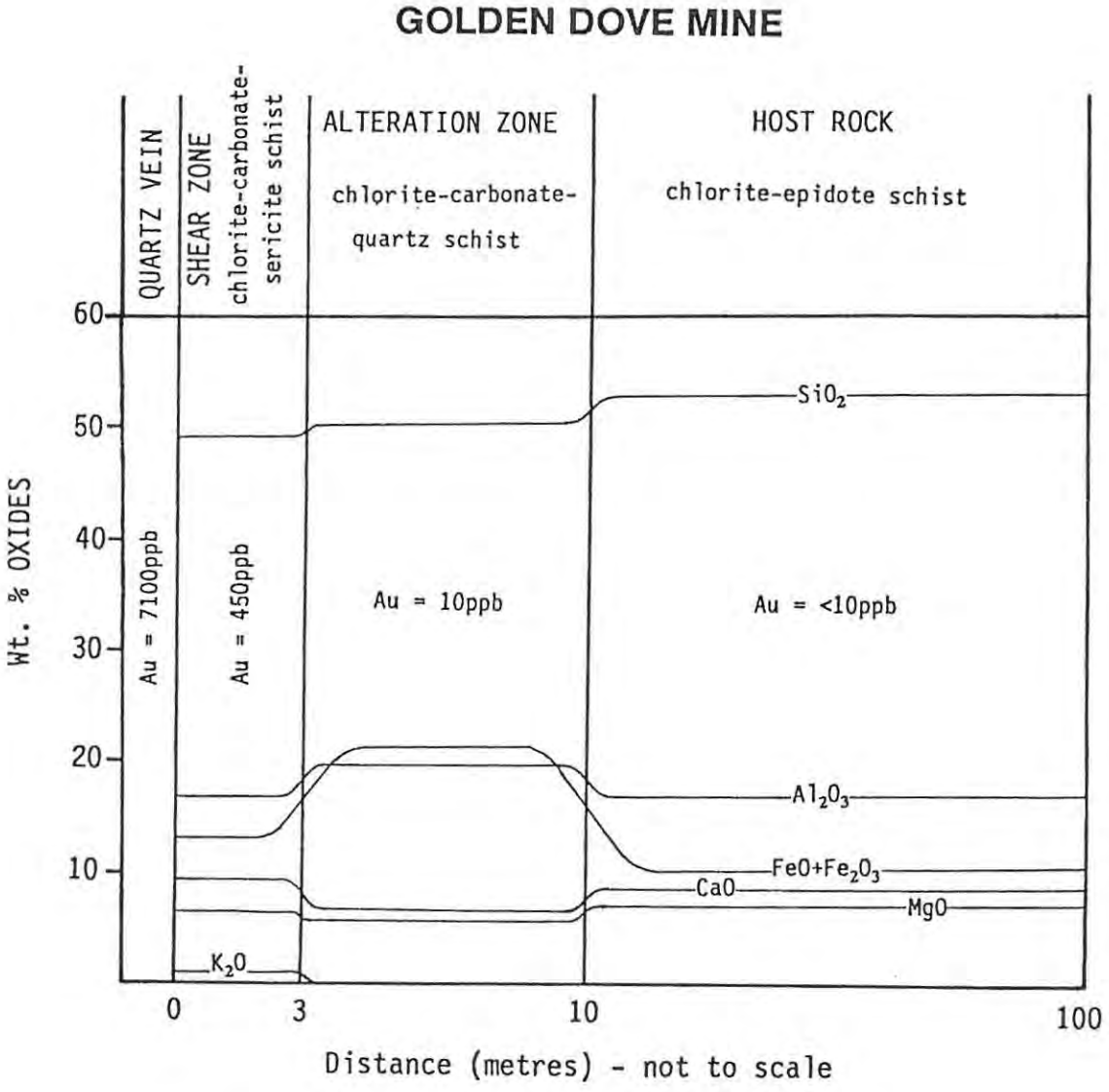

FIGURE 10. Chemical changes across strike at the Golden Dove Mine.

chlorite and carbonate, in the absence of sericite. Minor amounts of quartz are also present. This grades into unaffected host rock that may be described as a chlorite-epidote schist, showing minor feldspathization and carbonate alteration.

4.2.5 Buffalo River Mine

The Buffalo River Mine is located south of the exposed graphitic schist horizon shown in **Fig. 7** and is hosted by a sericite-quartz chlorite schist. Exposure in the vicinity of the mine is poor and it was not possible to examine underground exposures. Consequently geological controls on mineralization are not well constrained and a zone of shearing could not be defined. Nor was it possible to delineate an alteration zone associated with the mineralization, and hence a chemical diagram is not provided. The old workings are situated close to the eastern margin of a metagabbroic intrusion and mineralized quartz veins up to 70cm in width were observed in a shallow pit at the mine locality. These veins strike 086° and dip steeply to the south and the style of mineralization is somewhat different to that observed at the previously described localities. At Buffalo River Mine significant amounts of base metals are associated with the gold and the expression of mineralization at surface occurs as 'blobs' of gossan contained within quartz veins. The gossan enclaves vary in size from approximately 5 to 30cm in diameter and their quartz vein hosts show only slight deformation.

Carbonate alteration, in the form of siderite, is extremely intense and pervasive at this locality and, in places, has largely replaced the quartz vein material. This feature is shown in **Plate 12** from an outcrop exposed in the shallow pit and **Plate 13** shows a photomicrograph of siderite veinlets fragmenting and replacing quartz. The sideritic nature of carbonate is unique to the Buffalo River Mine, as all other mineral occurrences contain calcite as the dominant carbonate phase. The presence of siderite suggests that the late CO_2-rich fluids encountered a zone of iron-enrichment, thus precipitating siderite, and in this case, iron could have been supplied by pyrite contained within the sulphide enclaves in quartz veins. This may account for the

PLATE 12. Shows pervasive siderite alteration replacing quartz vein material at the Buffalo River Mine.

PLATE 13. Photomicrograph illustrating the replacement of quartz by siderite on a micro-scale. (Bar scale = 1mm).

seemingly preferential replacement of quartz vein material by siderite.

Gold mineralization appears to be confined to the gossan enclaves and thereby associated with the sulphide mineralization, it does not occur in pure quartz vein material. This is borne out by the following analyses:-

	NB-1	NB-4	NB-5	NB-6	
Cu	22345	14127	116	98	ppm
Pb	46	170	7	279	ppm
Zn	670	741	112	75	ppm
Ni	811	631	36	394	ppm
Ag	2	2	<1	<1	ppm
Au	1600	600	10	10	ppb

NB-1 = Gossan material from quartz vein.
NB-4 = Composite sample of gossan-bearing quartz vein.
NB-5 = Pure quartz vein material.
NB-6 = Quartz vein + siderite (no gossan material present).

4.2.6 Phoenix Mine

The Phoenix Mine represents an example of shear zone hosted gold mineralization located within the upper-amphibolite facies metamorphic terrane of the Tugela Group. The style of mineralization is similar to that described at the H.M.S., Champion Reef and Golden Dove mines, although gold-bearing quartz veins are generally thicker here (up to 75cm wide). The mineralized shear is hosted by a metagabbro and is approximately 3m in width, striking 097° and dipping between 60 and 70°S. **Plate 14** shows the dipping shear zone containing mineralized quartz veins outcropping above the entrance to an adit at the mine. The adit is developed for a distance of 120m along strike of the shear zone and Hatch (1910) reports a grade of 5.49 g/t Au over a width of 0.6m along the last 50m of the adit. This however could not be repeated during the present study and analyses of quartz vein material

PLATE 14. Shows the shear zone developed above the entrance to an adit at the Phoenix Mine. Mineralized quartz veins can be seen (marked with arrows). At Phoenix Mine gold-bearing quartz veins may reach 75cm in thickness.

returned a maximum value of 1000ppb Au, and the shear zone material (excluding quartz veins) assayed at 20ppb Au.

The chemical changes observed in a traverse across the shear are shown in Fig. 11. The shear zone material consists almost entirely of chlorite and biotite, with chlorite being dominant. Aggregates of fine-grained quartz are also present, as are minor amounts of epidote. No zone of alteration adjacent to the shear could be identified and the host rock is comprised by a medium-grained actinolite-clinozoisite-sericite metagabbro. The major chemical changes in the shear zone, with respect to the host rock, display a substantial loss in calcium and gains in silica, iron and magnesium. The calcium depletion is explained by the breakdown of actinolite and clinozoisite within the shear, resulting in the release and removal of calcium from the system. Iron and magnesium may also be derived from the breakdown of actinolite and are concentrated in the shear during formation of the new minerals chlorite and biotite.

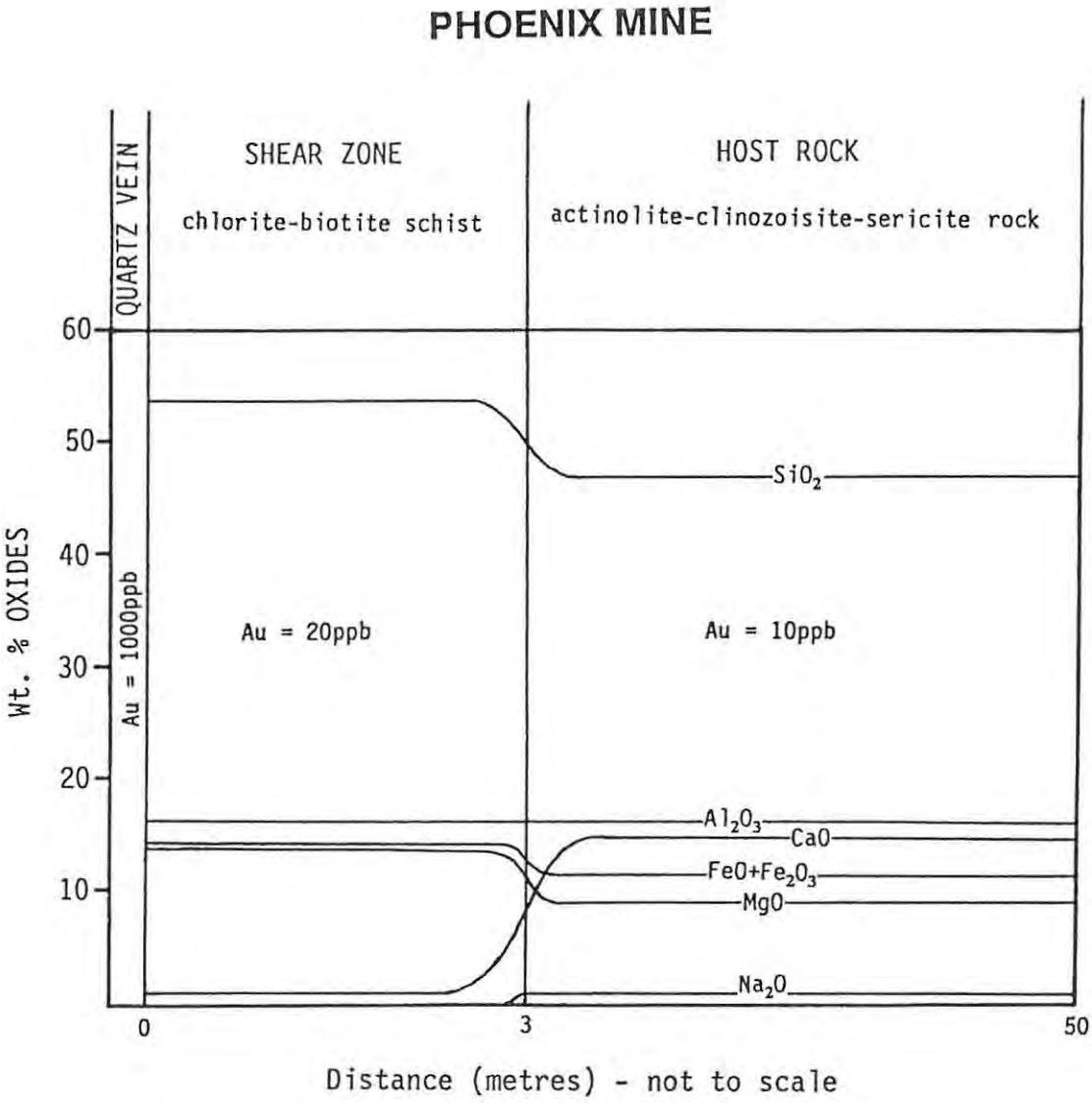

FIGURE 11. Chemical changes across strike at the Phoenix Mine. Note the absence, in this case, of an altered wall rock zone adjacent to the shear.

5. STUDY AREA B

The local geology of study area B is shown in Fig. 12 at a scale of 1:50 000 and is modified after mapping by Smalley (1980). The mineralized locality, studied in detail, is highlighted by the square on Fig. 12 and is represented by a sediment-hosted massive sulphide horizon of syngenetic exhaltive origin.

5.1 Structure, metamorphism and Age Determinations

Study area B, which forms part of the Tugela Nappe of the Natal Nappe Complex, is dominated by two lithologies, namely; amphibolites, that represent metamorphosed mafic lavas, and quartz-feldspar sheets, that represent metamorphosed psammitic to pelitic sediments. Smalley (1980) used the distribution and orientations of these quartz-feldspar sheets as a means to determining the gross structure of the area and a summary diagram of his findings is shown in Fig. 13 (to be viewed in conjunction with Fig. 12). Smalley (1980) recognizes at least three different deformational phases and describes them as follows:-

First Phase - D_1

These are tight to near isoclinal, generally flattened, flexural folds. They are reclined to semi-reclined with northwest to west dipping axial planes and are clearly defined by the thicker quartz-feldspar horizons. The large scale folding was confirmed by 'way-up' determinations from pillow structures, indicating a synclinal axis along the major fold closure defined by the outcrop pattern in Fig. 12.

Second Phase - D_2

The D_2 deformation is constituted by minor open upright, symmetrical, concentric folds with north-south trending axial planes and results in an antiformal structure trending north through the area (see Fig. 13). Fold axes plunge at shallow angles to the north and minor 'S' and 'Z' folds are found on the east and west limbs respectively.

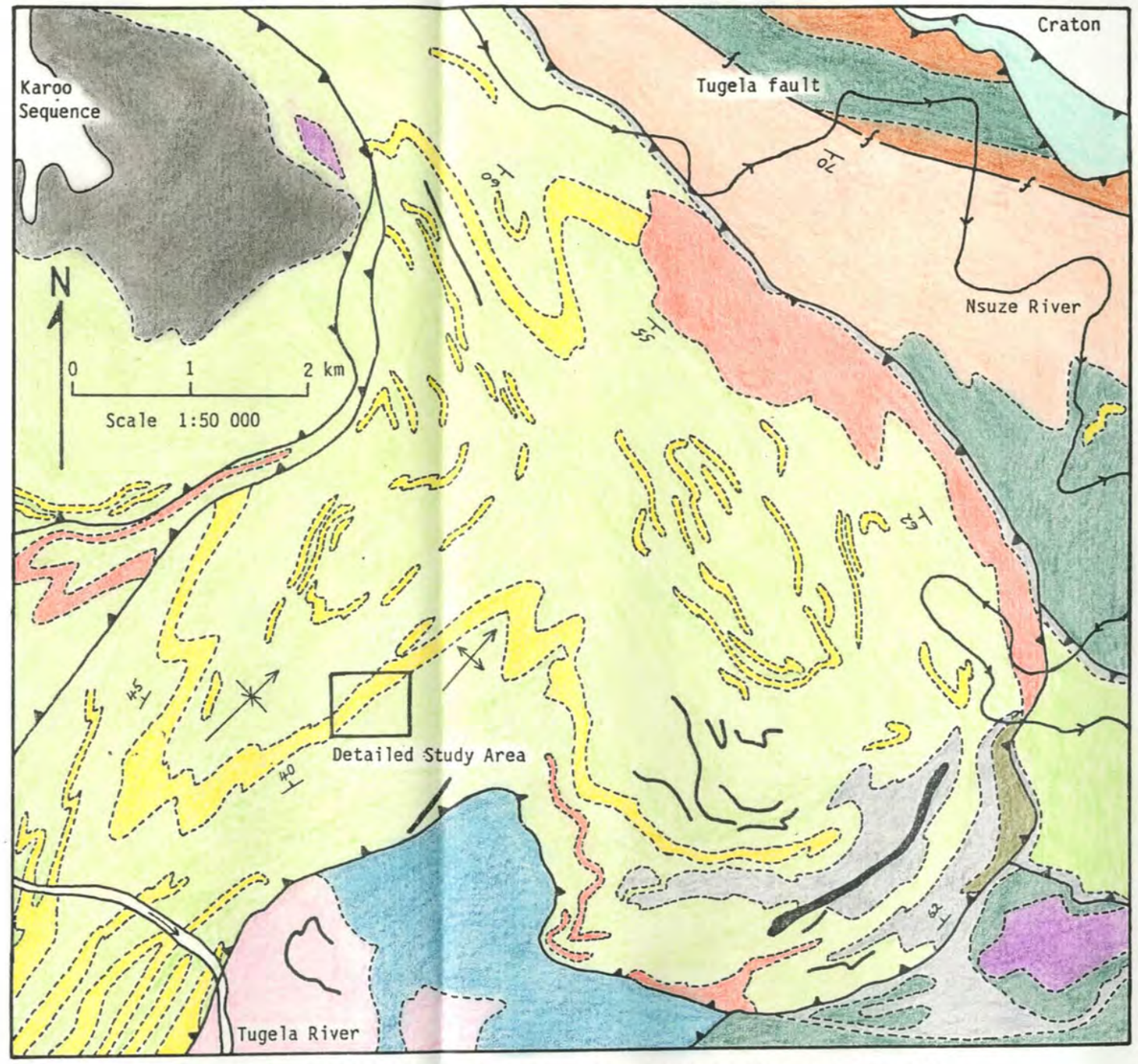

FIGURE 12. Geological map of study area B showing lithologies and major thrust faults. The locality of the detailed study area is highlighted by the square.

NATAL THRUST BELT	NATAL NAPPE COMPLEX		
	Tugela Nappe	Nkomo Nappe	Madidima Nappe
Group	Group	Group	Group
Ntingwe: conglomerate	Macala Complex	Halambu granite gneiss	Tugela: amphibolite, mica-garnet schist
Mfongosi: meta-argillite, metalava	hornblendite	Tugela: amphibolite	
	serpentinite		
	biotite-feldspar gneiss		
	Tugela: talc schist, magnetite quartzite, quartz-feldspar sheets, amphibolite		

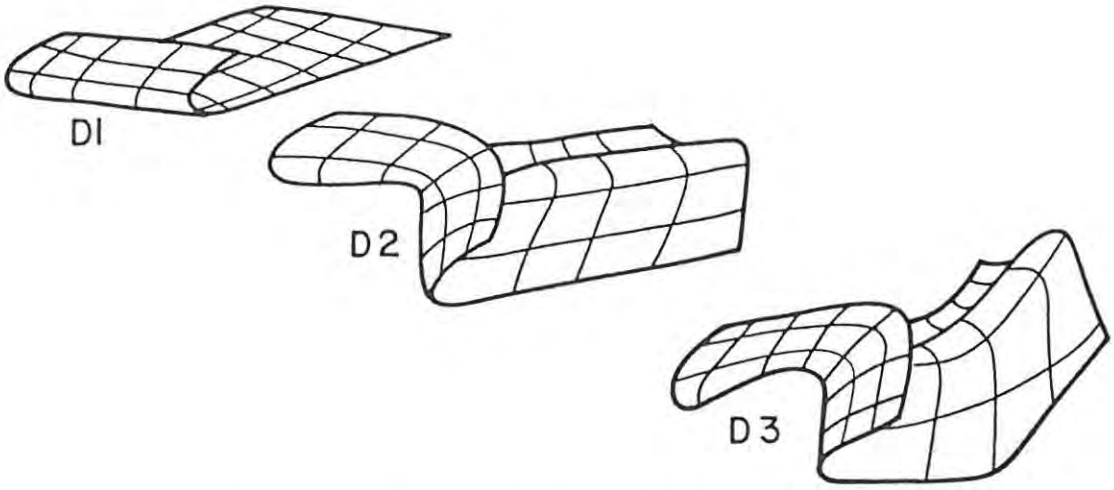

DIAGRAMMATIC SKETCH SHOWING
PROGRESSIVE STAGES OF DEFORMATION
(From Smalley, 1980)

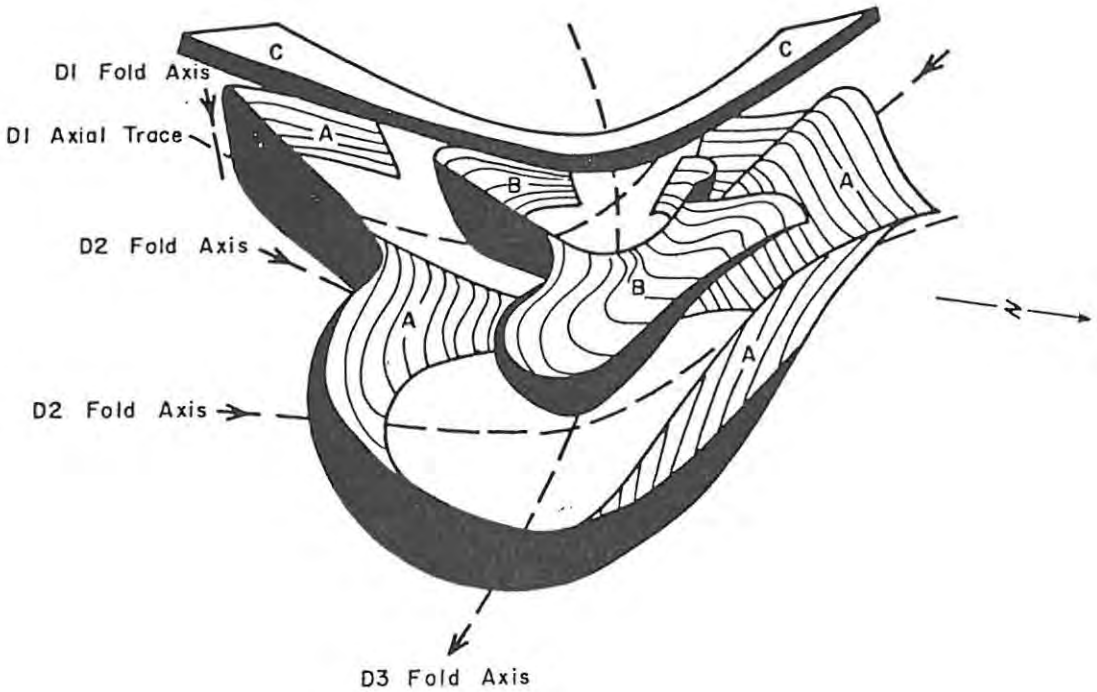

SCHEMATIC MODEL REPRESENTING THE STRUCTURE
OF THE TUMA FORMATION,
SHOWING D1, D2 & D3 DEFORMATION AXIS
(From Smalley, 1980)

A = Thicker quartz-feldspar horizon

B = Series of thin quartz-feldspar horizons from central part of study area B

C = Thrust fault to the west of study area B

FIGURE 13. Structural interpretation of study area B by Smalley (1980).

Third Phase - D_3

The axis of the antiform described above (D_2) appears to have been cross folded about an east-west axis, with the resulting structure representing a double plunging antiform (**Fig. 13**). Small scale crenulations, that may represent minor structures of this major east-west cross fold, plunge at shallow to moderate angles to the west on steep southerly dipping axial planes.

Harmer (1979) investigated the metamorphism affecting the present study area and points out that assemblages reflecting the peak metamorphism are infrequent because of the strong retrogressive metamorphic event produced by the later northward thrust movements. As a result, analyses of maximum P-T conditions were carried out using relict minerals no longer in clear equilibrium. Harmer (1979) assumes the following assemblages to have been stable at peak metamorphism:-

Pelitic rocks = kyanite + garnet + biotite + staurolite + quartz

Psammitic rocks = (i) muscovite + quartz
(ii) muscovite + quartz + biotite + garnet

Mafic rocks = blue-green hornblende + $anorthite_{30-36}$ + epidote

and demarcated the P-T field at peak metamorphism as 575 to 620°C at pressures in excess of 5.5 to 6.0 kbar. He also sets a lower limit of 350°C for temperature conditions during the retrogressive metamorphic event related to thrusting.

According to Harmer (1979) a Rb/Sr isochron age of 1218 Ma was obtained from a suite of metalavas within the present study area and was interpreted as dating the upper medium-grade metamorphic event, rather than representing the age of extrusion of the lavas. However, using the $^{87}Sr/^{86}Sr$ growth diagram, the low initial strontium ratio (0.7039) coupled with the low Rb/Sr ratio (0.29) of the suite, constrains the maximum possible age to 1425 Ma. This is significant as it implies that the amphibolites are clearly unrelated to to any of the Archaean metavolcanic formations exposed on the Kaapvaal Craton to

the north.

5.2 Detailed Study Area

Attention will now be focused on the geology and style of mineralization observed within the detailed study area. Fig. 14 provides a detailed geological map showing lithological variations and demonstrates the stratabound nature of the mineralized horizon.

5.2.1 Lithologies

The dominant rock types present include amphibolite, psammitic to pelitic quartz-feldspar horizons, thin magnetite quartzite units, a leucocratic fuchsite-bearing sheared horizon containing 10-50% pyrite and enhanced gold and silver values, and a biotite-chlorite-phlogopite schist unit. The following is a description of these lithologies and their possible modes of formation.

Amphibolite:

In general the amphibolites occur as fine- to medium-grained melanocratic rocks with partly foliated to massive textures. Hornblende and plagioclase occur in approximately equal proportions, together with minor amounts of quartz, epidote, biotite and pyrite. Chlorite is present as a retrogressive product of hornblende and is most strongly developed within, and close to, zones of shearing.

The amphibolites are considered to be derived from submarine mafic volcanism and they form the hosts to the psammitic to pelitic sedimentary horizons (Fig. 12), which in turn host the mineralization mapped in Fig. 14.

Psammitic to Pelitic Quartz-Feldspar Schists and Gneisses:

This unit is subdivided into various lithologically distinct zones and comprises most of the area mapped in Fig. 14. Quartz and plagioclase are the main minerals present, with plagioclase being subordinate to quartz. The more psammitic varieties may be described as quartz-feldspar-muscovite-biotite gneisses and are fine-grained and generally

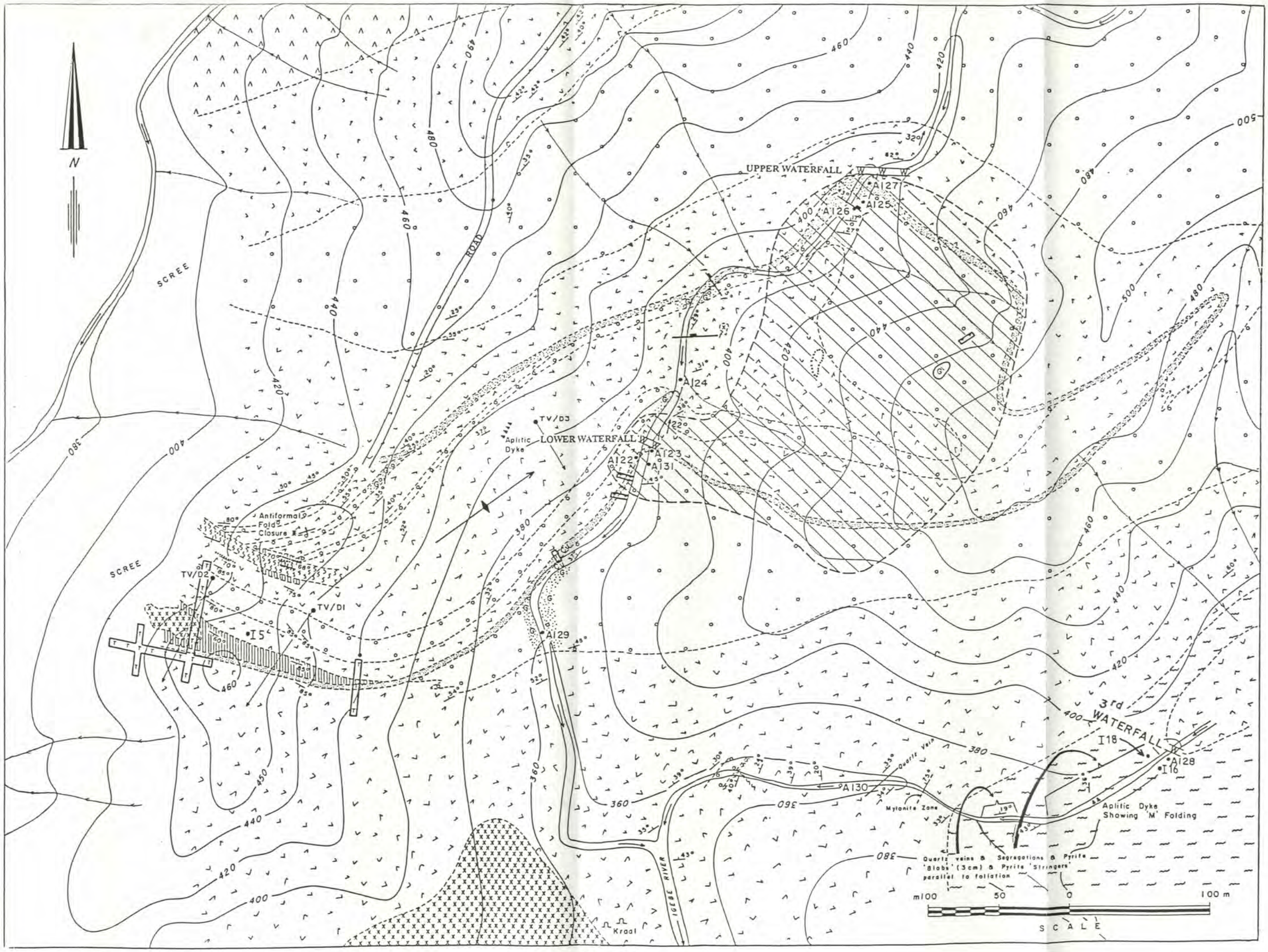
N
SCREE
ROAD
UPPER WATERFALL
A127
A125
A126
A124
TV/D3
Aplitic Dyke
LOWER WATERFALL
A122
A123
A131
Antiformal Fold Closure
TV/D2
TV/D1
I5
A129
SCREE
Kraal
IGJEE RIVER
3rd WATERFALL
I18
A128
I16
A130
Quartz Vein
Mylonite Zone
Aplitic Dyke Showing 'M' Folding
Quartz veins & Segregations & Pyrite 'Blobs' (3cm) & Pyrite 'Stringers' parallel to foliation
m100
50
0
100 m
SCALE

FIGURE 14.

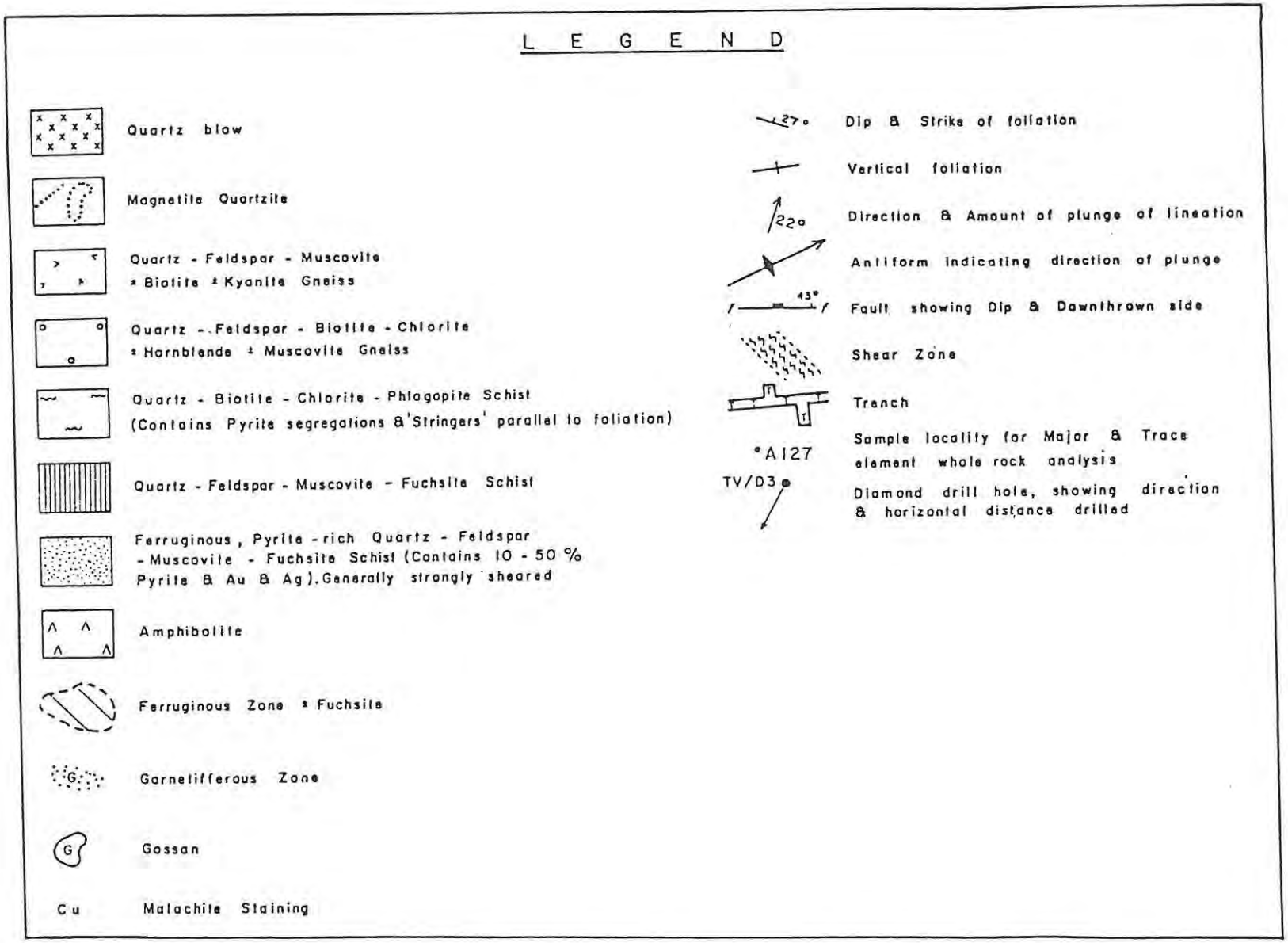

FIGURE 14. Geological map of the detailed study area showing lithological variations and the stratabound nature of the mineralized horizon.

poorly foliated. Accessory minerals include kyanite and sphene. The more pelitic varieties are also dominated by quartz and plagioclase but contain varying amounts of muscovite, biotite, chlorite, garnet, staurolite and kyanite, collectively comprising up to 20% of the rock. As the abundance of micaceous minerals increases with increasing pelitic character the rock can no longer be described as a gneiss and in places a strong schistose fabric is developed, with a gradation between the two end members. In the more pelitic members, Harmer (1979) describes large xenoblastic garnet crystals poikiloblastically enclosing small quartz, plagioclase, biotite and staurolite grains. Although garnet can form from pelites at moderate metamorphic grades, the presence of staurolite inclusions suggests that at least part of the garnet is derived from the breakdown of staurolite at higher temperatures by the reaction:-

$$\text{Staurolite} + \text{Quartz} \longrightarrow Al_2SiO_5 + \text{Almandine} + H_2O$$

Although this unit varies from psammitic to pelitic in composition it is considered to represent a single stratigraphic horizon within the metavolcanics, with the compositional variations being due to changes in composition of the sediment supply, e.g fluctuations in the clay content.

Samples A122-A131 (see **Fig. 14** and **Appendix A** and **B**) were plotted on a diagram proposed by de la Roche (1972) which distinguishes igneous from sedimentary rocks and serves to classify the rocks into broad catagories. The resulting diagram is shown in **Fig. 15** and consists of a rectangular plot employing three components only; Al, Na and K. Their choice is based on the general principals of geochemical opposition between magmatic and sedimentary formations. In the magmatic environment the two alkalis, Na and K, behave in a similar manner with regard to aluminium - a behaviour dominated by the feldspathic state. In the geochemical cycle on surface, dominated by the phyllitic state and by the intervention of the hydrosphere, sodium goes into marine waters, thus separating from potassium which alone remains linked to aluminium in common phyllites. The diagram exploits this contrast between magmatic and sedimentary formations and is

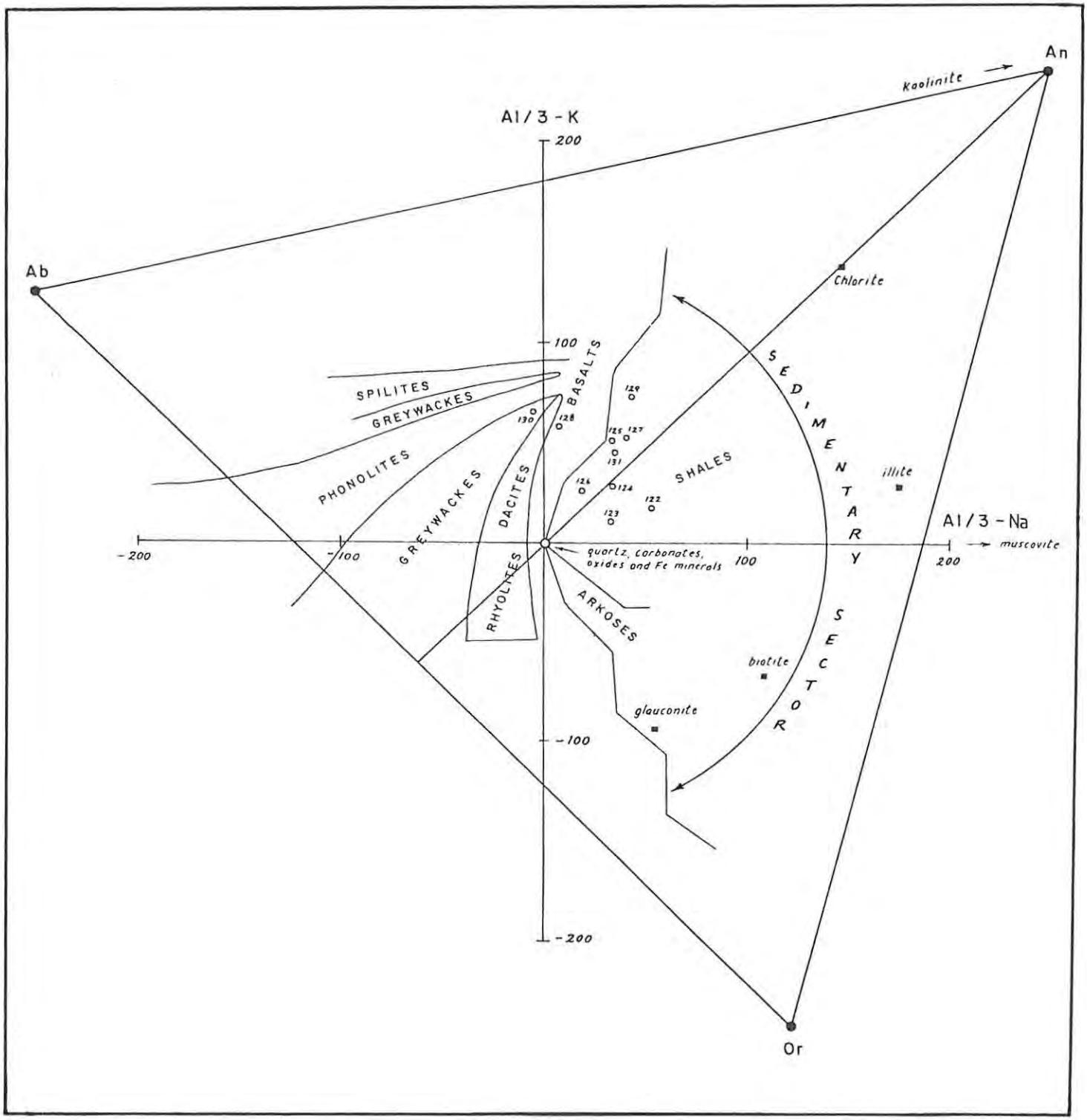

FIGURE 15. de la Roche diagram delineating major igneous and sedimentary rock types. The samples shown in Fig. 14 plot predominantly in the field of shales. (After de la Roche, 1972).

constructed from the parameters (Al/3)-Na on the abscissa and (Al/3)-K on the ordinate, calculated in milliatom-grams per 100g of rock material.

The feldspars An, Ab and Or are thus situated far from the origin of the axes, at the vertices of an almost equilateral triangle. On the other hand, all minerals that do not contain aluminium and alkalis are grouped at the origin (e.g. quartz, carbonates, oxides, iron ores etc.). All phyllitic minerals, with the exception of sodium montmorillonites, are distributed to the right of the ordinate and igneous minerals to the left (see **Fig. 15**). Evolved sedimentary formations stretch towards the right from the origin where the sandstones and limestones are located, to the clay zone where shales, argillites and carboniferous schists occur. The interference fringe between the igneous and sedimentary domains corresponds either to basic, little-evolved, clastic sediments, e.g. greywackes and arkoses, or to volcanosedimentary formations, both within igneous terranes.

All sample points, with one exception, plotted on **Fig. 15** fall within the fields of shale or greywacke, thus confirming a pelitic sedimentary origin. One sample plots within the basalt field and this may be taken as evidence for the volcanosedimentary nature of the sequence.

Sheared Leucocratic Sulphide-Bearing Fuchsitic Horizon:

This stratbound horizon contains the mineralization occurring in the detailed study area and comprises a stongly sheared quartz-feldspar-muscovite-fuchsite schist horizon approximately 2m wide and rich in sulphides. Fuchsite imparts a blueish-green colour to the shear zone and appears late in the paragenetic sequence. Fuchsitic alteration is probably a result of fluids moving through the shear zone and has also affected the host rock in the vicinity of boreholes TV/D1 and TV/D2 (**Fig. 14**). **Plate 15** shows a photomicrograph of this altered host rock, and fuchsite can clearly be seen replacing kyanite, indicating that the alteration is post-peak metamorphism. Pyrite concentrations within the shear vary between 10 and 50%, often grading into massive pyrite, and minor amounts of galena and sphalerite occur in the

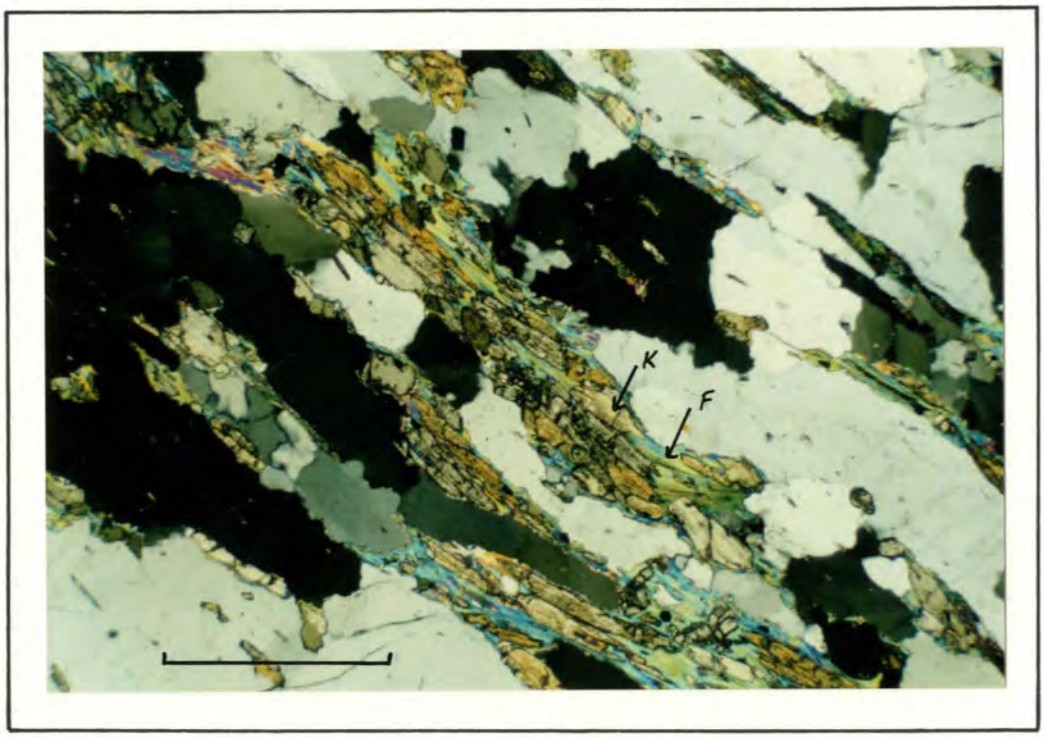

PLATE 15. Photomicrograph showing fuchsite (F) alteration replacing the metamorphic mineral kyanite (K). Fuchsite appears late in the paragenetic sequence and post-dates the peak of metamorphism. (Bar scale = 0.5mm).

massive sulphide domains. The mineralized horizon is poorly exposed along the sides of hills but may be traced along strike by occasional gossan outcrops. The best exposures are located in river beds where sulphides are still relatively unweathered and good examples of this are obtained at the upper and lower waterfalls (see **Fig. 14**). Enhanced gold and silver values were obtained from the shear zone and immediately adjacent host rock, and in particular are associated with massive sulphides.

Magnetite Quartzite:

Magnetite quartzite units occur as thin (1-2m thick) discontinuous lenses and may be traced for only a hundred metres or so along strike. They display a ferruginous staining and consist essentially of fine- to medium-grained quartz with disseminated magnetite and very minor garnet. Disseminated pyrite cubes are also visible in places. All magnetite quartzite units are developed in the hanging-wall to the sheared sulphide horizon and are considered to have originated as fine-grained cherty ferruginous chemical precipitates localized at, or near, exhalative vents and overlying the sulphide mineralization.

Biotite-Chlorite-Phlogopite Schist:

This rock type is seen outcropping in the southeast corner of **Fig. 14** as a dark coloured schist and contains abundant sulphide segregations up to 5cm in length that form lenticles parallel to the foliation and consist mainly of pyrite, with minor amounts of chalcopyrite. Numerous thin sulphide veinlets also occur parallel to the foliation. Thin quartz veins and segregations are common, and quartz and sulphide concentrations occur together. Where quartz and sulphide concentrations are high, the schist is strongly foliated and contains a high proportion of phlogopite. Minor amounts of tourmaline and andalusite are also present. **Plate 16** shows the mode of occurrence of the quartz and sulphide lenticles and veinlets. A poorly foliated, more massive, phlogopite-poor schist variety also occurs and contains only minor quartz and disseminated sulphides and accessory amounts of andalusite.

The sulphide-rich biotite-chlorite-phlogopite schist bears a strong

PLATE 16. Shows sulphide and quartz stringers and segregations in the footwall feeder zone. Sulphides consist predominantly of pyrite together with lesser amounts of chalcopyrite and up to 230ppb Au. The host rock is a biotite-chlorite-phlogopite schist.

PLATE 17. The massive, to semi-massive, sulphide horizon is seen here at the base of the lower waterfall. The river is flowing from right to left. The sulphide horizon is approximately 2m thick and can be recognized by the yellowish-orange colour it imparts to the rocks.

resemblance to the 'stringer' mineralization at the Maranda J Cu-Zn deposit in the Murchison Greenstone Belt, described by Maiden (1984). At Maranda J, the sulphide lenticles (pyrite-pyrrhotite-chalcopyrite-sphalerite) are interpreted as volcanogenic 'stringer' mineralization that has been transposed into foliation-parallel lenticles during deformation. The implications for the study area will be discussed in the following section.

5.2.2 Styles of Mineralization

The volcanosedimentary package, together with the development of magnetite quartzite horizons, observed in study area B represents a likely environment for the formation of volcanogenic massive sulphide deposits, and the sheared sulphide horizon mapped in the detailed study area is considered to be an example of this type of mineralization. Lithological mapping and geochemical sampling results strongly suggest a stratabound sediment-hosted exhalative origin for this mineralization and similarities can be drawn to the Maranda J (Maiden, 1984), Aggeneys (Ryan et al., 1986) and Gamsberg (Rozendaal, 1986) base metal deposits.

Mapping shows the mineralized shear zone to be stratabound and to have suffered the same deformational features as the surrounding host rock, indicating a pre-tectonic and probably syngenetic origin. The present disposition of the sulphide horizon outlines a major antiformal structure, with a northeast trending axial plane, affecting the central part of the area mapped in Fig. 14 and plunging at a shallow angle to the northeast. Both limbs of the fold dip to the northwest at about 40° and the antiform is considered to be a product of the D_1 deformation described by Smalley (1980).

Maiden (1984) describes sheared sulphide rock from the Maranda J copper-zinc deposit where the range of sulphide rock textures represented at the margins of the massive sulphide lens (from microbreccia to mylonite) indicates that there has been shearing along the interfaces between sulphide rock and silicate rock due to the competency contrast between the two rock types. A similar situation is

observed in the present study, and shearing is most intense at the margins of the sulphide horizon, decreasing in intensity towards the centre of the zone. The sulphide grain size also increases towards the centre of the zone where partial recrystallization has taken place. It is proposed that shearing took place during the D_1 deformation that produced the major anticlinal structure in the area.

Exposure of massive sulphides is best developed along strike south of the lower waterfall (**Plate 17**) and the horizon was extensively prospected for a strike length of 120m from the lower waterfall to the zone of malachite staining indicated on **Fig. 14**, with geochemical results supporting a volcanogenic exhalative origin. The following base metal, barium, gold and silver values were obtained over a 1m channel sample width along the 120m strike length investigated. Channel samples were situation 10m apart:-

	Cu	Pb	Zn	Ba	Au	Ag
HIGHEST/ppm	8341	17960	8103	11007	3.80	87.0
AVERAGE/ppm	2885	3236	1838	4320	1.25	27.0

The high base metal, barium and silver values obtained from the mineralized zone strongly suggest an element association similar to that found in large sediment-hosted syngenetic exhalative base metal deposits, e.g. the Aggeneys area in the north west Cape (Ryan et al., 1986). Although the grades are much lower in the study area, the environment of deposition appears to be very similar, with quartzofeldspathic gneisses, aluminous schists and gneisses, amphibolite and magnetite quartzite units also present in the Aggeneys stratigraphy. The Aggeneys Ore Formation which hosts the stratiform ore bodies may be described as a quartz-muscovite-biotite-sillimanite schist containing abundant feldspar, and is very similar to the sulphide host rocks in the study area. Although no barite ($BaSO_4$) was indentified, geochemical analyses show that barium is present in anomalous amounts within the sulphide horizon and the development of barite-rich layers would be expected in the hanging wall where conditions were more oxidizing.

The following is a brief summary, from Sangster and Scott (1976), of the proposed genesis of exhalative-type deposits. According to the exhalative concept, ore deposition takes place from hydrothermal solutions originating within the crust and rising along fractures or zones of weakness. In the present case, the fluids were likely to have been dominated by sea water as a result of circulation cells set up by rising mafic magmas which gave rise to the amphibolites. The passageway through which the fluids rose is preserved as an alteration pipe stratigraphically below the ore body, with extensive leaching, metasomatism and replacement by sulphides taking place within the pipe. Ore deposition takes place at, or near, the rock/sea interface between volcanic episodes and is contemporaneous with sedimentation. The actual locus of sulphide precipitation from the metal-bearing exhalations, whether at the fumarolic vent or further away, is dependant largely on the original salinity and temperature of the ascending fluid which dictates its mixing behaviour with sea water. Lower salinity and higher temperature fluids will precipitate closer to the fumarolic vent than higher salinity and lower temperature fluids.

The biotite-chlorite-phlogopite schist unit containing sulphide segregations and veinlets (described in chapter 5.2.1) is developed in the footwall to the sulphide horizon and is thought to represent a 'stringer' zone or feeder pipe for fumarolic emanations giving rise to the stratabound mineralization above. The passage of fluids through this zone has given rise to a strong alteration assemblage consisting of biotite-chlorite-calcite-phlogopite and minor amounts of tourmaline, and the zone is characterized by an increase in magnesium (samples I-16, I-18, A128 in **Appendix A**) relative to the host quartz-feldspar-muscovite gneiss. The original semi-pelitic character of the alteration zone is indicated by abundant fine-grained primary quartz and feldspar and the development of minor amounts of andalusite.Silica introduced by the pre-metamorphic mineralizing fluids forms medium-grained veins and segregations and is associated with the sulphides.

Gold is enriched in the feeder zone up to 230ppb, indicating that the mineralizing fluids were also gold-bearing and gave rise to the gold

mineralization associated with the massive sulphide horizon (i.e. gold was not introduced into the sheared massive sulphides as a result of an epigenetic event related to metamorphism, but forms part of the syngenetic mineralizing event).

Large et al. (1988) discuss the genesis of gold and its distribution in some volcanogenic massive sulphide deposits in Australia and they recognize two distinct spacial and mineralogical associations of gold:-

1) A gold-zinc association (together with lead and silver) which typically occurs throughout the massive ores, with gold concentrated in the stratigraphic hanging wall of the deposit.

2) A gold-copper association which typically occurs in the footwall stringer zone.

Fig. 16 shows the variation in gold grade with stratigraphic level at the Hellyer Zn-Cu-Au deposit in eastern Australia. The deposit shows a well developed metal zonation, with iron and copper enrichment at the base of the massive sulphide and zinc, lead, siver and gold enrichment at the top. Gold averages 2.3 g/t in the massive sulphide body but reaches 4.0 g/t in the pyritic silica cap which overlies the baritic horizon. A similar situation is preserved in the present study area where a lead-zinc-silver-gold association occurs in the massive sulphide horizon with average gold and silver values of 1.25 and 27.0 g/t respectively over a strike length of 120m (as described earlier). The sulphide association in the stringer zone consists of pyrite and chalcopyrite only, with pyrite being vastly dominant. Gold enrichment in this zone is in the region of 20 to 230ppb.

Large et al. (1988) consider the two gold associations outlined above to be directly related to different gold transport mechanisms. Under the hydrothermal conitions considered likely for volcanogenic massive sulphide formation, gold may be transported as a bisulphide complex or as a chloride complex according to the following reactions:-

$$4Au^0 + 8H_2S + O_2 \text{ ---> } 4Au(HS)_2^- + 2H_2O + 4H^+ \quad .....(1)$$

and

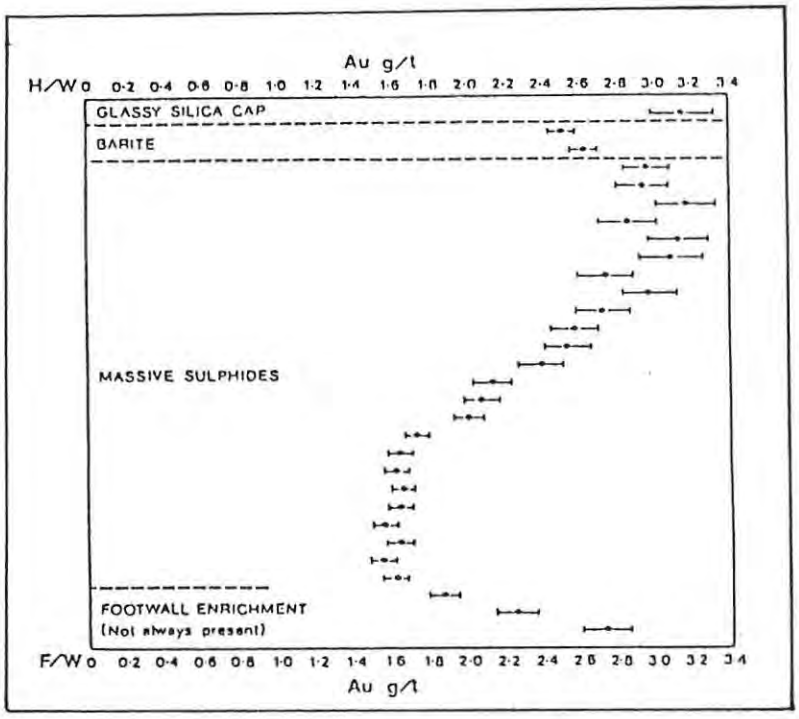

FIGURE 16. Variation in gold grade with stratigraphic height at the Hellyer Zn-Cu-Au deposit in eastern Australia. (After Large et al., 1988).

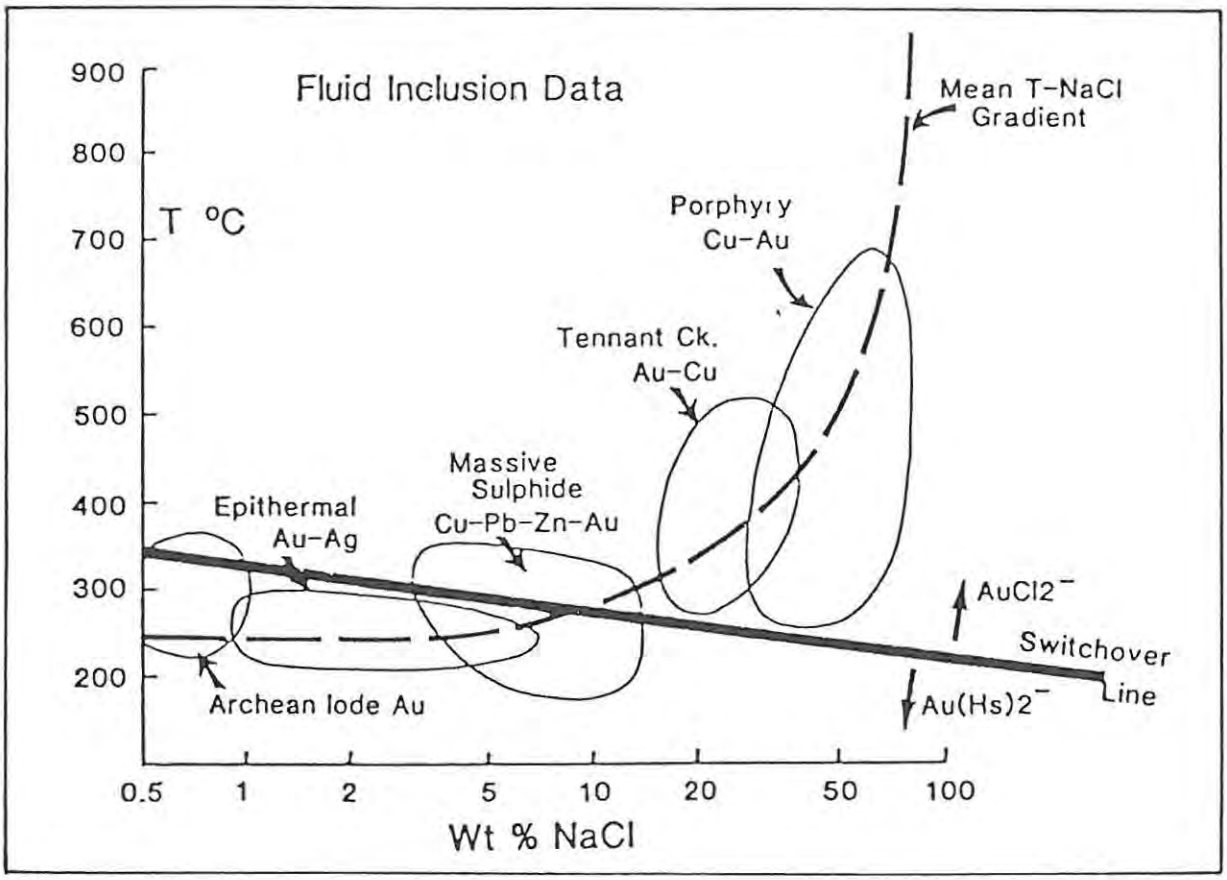

FIGURE 17 Fields of temperature-salinity for a range of common gold-bearing ores showing the split into $AuCl_2^-$ transport, and $Au(HS)_2^-$ transport fields. (After Large et al., 1988).

$$4Au^0 + 4H^+ + 8Cl^- + O_2 \text{ ---> } 4AuCl_2^- + 2H_2O \text{ .....(2)}$$

The relative importance of these two complexes in the ore fluid is controlled by temperature, aH_2S, pH, fO_2 and salinity, as defined by the equation:-

$$aAuCl_2^-/aAu(HS)_2^- = (K_1/K_2)\ [(aH^+)^2\ (aCl^-)^2/(aH_2S)^2]$$

Where K is the temperature dependent equilibrium constant for the respective reactions.

Calculations by Large et al. (1988) show that gold transport as the $[AuCl_2]^-$ complex is favoured by high temperature fluids (>300°C) with high salinity (>seawater), low pH (<4.5), low aH_2S ($<10^{-2.5}$M) and moderate to high fO_2 (pyrite or magnetite stable), and favour the mutual transport and deposition of copper and gold. On the other hand, gold transport as the $[Au(HS)_2]^-$ complex is favoured by lower temperature fluids (150-300°C) with low salinity (<seawater), moderate to alkaline pH (>4.5), high aH_2S ($>10^{-2.5}$M) and moderate fO_2 (pyrite field only). The above authors also classify other gold deposits according to the gold-copper or gold-zinc association and point out that high temperature and high salinity hydrothermal systems, such as porphyry coppers, show a gold-copper association indicative of transport as the chloride complex. Lower salinity, lower temperature and neutral pH hydrothermal systems, such as epithermal Au-Ag and most Archaean lode gold deposits, show the gold-zinc association indicative of bisulphide complexing. Fig 17 shows that various gold deposit types may be classified according to a spectrum of temperature and salinity conditions and these dictate the type of complexing involved in gold transport.

Huston and Large (1989) present a model to explain the concentration of gold in volcanogenic massive sulphide deposits and their model is shown in Fig. 18 and outlined below:-

Stage 1

In the early, low temperature stages of massive sulphide deposition,

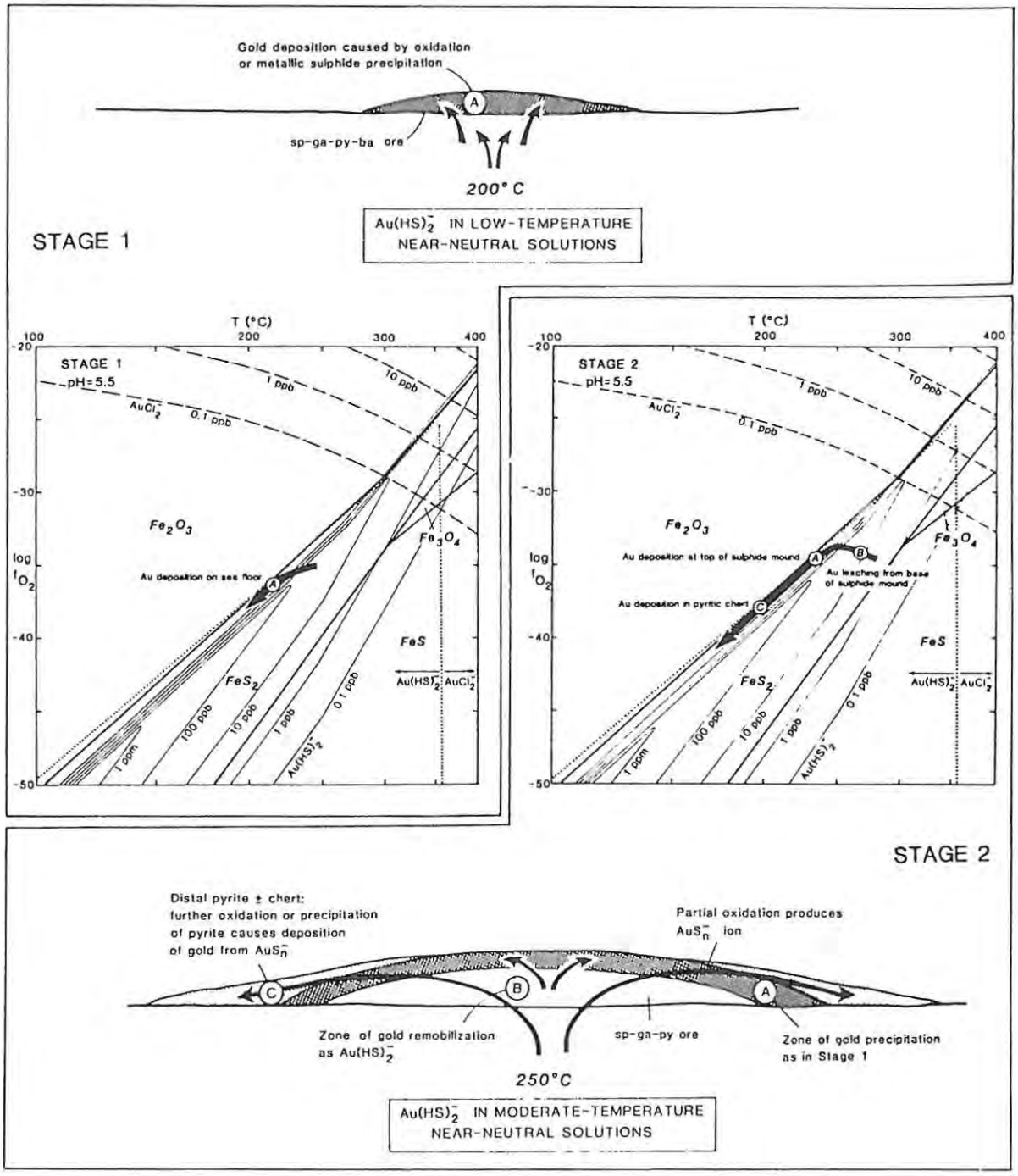

FIGURE 18. Geochemical model of gold transport and deposition in volcanogenic massive sulphide deposits. (After Huston and Large, 1989).

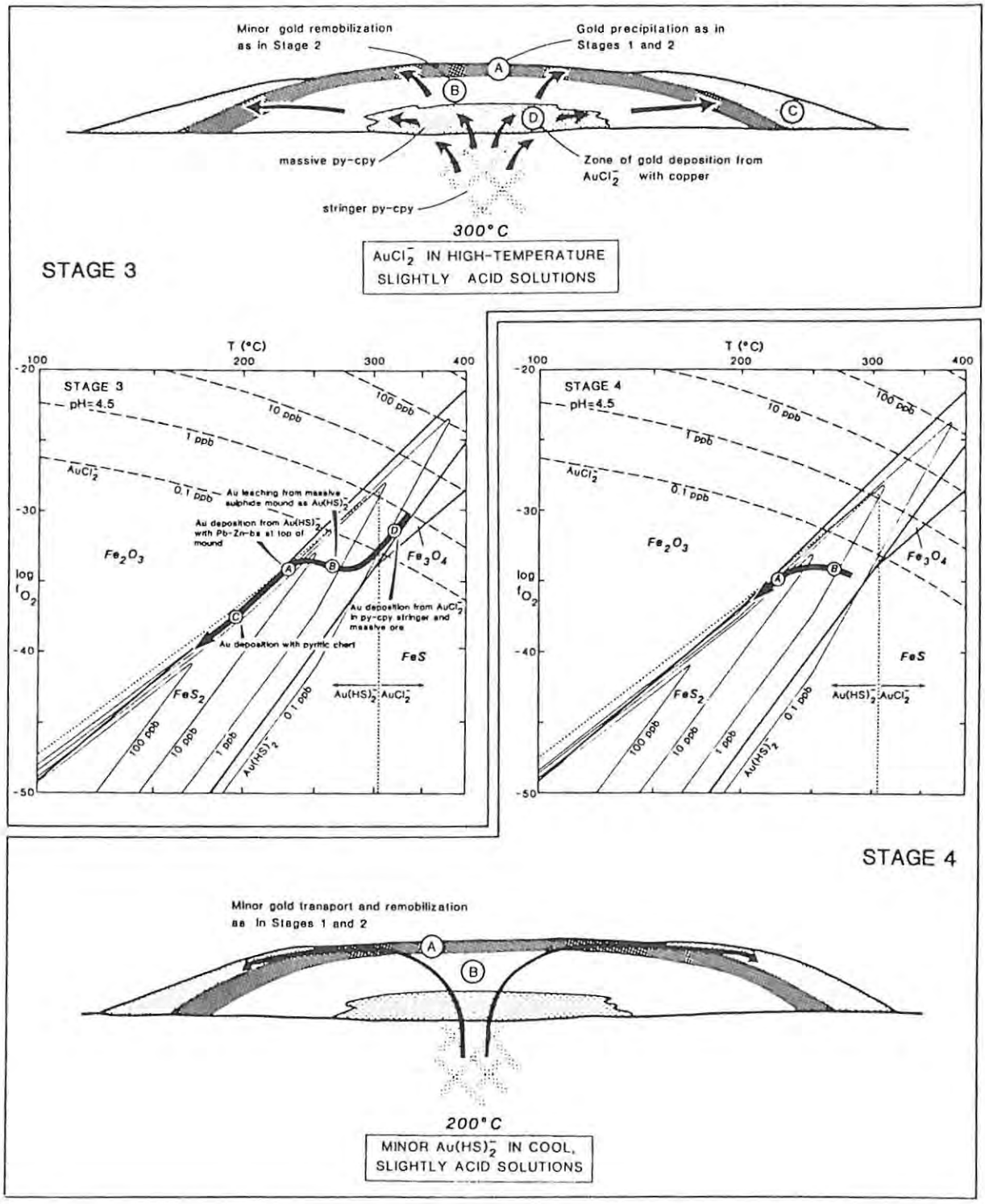

FIGURE 18. (continued)

gold (as $[Au(HS)_2]^-$) is transported with silver, lead and zinc (all as chlorocomplexes) to the seawater interface where all metals are deposited. Precipitation of lead, zinc and silver is caused by cooling when the hydrothermal fluids mix with seawater. Gold, however, precipitates by oxidation of the fluids caused by mixing and precipitation of metallic sulphides (point A), and both processes reduce the activity of reduced sulphur. Since $[Au(HS)_2]^-$ transport is favoured by near neutral pH, high grade gold ore is favoured in deposits where there is evidence of near neutral fluids in or around the massive sulphide ore (e.g. significant feldspar or carbonate gangue).

Stage 2

As the fluids warm and the sulphide mound grows, gold is mobilized as $[Au(HS)_2]^-$ from the base (point B) and deposited near the top, or in the barite zone (point A), again by a reduction in the activity of reduced sulphur caused by the precipitation of metallic sulphides. Partial oxidation of reduced sulphur caused by mixing with seawater may produce partially oxidized sulphur species which may then mobilise gold as an $[AuS_n]^-$ complex where $n>2$. This gold may be transported and deposited in the distal parts of the massive sulphide by continued oxidation or precipitation of pyrite (point C).

Stage 3

As the fluids continue to warm, gold will become less soluble as $[Au(HS)_2]^-$, and when temperatures reach 300°C, pyrite-chalcopyrite ore begins to replace sphalerite-galena-pyrite ore, with the higher temperatures allowing gold transport as the chloride complex. As this replacement proceeds, pH increases and temperature and fO_2 both decrease, causing gold precipitation (point D). Gold solubility as $[AuCl_2]^-$ increases with decreasing pH, therefore enhanced gold grades, together with copper, will occur in deposits precipitated from more acid and saline hydrothermal fluids, as indicated by the presence of kaolinite gangue. When the hydrothermal fluids migrate up through the mound and cool to a point where sphalerite and galena are again precipitated, transport switches over from $[AuCl_2]^-$ to $[Au(HS)_2]^-$ and the processes described in stages 1 and 2 apply as pH and fO_2

increase.

Stage 4

As the hydrothermal system wanes and fluid temperatures cool, gold transport returns to $[Au(HS)_2]^-$ and the processes described in stages 1 and 2 apply.

In conclusion, it would appear that the mineralization occurring within the detailed study area represents an, as yet unrecognized, example of syngenetic, sediment-hosted, volcanogenic exhalative massive sulphide mineralization with significant gold enrichment. During the scope of this study it has become apparent that the environment of mineralization is similar to other deposits of this type, e.g. Aggeneys base metal deposits and the Maranda J Cu-Zn deposit. The mineral associations and the occurrence of gold also conform well to the observations made by Large et al. (1988) and Huston and Large (1989), although further work is needed to better define the zones of gold enrichment.

6. STUDY AREA C

6.1 Petrography and Local Geology

The local geology of study area C (Fig. 4), together with the location of the Nkunzana Mine, is shown in Fig. 19. The old mine workings are situated on a well defined shear zone, striking 100° and dipping 70°S, developed within quartz-biotite-muscovite schists of the Mfongosi Group. The mineralized shear zone is located approximately 200m north of the Tugela fault. The fault is not considered to have influenced mineralization in any way since it is very late in the geological history of the area and displaces Karoo Sequence formations, although it is possible that this major structural lineament has been reactivated at times during the geological evolution of the area.

Granite gneiss and amphibolites of the Nkomo Nappe are exposed to the south of the Tugela fault, and these formations are highly defomed and show evidence of partial melting. Anatexis and migmatization is displayed by the amphibolitic formations and extensive quartzofeldspathic sheets (up to 10m thick) intrude the amphibolites. These sheets are believed to have been derived from partially molten granite gneiss material that was injected into the amphibolitic horizons and show dramatic effects of folding related to the later deformation produced by northward thrusting of the nappe complex. Plate 18 shows an example of this deformation in which a quartzofeldspathic sheet is deformed into north verging folds by nothward movement, with detachment takeing place to form a miniature thrust and nappe structure.

6.2 Nature of Mineralization and Geochemistry

Surface exposure in the vicinity of Nkunzana Mine is very poor but access to underground workings is generally good. The underground development consists of four levels developed along strike of the shear zone with regularly spaced cross-cuts, thus facilitating

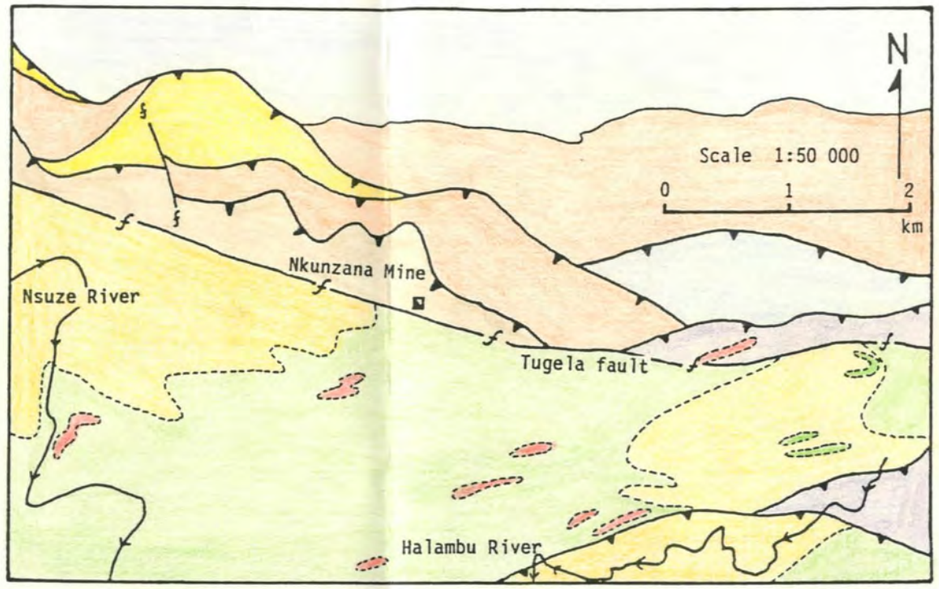

FIGURE 19. Geological map of study area C showing lithologies, major structural features and the location of Nkunzana Mine.

CRATONIC SEQUENCES	NATAL THRUST BELT	NATAL NAPPE COMPLEX
Group	Group	Group
Nsuze — quartzite and schist	Ntingwe — conglomerate and grit	quartzofeldspathic sheets
granite gneiss	Mfongosi — quartz-sericite schist; chlorite, quartz-chlorite schist	Tugela (Nkomo Nappe) — amphibolite
		Halambu granite gneiss

PLATE 18. Shows northward verging folds, highlighted by the quartzofeldspathic sheet, and developed in response to the northward obduction of the Natal Nappe Complex. The host rock is amphibolite of the Nkomo Nappe.

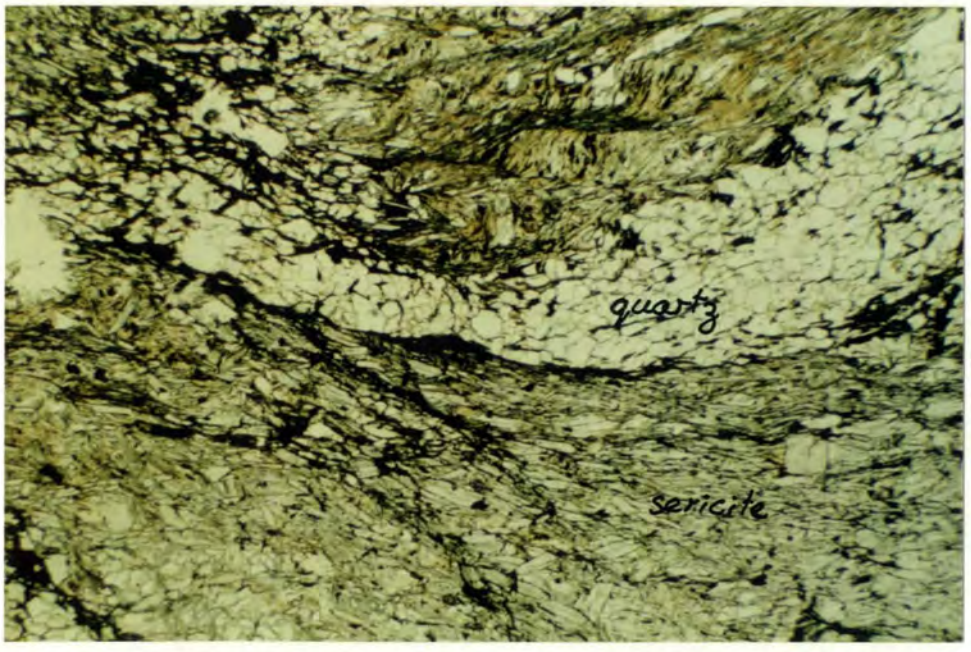

PLATE 19. Photomicrograph illustrating the intense sericitic alteration that characterizes the shear zone mineral assemblage at Nkunzana Mine. Segregations of fine-grained quartz (as seen here) may be common in places but are not ubiquitous. (Bar scale = 0.5mm).

sampling of the shear zone and adjacent alteration zone. Samples of unaffected host rock were obtained from core at a diamond drill site situated approximately 120m south of the shear zone.

The mineralized shear zone, exposed underground, varies in width from 2 to 3m and parallels the regional foliation. The rock within this zone exhibits a very strong schistose fabric, is highly weathered, displays a ferruginous staining, and the style of mineralization observed here is almost identical to that described at the Champion Reef Mine (chapter 4.2.3). Gold occurs in thin (up to 1cm thick) relatively undeformed quartz veins that parallel the shear fabric and a maximum value of 1300ppb Au was obtained from this shear-hosted quartz vein material. Thin section examinations show that strong sericitic alteration has taken place in the shear zone and fine-grained quartz grains show strained extinction and are often fragmented. At Nkunzana the alteration appears to have developed alternating bands of quartz-rich and sericite-rich material, as shown in **Plate 19**, and a strong crenulation cleavage is apparent in the sericite-rich zones. Analysis of shear zone material returned a value of 30ppb Au.

Fig. 20 shows the chemical changes across strike, from mineralized quartz veins within the shear, through the alteration zone, and into the unaffected host rock. It was however not possible to determine the width of the alteration zones, adjacent to the shear margins, from underground exposures. The most striking features of **Fig. 20** are the strong depletion in silica as one moves into the shear zone and a large increase in potassium within the shear, relative to the unaltered host rock. The silica depletion (also noted in study area A) is ascribed to the mobilization of silica from the shear zone and adjacent alteration zone by the passage of hydrothermal fluids through the shear. Mineralization may result from deposition of this mobilized silica as gold-bearing quartz veins within the shear. The strong potassium enrichment results from the intense sericitic alteration developed in the shear (**Plate 19**) and is also associated with an increase in aluminium. Iron is also enriched in the shear zone and is manifested as a ferruginous staining, probably resulting from the weathering of disseminated pyrite.

NKUNZANA MINE

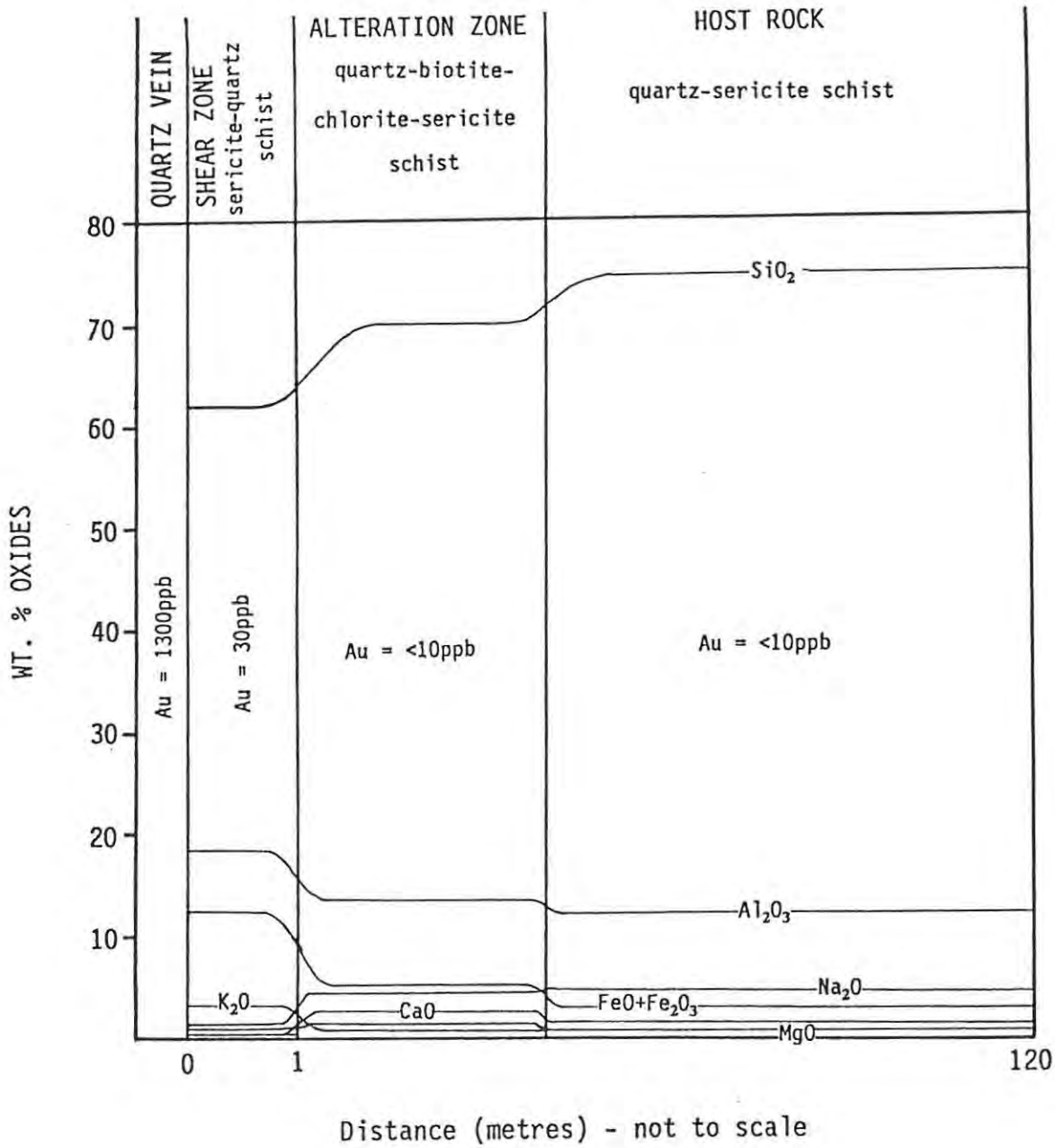

FIGURE 20. Chemical changes across strike at the Nkunzana Mine.

The alteration zone adjacent to the margins of the shear is characterized by chlorite, and is analogous to the propylitic zone developed at the Champion Reef Mine (chapter 4.2.3) although epidote is absent in this case. Sericite is minor and is thought to represent an original component of the metamorphic rock (i.e. it is not an alteration mineral). Carbonate is abundant as late-stage cross-cutting veinlets and finely disseminated pyrite is also present. It appears that thin fractures (thin section scale) are developed in the alteration zone and occur sub-parallel to the main shear zone, cross-cutting the regional foliation at a shallow angle. Where these fractures intersect a biotite-rich layer within the host rock, the biotite is partially replaced by chlorite.

The unaffected host rock consists of a quartz-sericite-biotite schist, with the micas concentrated into thin parallel layers defining the foliation.

7. STUDY AREA D

7.1 Local Geology and Mineralization

The location of study area D is shown in Fig. 4 and is situated within the Madidima Nappe. The mineralized occurrences in this area represent examples of shear zone hosted mineralization developed within the amphibolite facies Tugela Group rocks. Fig. 21 shows the local geology at a scale of 1:50 000, together with the two old workings investigated. The old workings are located within the Mbongolwane Flats, an area covered by eluvial overburden, and bed-rock exposures are almost non-existent except where access is available to underground workings.

The Madidima Nappe comprises mainly amphibolites derived from mafic volcanics and quartz-feldspar-biotite gneiss of sedimentary origin, while intrusive rocks into the nappe include serpentinites and metagabbros. The mineralization at both Rebellion Reef and Coopers Shaft is hosted by shear zones developed within metagabbro, and in this respect it is similar to the mineralization occurring at Phoenix Mine (chapter 4.2.6). The metagabbro host (sample R-1, Appendix A) consists of medium-grained hornblende porphyroblasts set in a fine-grained groundmass of strongly sericitized feldspar crystals that show a well developed triple-junction relationship. In places, sericitization has proceeded to the extent where feldspars are no longer recognizable and the groundmass is comprised by an extremely fine-grained mat of sericite. Biotite is abundant and is seen replacing hornblende, and quartz and sphene are present in more than accessory amounts.

Coopers Shaft:

The Coopers Shaft Mine consists of a vertical shaft and an unknown amount of underground development. Unfortunately the shaft has been largely filled in and access to the old workings is not possible. According to Hatch (1910) mineralization occurs as a northeast striking gold-bearing quartz vein, dipping 85°E, located in sheared metagabbro. The quartz vein varies between 0.41 and 0.91m in width and

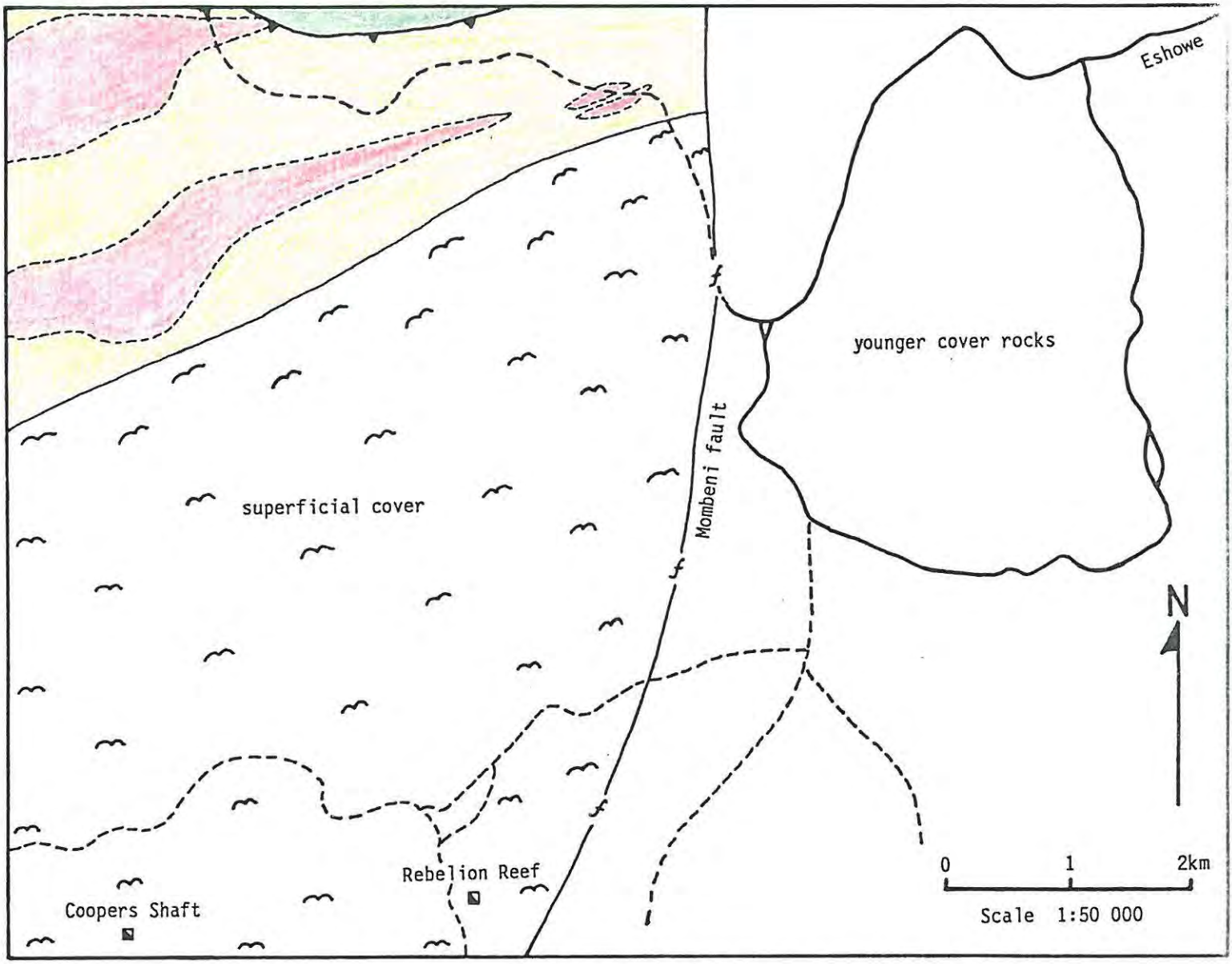

FIGURE 21. Geological map of study area D showing lithologies and the locations of mineralized occurrences.

NATAL NAPPE COMPLEX

Tugela Group

Madidima Nappe — amphibolite; biotite-feldspar gneiss

Nkomo Nappe — amphibolite

major roads

minor roads

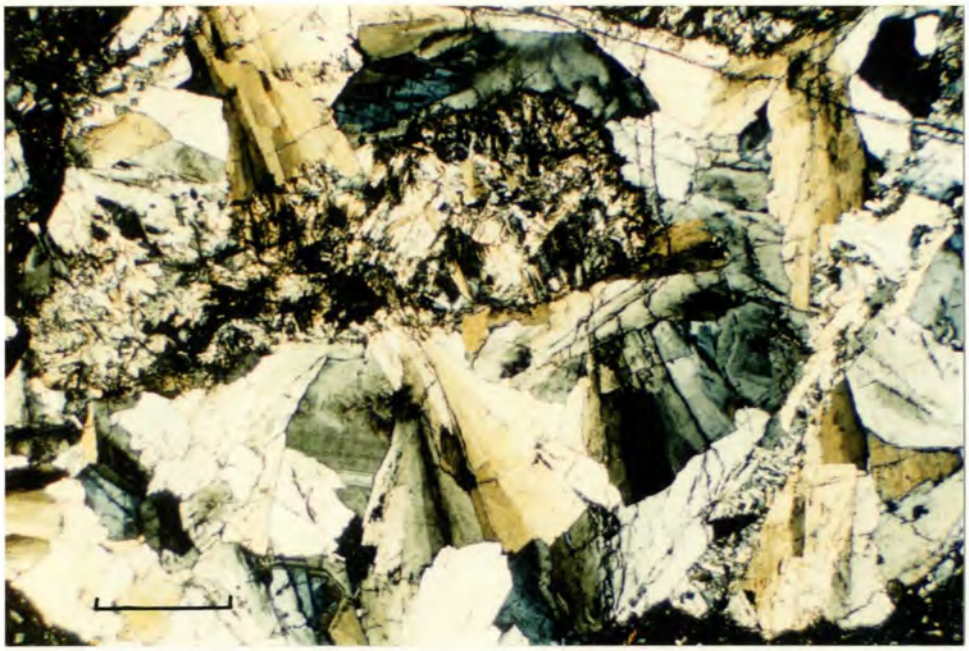

PLATE 20. Photomicrograph illustrating the highly strained and fragmented nature of quartz aggregates within the mineralized shear zone at Rebellion Reef Mine. (Bar scale = 1mm).

two samples collected by Hatch (1910) assayed at 40.28 and 50.57 g/t Au respectively. In the present study, quartz vein material containing pyrite, collected from a nearby dump, assayed at 2600ppb Au and 3.4ppm Ag. A sample of sheared metagabbro (sample C-3, **Appendix A**) containing abundant disseminated pyrite, from the same dump, assayed at 350ppb Au.

Rebellion Reef Mine:

The Rebellion Reef Mine consists of a single adit developed along a 1m wide shear zone striking 025° and dipping 75°E. The sheared metagabbro (sample R-3, **Appendix A**) consists of aggregates of fragmented quartz, showing extreme examples of strained extinction, surrounded by a groundmass of very fine-grained feldspar, sericite and chlorite. Minor amounts of epidote and finely disseminated pyrite are also present. **Plate 20** illustrates the fragmented nature and strained extinction shown by quartz aggregates in thin section (note that the section is slightly thick). Relatively undeformed quartz veins, up to 5cm in thickness, are developed parallel to the shear fabric and display a ferruginous staining. In places, pyrite segregations, up to 3cm in diameter, are developed within the veins and these are associated with a particularly ferruginous appearance of the surrounding vein material. However, assays of the sulphide-rich quartz veins returned values not exceeding 30ppb Au, while assays of the shear zone material returned values of <10ppb Au. It therefore appears that, although gold and sulphides are related to the same mineralizing event, they do not necessarily occur in direct association with one another.

8. FLUID INCLUSIONS

Samples of mineralized quartz vein material were selected from the Golden Dove shear zone for fluid inclusion studies. This material returned values of >7 g/t Au and displayed a slight ferruginous staining. Thin slices were cut, mounted on glass slides and ground to a thickness of 100 microns. Further preparation involved the polishing of both sides of the specimens. Numerous primary inclusions were present in all samples, with inclusion sizes varying up to about 30 microns in diameter. Trails of secondary inclusions were also common.

Heating and freezing measurements were carried out on primary inclusions and the data obtained are shown in **Figs. 22** and **23**. Melting temperatures (T_m) were recorded where, upon freezing and being allowed to heat up slowly, the last visible ice in the inclusion melted. The T_m values are used to calculate the equivalent wt. % NaCl of the inclusion using the phase diagram shown in **Fig. 24**, and **Fig. 25** shows a plot of salinities *vs.* homogenization temperatures (T_h). The average salinity measured lies in the range 4 to 5 equivalent wt. % NaCl and is consistent with a metamorphically derived hydrothermal fluid.

The homogenization temperatures shown in **Fig. 23** display a bimodal distribution with peaks at 150°C and 270°C respectively. This feature may be indicative of the existance of two fluid populations and may be significant in the genesis of the epigenetic gold occurrences. Craw and Koons (1989) describe tectonically induced hydrothermal activity and gold mineralization adjacent to major faults in New Zealand. They point out that some combination of meteoric fluid flow and rise of metamorphic fluids from deeper levels has been responsible for gold mineralization.

It may therefore be possible that the lower temperature T_h peak at about 150°C could represent meteoric fluids circulating in the highly permeable, sheared and foliated, thrust front (i.e. the Mfongosi

FLUID INCLUSION DATA

Melting Temperature (H2O)

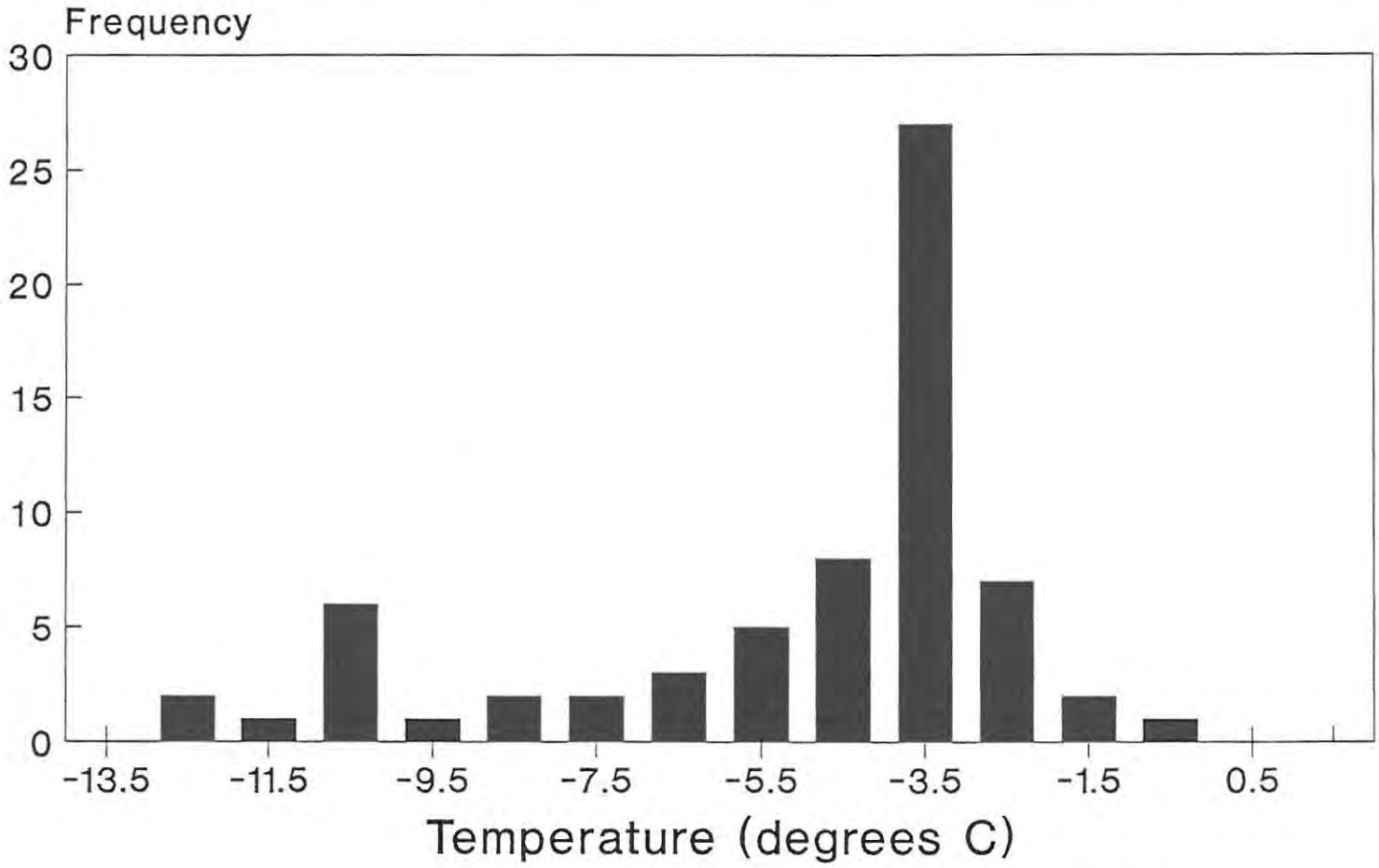

FIGURE 22. Histogram showing the distribution of melting point temperature measurements carried out on mineralized quartz vein material from the Golden Dove mine.

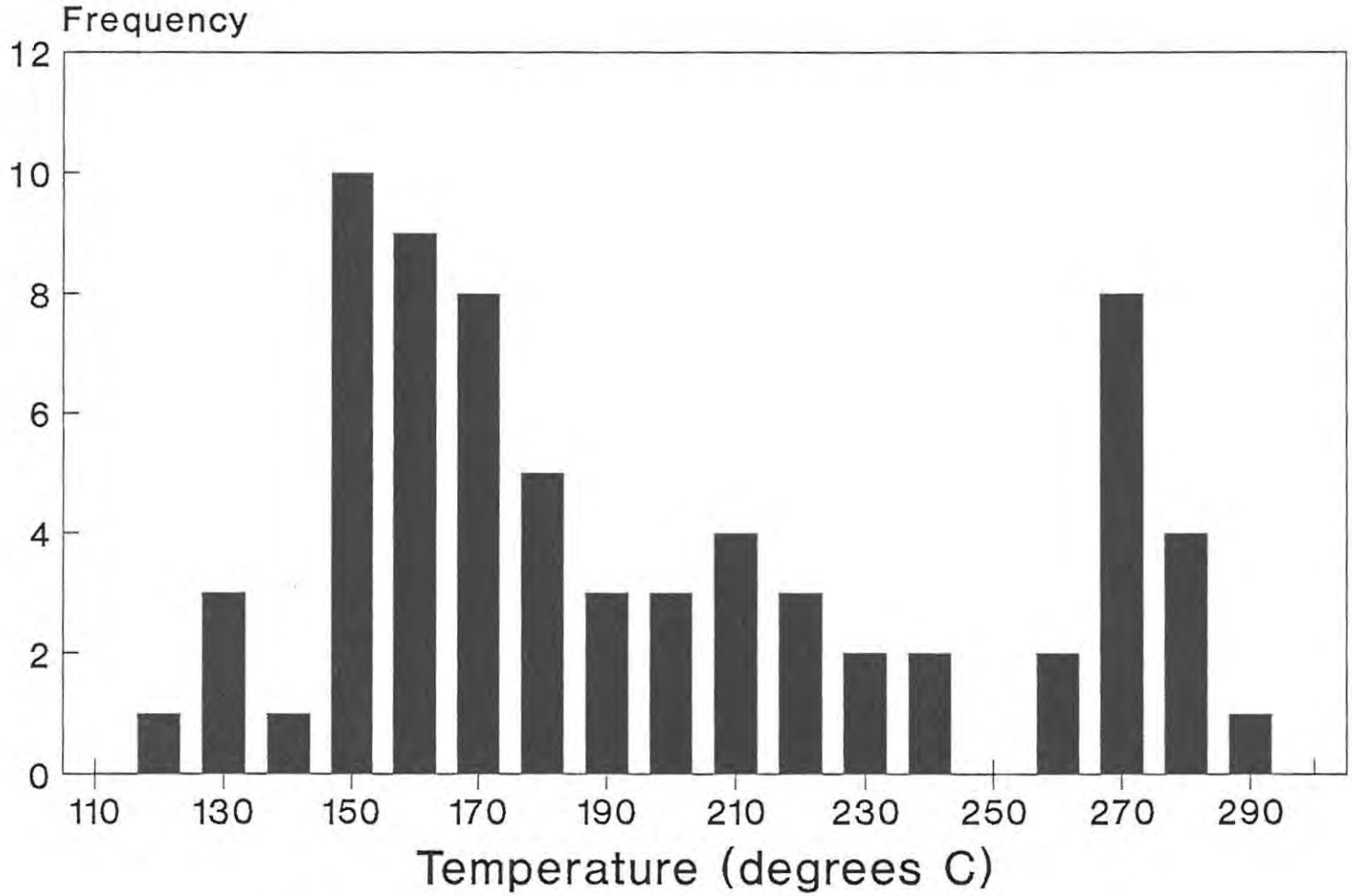

FIGURE 23. Histogram showing the distribution of homogenization temperature measurements carried out on mineralized quartz vein material from the Golden Dove mine. Note the bimodal distribution which may indicate the presence of both metamorphic and meteoric fluids.

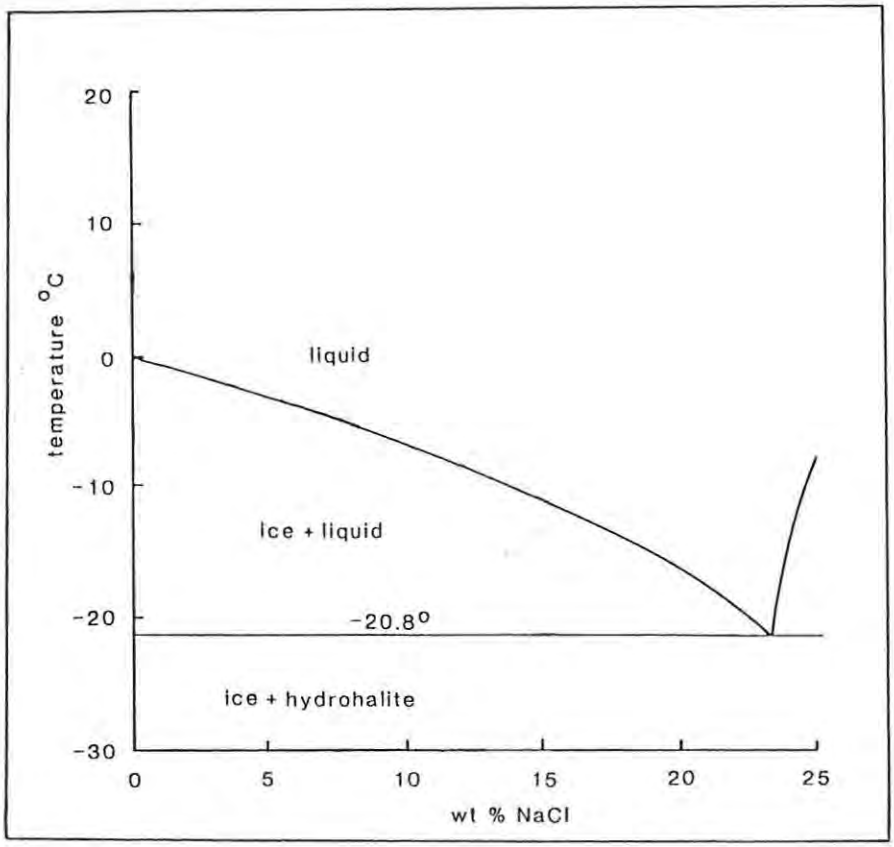

FIGURE 24. Diagram showing the temperatures at which major phase changes occur in an aqueous inclusion with varying NaCl concentration. T_m values were plotted on this diagram in order to obtain salinities in equivalent wt. % NaCl.

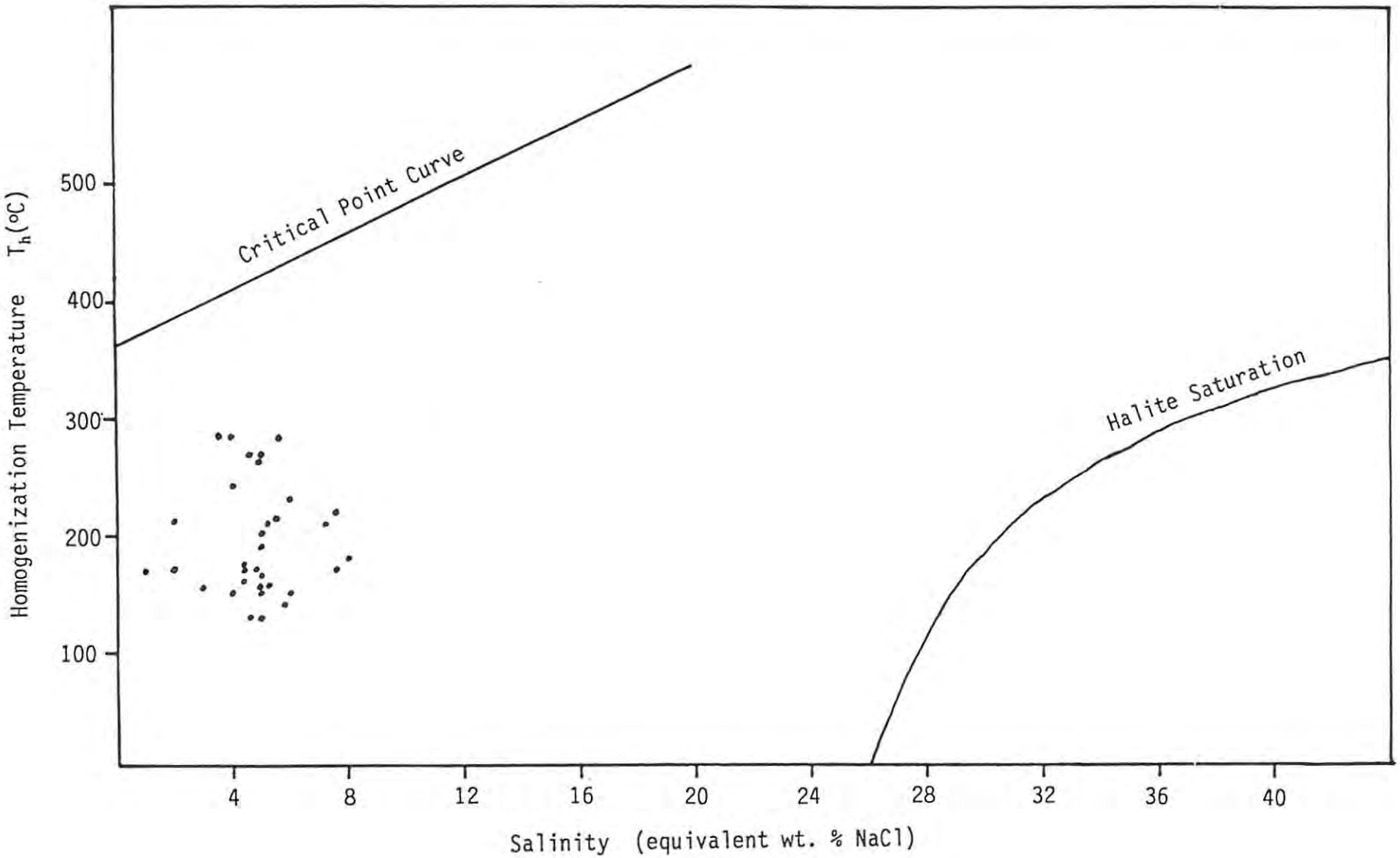

FIGURE 25. Shows the salinities of fluid inclusions from the Golden Dove mine plotted against homogenization temperature (T_h).

Schists), while the 270°C T_h peak may represent the mineralizing metamorphic fluids. The 'grey' area between the two peaks could identify a zone of mixing between meteoric and metamorphic fluids, and it is in this zone that gold deposition has taken place.

Fluid inclusion studies carried out at the syngenetic exhalative iThuma prospect proved to be inconclusive. Primary inclusions were particularly difficult to find and the results obtained were very similar to those outlined above. The average salinity was 5 equivalent wt. % NaCl, with a T_h peak at 280°C. It is therefore concluded that the upper-amphibolite facies metamorphism which has affected the area has destroyed the earlier syngenetic fluid signature.

9. CONCLUSIONS

In this concluding section attention will be focussed on the genesis of the epigenetic deposits already discussed, and an attempt will be made to relate this to the tectonic evolution of the Northern Marginal Zone. The relevant points to be borne in mind while developing a genetic model are:-

1) The fluids giving rise to the epigenetic mineralization appear late in the tectonic evolution of the area. That is to say, they post-date the last major deformational event which involved the northward obduction of the major thrust sheets.

2) The majority of gold occurrences in the Northern Marginal Zone are concentrated in the low-grade greenschist facies rocks of the Natal Thrust Belt.

3) Both the Natal Thrust Belt and the Natal Nappe Complex contain large volumes of mafic volcanics which could act as a gold source through the leaching of these rocks by metamorphic fluids. There is also some evidence to suggest that the tourmaline-rich horizons in the Natal Thrust Belt may have formed through syngenetic exhalative processes and are enriched in gold - thus providing a potential protore.

It is envisaged that the mineralizing fluids were generated as a consequence of the northward obduction of the Northern Marginal Zone onto the southern flank of the Kaapvaal Craton, and were channelled along the major detachment zones separating the various nappes. Fyfe and Kerrich (1985) describe the processes by which large volumes of fluids may be generated during thrusting. During the development of large-scale low-angle thrust faults the hotter base of the overthrust block comes to rest on the cooler top of the underthrust block, resulting in an inversion of the geothermal gradient at the boundary between the two blocks. This thermal disequilibrium may result in prograde metamorphism and devolatilization reactions within the upper

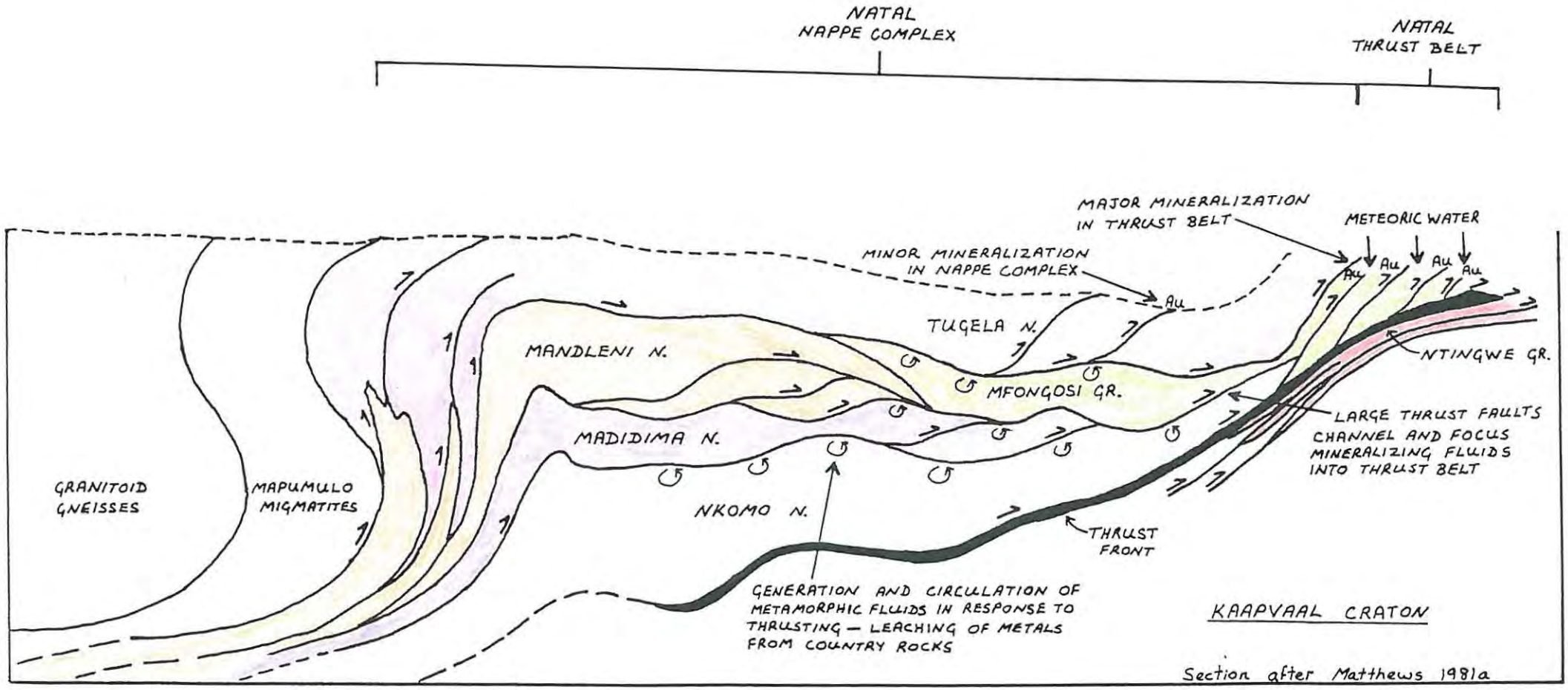

FIGURE 26. Schematic section to illustrate the genetic model proposed to account for the epigenetic shear zone-hosted gold mineralization.

portion of the cooler underthrust block. In addition, convective cells of circulating hydrothermal fluids may be set up in the underthrust block. Thermal expansion of the fluids during prograde metamorphism encourages hydraulic fracturing, thus increasing the permeability of rocks and facilitating fluid movement, allowing gold to be leached from a large volume of rock. In the case of the Northern Marginal Zone, the increased rock permeability may also tap metamorphic fluids generated during the peak of metamorphism, which occurred slightly earlier than the major thrusting event.

It therefore appears that thrusting played an important role in the genesis of these epigenetic gold deposits for the following reasons:-

1) It enhanced the production of hydrothermal fluids.

2) It gave rise to circulating hydrothermal fluids in the lower thrust blocks.

3) It resulted in an increase in the rock permeability through processes of thrusting, shearing and hydraulic fracturing - thus facilitating the movement of hydrothermal fluids.

4) The major detachment zones formed channelways through which the mineralizing fluids could be focussed.

The schematic section shown in Fig. 26 illustrates these processes. The mineralizing fluids migrated along the major thrust faults separating the nappes towards the lower temperature and pressure regimes of the thrust front. Here, gold and silica were deposited in subsidiary shears at the thrust front where the mineralized metamorphic fluids encountered cooler oxidizing meteoric fluids. This accounts for the observed concentration of gold occurrences in the Mfongosi Schists of the Natal Thrust Belt.

REFERENCES

Burger, A.J. and Coertze, F.J. (1975-76). Summary of age determinations carried out during the period April 1974 to March 1975. *Ann. geol. Surv. S. Afr., Vol. 11,* 317-321.

Cain, A.C. (1975). A preliminary review of the stratigraphic relationships and distribution of metamorphism in the northern part of the Natal-Namaquarides, South Africa. *Geologische Rundschau, Vol. 64,* 192-216.

Craw, D. and Koon, P.O. (1990). Tectonically induced hydrothermal activity and gold mineralization adjacent to major fault zones. *In: Keays, R., Ramsay, R. and Groves D., Eds., The geology of gold deposits: The perspective in 1988. Econ. Geol. Monograph 6.* 471-478.

de la Roche, H. (1972). Some chemico-mineralogical diagrams for the study of igneous and sedimentary associations and their metamorphic derivatives. *Science de la Terra, Vol. 17,* 31-46.

Eglington, B.M. and Harmer, R.E. (1984). Age and geochemical character of granitoids from southern Natal. *Abstr. Conf. Mid- to Late-Proterozoic Lithosphere Evolution,* PRU, 14-16.

------, ------ and Kerr, A. (1986a). Some geochemical constraints on the evolution of the crust in south-central Natal. *Extended Abstracts - Geocongress 86,* Geol. Soc. S. Afr., 781-786.

------, ------ and ------ (1986b). Petrogenetic, Rb-Sr isotope and geochemical characteristics of intrusive granitoids from the Port Edward - Port Shepstone area, Natal. *Trans. geol. Soc. S. Afr., Vol. 89,* 199-213.

------, ------ and ------ (1988). Development of Proterozoic lithosphere in Natal - Towards a model. *Abstracts - Geocongress 88,* Geol. Soc. S. Afr., 177-178.

------, Kerr, A. and Auret, J.M. (1988). The bearing of rare-earth element data on the genesis of the Natal Structural and Metamorphic Province. *Abstracts - Geocongress 88,* Geol. Soc. S. Afr., 175-176.

Fyfe, W.S. and Kerrich, R. (1985). Fluids and thrusting. *Chemical Geology, Vol. 49,* 353-362.

Harmer, R.E. (1979). *Pre-Cape geology of the Tugela Valley north of Kranskop, Natal.* M.Sc. Thesis (unpubl.), Dept. of Geology, University of Natal.

Hatch, F.H. (1910). Report on the mineral resources of Natal. Natal Government. 155pp.

Huston, D.L. and Large, R.R. (1989). A chemical model for the concentration of gold in volcanogenic massive sulphide deposits. *Ore Geology Reviews, Vol. 4,* 171-200.

Kroner, A. (1976). Proterozoic crustal evolution in parts of southern Africa and evidence for extensive sialic crust since the end of the Archaean. *Phil. Trans. R. Soc. Lond., Vol. A280,* 541-553.

Large, R., Huston, D., McGoldrick, P., McArthur, G. and Ruxton, P. (1988). Gold distribution and genesis in Palaeozoic volcanogenic massive sulphide systems, eastern Australia. *In: Goode, A.D.T. and Bosma, L.I., Compls., Bicentenial Gold '88, Extended Abstracts - Oral Programme,* Geol. Soc. Aust., 121-126.

Maiden, K.J. (1984). Metamorphic features of the Maranda J copper-zinc deposit, Murchison Greenstone Belt, Transvaal. *Trans. geol. Soc. S. Afr., Vol. 87,* 335-345.

Matthews, P.E. (1959). The metamorphism and tectonics of the pre-Cape formations in the post-Ntingwe thrust belt, S.W. Zululand, Natal. *Trans. geol. Soc. S. Afr., Vol. 62,* 257-324.

------ (1972). Possible Precambrian obduction and plate tectonics in southeastern Africa. *Nature, Vol. 240,* 37-39.

------ (1981a). Eastern or Natal sector of the Namaqua-Natal mobile belt in southern Africa, 705-715. *In:* Hunter,D.R., Ed., *Precambrian of the southern hemisphere.* Elsevier, Amsterdam, 882pp.

------ (1981b). A new tectonic model for the northern region of the Namaqua-Natal belt in Natal. *Abstracts - Geocongress '81,* Geol. Soc. S. Afr., 150-151.

------ and Charlesworth, E.G. (1981). Tectonics of the Natal Thrust Belt. *Abstracts - Geocongress '81,* Geol. Soc. S. Afr., 148-149.

McIver, J.R. (1966). Orthopyroxene-bearing granitic rocks from southern Natal. *Trans. geol. Soc. S. Afr., Vol. 69,* 99-117.

Nicolaysen, L.O. and Coertze, F.J. (1965). Note on an extensive zone of 1000 million-year old metamorphic and igneous rocks in southern Africa. *Sciences de la Terra, Vol. 10,* 497-516.

Plimer, I.R. (1987). The association of tourmalinite with stratiform scheelite deposits. *Mineral. Deposita, Vol. 22,* 282-291.

Rozendaal, A. (1986). The Gamsberg zinc deposit, Namaqualand district. *In: Anhaeusser, C.R. and Maske, S., Eds., Mineral deposits of southern Africa.* Geol. Soc. S. Afr., 1477-1488.

Ryan, P.J., Lawrence, A.L., Lipson, R.D., Moore, J.M., Paterson, A. and Stedman, D.P. (1986). The Aggeneys base metal sulphides deposits, Namaqualand district. *In: Anhaeusser, C.R. and Maske, S., Eds., Mineral deposits of southern Africa.* Geol. Soc. S. Afr., 1447-1473.

Sangster, D.F. and Scott, S.D. (1976). Precambrian, stratabound, massive Cu-Zn-Pb sulphide ores of North America. *In: Wolf, K.H., Ed., Handbook of stratabound and stratiform ore deposits - Volume 6,* Elsevier, Amsterdam. 129-222.

Slack, J.F. (1982). Tourmaline in Appalachian-Caledonian massive sulphide deposits and its exploration significance. *Institution of Mining and Metallurgy, Vol. 91,* B81-B89.

------, Herriman, N., Barnes, R.G. and Plimer, I.R. (1984). Stratiform tourmalinites in metamorphic terranes and their geologic significance. *Geology, Vol. 12,* 713-716.

Smalley, T.J. (1980). *Structure and metamorphism of the Tugela Group within the northern zone of the Natal Mobile Belt.* Ph.D. Thesis (unpubl.), Dept. of Geology, University of Natal.

Tankard, A.J., Jackson, P.A., Eriksson, K.A., Hobday, D.K., Hunter, D.R. and Minter, W.E.L. (1982). *Crustal evolution of southern Africa.* Springer - Verlag, New York, 523pp.

APPENDIX A

Appendix A lists some selected analyses illustrating important features such as shear zone, alteration zone and host rock compositions.

H.M.S. MINE

RAW DATA

	NH-2	NH-5	NH-7	NH-9	NH-10	NH-11	NH-17
SiO2	40.85	70.03	53.09	67.85	47.08	47.12	42.40
TiO2	2.96	0.90	0.62	1.22	1.64	2.04	4.55
Al2O3	9.36	12.78	22.19	12.86	17.07	15.33	16.73
Fe2O3	2.09	0.42	0.74	0.46	1.50	1.57	2.17
FeO	15.09	3.00	5.36	3.30	10.83	11.35	13.63
MnO	0.03	0.01	0.10	0.03	0.19	0.21	0.30
MgO	0.80	1.81	3.59	1.26	6.28	4.88	3.36
CaO	0.96	0.10	3.11	2.12	10.54	11.33	4.18
Na2O	3.45	0.46	2.22	2.16	0.78	0.52	1.01
K2O	0.44	4.41	3.77	2.22	0.05	0.10	1.98
P2O5	0.30	0.44	0.25	0.47	0.20	0.39	0.67
Cr2O3	0.00	0.07	0.05	0.03	0.09	0.05	0.01
NiO	0.00	0.00	0.00	0.00	0.01	0.01	0.02
H2O-	1.61	0.50	0.36	1.04	0.53	0.28	0.43
LOI	13.09	4.69	4.63	4.30	4.25	6.17	4.28
	91.03	99.60	100.08	99.32	101.06	101.37	97.72
Zn	26	6	64	38	109	101	209
Cu	42	3	23	67	243	115	216
Ni	8	3	22	37	89	55	39
Co	4	1	14	11	55	43	23
Ga	21	23	21	19	20	22	44
Mo	10	55	0	12	0	0	0
Nb	30	13	10	42	10	9	46
Zr	235	161	95	365	118	137	345
Y	7	2	10	80	29	36	76
Sr	164	66	311	131	283	297	102
Rb	2	55	139	42	1	2	40
U	0	28	4	19	0	0	10
Th	6	3	1	8	0	4	0
Pb	9	5	16	21	4	12	1
La	22	17	19	17	18	19	75
Ce	23	26	18	14	24	19	190
Nd	19	20	24	17	21	24	122
Te	25	26	22	20	26	25	20
Ba	877	3780	1518	1102	65	121	941
S	24282	5342	192	343	126	103	5270
As	39	30	10	27	7	5	10
Se	0	8	0	5	0	0	5
Ag	0.50	0.50	0.50	0.50	0.50	0.50	0.50
Au(ppb)	5	30	5	350	5	20	5

RECAL DRY

	NH-2	NH-5	NH-7	NH-9	NH-10	NH-11	NH-17
SiO2	53.52	74.16	55.83	72.20	48.91	49.65	45.59
TiO2	3.88	0.95	0.65	1.30	1.70	2.15	4.89
Al2O3	12.26	13.53	23.34	13.68	17.73	16.15	17.99
Fe2O3	2.74	0.44	0.78	0.49	1.56	1.65	2.33
FeO	19.77	3.18	5.64	3.51	11.25	11.96	16.80
MnO	0.04	0.01	0.11	0.03	0.20	0.22	0.32
MgO	1.05	1.92	3.78	1.34	6.52	5.14	3.61
CaO	1.26	0.11	3.27	2.26	10.95	11.94	4.49
Na2O	4.52	0.49	2.33	2.30	0.81	0.55	1.09
K2O	0.58	4.67	3.96	2.36	0.05	0.11	2.13
P2O5	0.39	0.47	0.26	0.50	0.21	0.41	0.72
Cr2O3	0.00	0.07	0.05	0.03	0.09	0.05	0.01
NiO	0.00	0.00	0.00	0.00	0.01	0.01	0.02
	100.00	100.00	100.00	100.00	100.00	100.00	100.00

CHAMPION REEF MINE

RAW DATA

	NC-2	NC-6	NR-1A	NR-1B
SiO2	52.89	40.70	52.24	41.69
TiO2	1.53	1.13	1.72	0.89
Al2O3	15.42	15.00	14.12	18.29
Fe2O3	0.91	1.11	1.31	0.91
FeO	6.58	8.03	9.44	6.58
MnO	0.15	0.17	0.22	0.20
MgO	4.87	6.10	5.05	2.60
CaO	8.58	12.14	8.18	9.92
Na2O	2.19	0.70	3.19	0.36
K2O	1.75	1.67	0.35	4.24
P2O5	0.13	0.19	0.29	0.18
Cr2O3	0.02	0.05	0.00	0.02
NiO	0.00	0.01	0.01	0.00
H2O-	0.63	0.36	0.71	0.56
LOI	3.84	12.27	3.22	11.27
	99.50	99.64	100.05	97.71

Zn	91	74	108	88
Cu	70	52	68	62
Ni	23	67	4	7.2
Co	57	34	3	6.7
Ga	20	15	26	37
Mo	0	0	0	0
Nb	7.9	4.8	7	7
Zr	119	81	123	62
Y	26	22	39	23
Sr	166	49	265	126
Rb	35	50	0.2	91
U	5	0	6.7	0
Th	3.3	0	0	1.2
Pb	2.6	6.6	26	0
La	19	20	113	90
Ce	23	16	103	53
Nd	14	20	84	74
Te	22	22	20	15
Ba	781	406	72	3139
S	8330	143	5270	92
As	0	4.9	3	3
Se	4.3	3.8	5	4
Ag	0.5	0.5	0.5	0
Au(ppb)	5	5	10	0

RECAL DRY

	NC-2	NC-6	NR-1A	NR-1B
SiO2	55.66	46.78	54.35	48.54
TiO2	1.61	1.30	1.79	1.04
Al2O3	16.23	17.24	14.69	21.30
Fe2O3	0.96	1.28	1.36	1.06
FeO	6.92	9.23	9.82	7.66
MnO	0.16	0.20	0.23	0.23
MgO	5.13	7.01	5.25	3.03
CaO	9.03	13.95	8.51	11.55
Na2O	2.30	0.80	3.32	0.42
K2O	1.84	1.92	0.36	4.94
P2O5	0.14	0.22	0.30	0.21
Cr2O3	0.02	0.06	0.00	0.02
NiO	0.00	0.01	0.01	0.00
	100.00	100.00	100.00	100.00

GOLDEN DOVE MINE

	RAW DATA			RECAL DRY		
	NG-2	NG-3	NG-5	NG-2	NG-3	NG-5
SiO2	48.07	47.50	48.08	51.62	50.04	49.93
TiO2	1.45	1.97	1.60	1.56	2.08	1.66
Al2O3	15.05	18.60	15.78	16.16	19.60	16.39
Fe2O3	1.28	1.57	1.51	1.37	1.65	1.57
FeO	9.21	11.34	10.92	9.89	11.95	11.34
MnO	0.18	0.18	0.19	0.19	0.19	0.20
MgO	5.81	5.59	6.17	6.24	5.89	6.41
CaO	9.47	5.79	9.26	10.17	6.10	9.62
Na2O	2.12	1.97	2.07	2.28	2.08	2.15
K2O	0.19	0.02	0.38	0.20	0.02	0.39
P2O5	0.24	0.32	0.27	0.26	0.34	0.28
Cr2O3	0.05	0.06	0.05	0.05	0.06	0.05
NiO	0.01	0.01	0.01	0.01	0.01	0.01
H2O-	0.39	0.33	0.15			
LOI	5.69	4.85	2.66			
	99.12	100.10	99.09	100.00	100.00	100.00

Zn	81	97	112
Cu	62	92	97
Ni	55	72	80
Co	34	76	45
Ga	22	24	20
Mo	0	0	0
Nb	6.5	6.8	7.5
Zr	93	120	108
Y	26	36	30
Sr	185	138	258
Rb	0	0	8.5
U	0	0	1.5
Th	0	4.2	2.5
Pb	5	8.5	9.5
La	18	17	18
Ce	19	19	18
Nd	15	20	21
Te	21	22	25
Ba	92	95	5440
S	137	212	107
As	20	23	20
Se	0	0	2.8
Ag	0.5	0.5	0.5
Au(ppb)	5	20	450

PHOENIX MINE

	RAW DATA		RECAL DRY	
	PH-3	PH-6	PH-3	PH-6
SiO2	49.72	44.44	53.87	45.19
TiO2	0.37	0.54	0.40	0.55
Al2O3	14.28	16.04	15.47	16.31
Fe2O3	1.77	1.59	1.92	1.62
FeO	12.77	11.46	13.84	11.65
MnO	0.14	0.20	0.15	0.20
MgO	12.40	8.69	13.43	8.84
CaO	0.54	14.85	0.59	15.10
Na2O	0.00	0.40	0.00	0.41
K2O	0.02	0.07	0.02	0.07
P2O5	0.13	0.00	0.14	0.00
Cr2O3	0.14	0.05	0.15	0.05
NiO	0.02	0.01	0.02	0.01
H2O-	0.57	0.29		
LOI	6.99	1.89		
	99.86	100.52	100.00	100.00

Zn	102	71
Cu	97	65
Ni	185	51
Co	29	49
Ga	15	9.7
Mo	0	0
Nb	3.4	0
Zr	29	5.5
Y	5.5	2.4
Sr	6.1	185
Rb	2.9	1.1
U	3.5	0
Th	0	0
Pb	2.6	0
La	22	20
Ce	22	21
Nd	18	18
Te	20	22
Ba	24	97
S	183	289
As	6.9	11
Se	1.1	4.1
Ag	0.5	0.5
Au(ppb)	20	10

STUDY AREA B

RAW DATA

	I-5	I-16	I-18	A122	A123	A124
SiO2	79.94	65.60	60.56	60.60	76.40	76.90
TiO2	0.18	0.19	0.20	0.30	0.15	0.26
Al2O3	12.28	10.84	9.38	10.90	6.05	12.40
Fe2O3	0.16	0.82	1.53	11.40	9.35	2.56
FeO	1.18	5.89	11.03	0.00	0.00	0.00
MnO	0.01	0.09	0.07	0.00	0.00	0.04
MgO	0.16	6.52	4.53	1.67	0.40	0.86
CaO	0.56	2.38	2.16	1.79	0.02	1.83
Na2O	3.64	2.24	2.16	0.60	0.20	1.50
K2O	1.62	0.73	0.86	2.60	1.40	2.49
P2O5	0.03	0.09	0.11	0.09	0.01	0.05
Cr2O3	0.05	0.15	0.13	0.01	0.00	0.01
NiO	0.00	0.02	0.02	0.00	0.00	0.00
S	0.00	0.51	2.82	1.91	4.41	0.02
H2O-	0.07	0.13	0.36	0.00	0.00	0.00
LOI	1.02	4.54	7.03	7.90	5.52	0.82
	100.91	100.74	102.95	99.77	103.91	99.74

Zn	127	96	49	2064	788	41
Cu	23	33	289	1390	72	19
Ni	15	134	159			
Co	7.1	8.9	47	0	8	0
Ga	11	11	5.6	12	10	10
Mo	3.6	5.9	0			
Nb	6.3	5.1	4.6	21	5	3
Zr	120	77	69	111	39	100
Y	17	11	5.3	0	0	17
Sr	77	99	148	101	16	83
Rb	29	22	26	98	14	40
U	1.8	2.4	0			
Th	1.5	1.8	0			
Pb	6.7	17	27	6560	1590	21
La	18	26	76			
Ce	20	23	124	30	30	30
Nd	19	26	77			
Te	25	25	20			
Ba	327	517	588	6386	4534	379
S	115	5125	28200			
As	7.7	1.2	3			
Se	2.5	4.1	5			
Ag	0.5	0.5	0.5	42	4.9	0
Au(ppb)	5	230	5	1100	280	0

	A125	A126	A128	A129	A130	A131
SiO2	72.50	46.20	62.80	69.10	75.40	65.70
TiO2	0.23	0.27	0.28	0.39	0.34	0.23
Al2O3	11.50	6.69	11.50	13.20	12.50	12.10
Fe2O3	5.22	32.80	10.40	6.45	2.88	4.69
FeO	0.00	0.00	0.00	0.00	0.00	0.00
MnO	0.02	0.10	0.04	0.07	0.02	0.07
MgO	2.22	1.18	4.75	2.03	1.56	3.87
CaO	2.90	0.83	2.05	4.19	1.82	6.16
Na2O	1.30	0.80	2.10	1.30	2.70	1.40
K2O	1.23	0.78	0.82	0.63	0.83	1.68
P2O5	0.01	0.05	0.01	0.13	0.05	0.02
Cr2O3	0.00	0.02	0.00	0.00	0.00	0.00
NiO	0.00	0.00	0.00	0.00	0.00	0.00
S	1.28	2.15	2.36	0.03	0.10	0.09
H2O-	0.00	0.00	0.00	0.00	0.00	0.00
LOI	1.84	10.18	4.31	1.77	1.06	3.19
	100.25	102.05	101.42	99.29	99.26	99.20
Zn	98	184	70	89	68	60
Cu	13	1435	154	12	48	29
Ni						
Co	7	7	6	6	4	11
Ga	12	13	10	15	15	13
Mo						
Nb	3	1	2	6	4	1
Zr	76	71	99	76	111	82
Y	8	4	11	20	13	11
Sr	124	74	160	393	109	89
Rb	25	21	20	21	18	41
U						
Th						
Pb	74	208	30	9	18	6
La						
Ce	30	30	30	30	30	30
Nd						
Te						
Ba	754	1939	623	383	244	340
S						
As						
Se						
Ag	0	1.7	0	0	0	0
Au(ppb)	20	240	10	0	0	10

RECAL DRY

	I-5	I-16	I-18	A122	A123	A124
SiO2	80.09	68.28	63.37	65.96	77.65	77.74
TiO2	0.18	0.20	0.21	0.33	0.15	0.26
Al2O3	12.30	11.28	9.82	11.86	6.15	12.54
Fe2O3	0.16	0.85	1.60	12.41	9.50	2.59
FeO	1.18	6.13	11.54	0.00	0.00	0.00
MnO	0.01	0.09	0.07	0.00	0.00	0.04
MgO	0.16	6.79	4.74	1.82	0.41	0.87
CaO	0.56	2.48	2.26	1.95	0.02	1.85
Na2O	3.65	2.33	2.26	0.65	0.20	1.52
K2O	1.62	0.76	0.90	2.83	1.42	2.52
P2O5	0.03	0.09	0.12	0.10	0.01	0.05
Cr2O3	0.05	0.16	0.14	0.01	0.00	0.01
NiO	0.00	0.02	0.02	0.00	0.00	0.00
S	0.00	0.53	2.95	2.08	4.48	0.02
	100.00	100.00	100.00	100.00	100.00	100.00

	A125	A126	A128	A129	A130	A131
SiO2	73.67	50.29	64.67	70.86	76.78	68.43
TiO2	0.23	0.29	0.29	0.40	0.35	0.24
Al2O3	11.69	7.28	11.84	13.54	12.73	12.60
Fe2O3	5.30	35.70	10.71	6.61	2.93	4.88
FeO	0.00	0.00	0.00	0.00	0.00	0.00
MnO	0.02	0.11	0.04	0.07	0.02	0.07
MgO	2.26	1.28	4.89	2.08	1.59	4.03
CaO	2.95	0.90	2.11	4.30	1.85	6.42
Na2O	1.32	0.87	2.16	1.33	2.75	1.46
K2O	1.25	0.85	0.84	0.65	0.85	1.75
P2O5	0.01	0.05	0.01	0.13	0.05	0.02
Cr2O3	0.00	0.02	0.00	0.00	0.00	0.00
NiO	0.00	0.00	0.00	0.00	0.00	0.00
S	1.30	2.34	2.43	0.03	0.10	0.09
	100.00	100.00	100.00	100.00	100.00	100.00

NKUNZANA MINE

RAW DATA

	NK-6	NK-7	NK-8
SiO2	58.95	68.45	73.21
TiO2	1.10	0.32	0.41
Al2O3	18.73	13.20	11.57
Fe2O3	1.46	0.62	0.50
FeO	10.52	4.47	2.16
MnO	0.03	0.17	0.07
MgO	0.40	1.82	1.59
CaO	0.11	2.76	1.88
Na2O	0.45	4.06	4.11
K2O	3.14	1.20	1.37
P2O5	0.14	0.18	0.19
Cr2O3	0.12	0.04	0.01
NiO	0.02	0.01	0.02
H2O-	1.19	0.37	0.51
LOI	4.57	3.03	3.22
	100.94	100.68	100.82

RECAL TO 100% DRY

	NK-6	NK-7	NK-8
SiO2	61.94	70.35	73.40
TiO2	1.16	0.33	0.42
Al2O3	19.68	13.57	11.92
Fe2O3	1.53	0.64	0.51
FeO	11.05	4.59	2.22
MnO	0.03	0.17	0.07
MgO	0.42	1.87	1.64
CaO	0.12	2.84	1.94
Na2O	0.47	4.17	4.23
K2O	3.30	1.23	1.41
P2O5	0.15	0.18	0.20
Cr2O3	0.13	0.04	0.01
NiO	0.02	0.01	0.02
	100.00	100.00	100.00

Zn	32	99	40
Cu	76	46	19
Ni	103	6.2	11
Co	1.3	3.7	1.2
Ga	29	15	22
Mo	0	0	0
Nb	18	5.3	8.1
Zr	232	107	87
Y	9.7	48	52
Sr	50	97	106
Rb	143	19	121
U	10	4.4	5.1
Th	5.4	6.6	4.2
Pb	16	11	18
La	61	71	52
Ce	63	56	59
Nd	39	43	73
Te	20	20	20
Ba	509	540	330
S	59	382	111
As	26	6	5
Se	5	5	5
Ag	0.5	0.5	0
Au(ppb)	30	5	5

STUDY AREA D

RAW DATA

	R-1	R-3	C-3
SiO2	52.88	48.98	53.29
TiO2	1.01	0.94	1.06
Al2O3	17.03	18.70	17.04
Fe2O3	0.93	0.81	0.94
FeO	6.72	5.83	6.76
MnO	0.12	0.09	0.12
MgO	6.35	3.98	5.80
CaO	7.13	12.86	7.34
Na2O	2.25	0.70	3.19
K2O	1.31	3.69	0.79
P2O5	0.37	0.33	0.39
Cr2O3	0.06	0.08	0.05
NiO	0.02	0.01	0.01
H2O-	0.46	0.54	0.31
LOI	2.25	3.48	1.86
	98.90	101.01	98.95

RECAL DRY

	R-1	R-3	C-3
SiO2	54.98	50.49	55.06
TiO2	1.05	0.97	1.10
Al2O3	17.71	19.28	17.61
Fe2O3	0.97	0.84	0.97
FeO	6.99	6.01	6.98
MnO	0.12	0.09	0.12
MgO	6.60	4.10	5.99
CaO	7.41	13.26	7.58
Na2O	2.34	0.72	3.30
K2O	1.36	3.80	0.82
P2O5	0.38	0.34	0.40
Cr2O3	0.06	0.08	0.05
NiO	0.02	0.01	0.01
	100.00	100.00	100.00

Zn	91	79	82
Cu	30	34	16
Ni	150	91	121
Co	20	24	28
Ga	24	30	21
Mo	0	0	1.5
Nb	10	9.2	5.4
Zr	133	118	109
Y	21	18	22
Sr	829	360	870
Rb	20	49	20
U	0	0	5.2
Th	3.3	6.3	0
Pb	3.5	11	7
La	19	22	19
Ce	25	22	23
Nd	23	20	13
Te	21	22	25
Ba	2202	680	388
S	422	759	100
As	0	4.1	0
Se	6.4	0	3.2
Ag	0.5	0.5	0.5
Au(ppb)	5	5	350

APPENDIX B

ROCK DESCRIPTIONS OF ANALYSES REFLECTED IN APPENDIX A

H.M.S. MINE

NH - 2

Highly weathered gossan sample containing boxwork textures and few pyrite cubes. The gossan outcrop is located 200m east of the H.M.S. Mine.

NH - 5

Quartz - Muscovite - Sericite Schist.

This represents shear zone material from the H.M.S. Mine and is strongly silicified, consisting essentially of fine-grained polyhedral quartz grains. Chlorite is present and is generally altered to sericite. Few larger muscovite flakes are also present in random orientation.

NH- 7

Sericite - Chlorite - Quartz - Carbonate Schist.

This sample represents altered host rock adjacent to the H.M.S. shear. Sericite is dominant and plagioclase porphyroblasts containing muscovite inclusions are abundant. Chlorite is common and is replaced by sericite. Minor biotite is also present and appears to be replacing chlorite. Abundant fine-grained zircon occurs disseminated throughout. Fine quartz and calcite veins are apparent and few carbonate segregations are visible.

NH - 9

Graphite Schist.

This graphite schist sample (shown in Plate 6) is strongly carbonated and contains about 20% tourmaline which occurs as very fine-grained needles. Abundant fine-grained quartz is also present.

NH - 10

Chlorite - Epidote Schist.

This fine-grained rock represents the host rock at H.M.S. Mine and is unaffected by the mineralization and its associated alteration. It consists predominantly of chlorite and epidote together with minor amounts of sericite and disseminated carbonate.

NH - 11

Chlorite - Epidote - Quartz Schist.

This rock is similar to NH - 10 and also represents host rock far removed from the mineralization. It however contains slightly more quartz and less epidote than NH - 10 and rare plagioclase porphyroblasts occur associated with carbonate segregations.

NH - 17

Sericite - Quartz - Schist.

Float sample from nearby dump. The speciman shows typical quartz - sericite - pyrite alteration and contains about 5% disseminated pyrite. The rock is very similar to that encountered in the alteration zone adjacent to the shear.

CHAMPION REEF MINE

NC - 2

Graphite Schist.

This sample is located in the graphite schist horizon adjacent to the Champion Reef Mine. It consists mainly of graphite and sericite together with minor amounts of carbonate and fine-grained tourmaline. Abundant fine-grained quartz is also present, as well as rare plagioclase porphyroblasts.

NC - 6

Carbonate - Sericite Schist.

This shear zone material from the Champion Reef Mine consists of approximately 70% carbonate, occurring as medium to coarse grained segregations and veinlets. The remainder of the rock is made up of sericite together with minor amounts of chlorite.

NC - 1B

Sericite - Carbonate Schist.

This sample is typical of the sericite - carbonate alteration zone immediately adjacent to the shear zone. The rock consists of fine-grained muscovite and chlorite. Late-stage carbonate veining is common and rare disseminated fine-grained pyrite is visible.

NC - 1A

Epidote - Chlorite - Plagioclase - Sericite Schist.

This sample is representative of the outer epidote - chlorite alteration halo. In handspeciman the rock displays a ferruginous staining and is dominated by fine-grained epidote and chlorite. Sericite and plagioclase porphyroblasts make up the less abundant constituents together with minor fine-grained quartz and carbonate.

GOLDEN DOVE MINE

NG - 2

Chlorite Schist.

This sample is typical of the chlorite schist host rock at Golden Dove Mine and is unaffected by the alteration associated with mineralization. The rock consists mainly of chlorite with abundant fine-grained disseminated epidote. Altered plagioclase porphyroblasts are common together with moderate amounts of carbonate and minor amounts of fine-grained quartz.

NG - 3

Chlorite - Carbonate Schist.

This sample was taken immediately adjacent to the mineralized shear zone. It is similar in appearance to NG - 2 and an alteration zone is not clearly developed here. However the rock is characterized by a greater abundance of carbonate veining than in NG - 2. Minor amounts of quartz and pyrite are also present.

NG - 5

Chlorite - Carbonate - Sericite Schist.

This is a sample of mineralized shear zone material from the Golden Dove Mine. Chlorite is the dominant mineral together with lesser amounts of sericite and pyrite. Sericite and carbonate form pseudomorphs after plagioclase porphyroblasts. Carbonate veins and fine-grained zircon are abundant.

PHOENIX MINE

PH - 3

Chlorite - Biotite - Quartz - Epidote Schist.

This shear zone material from the Phoenix Mine consists mainly of chlorite and lesser amounts of biotite. Aggregates of fine-grained quartz are present together with minor amounts of epidote. Quartz grains show strained extinction.

PH - 6

Metagabbro.

This metagabbroic host to the Phoenix shear zone consists of medium-to coarse-grained sericitized feldspar and altered pyroxene. Clinozoisite and actinolite are common and biotite is absent. Chlorite is much less abundant than in PH - 3.

I - 16

Biotite - Chlorite - Calcite - Phlogopite Schist.

The sample represents mineralized footwall alteration with the alteration assemblage consisting of biotite - chlorite - calcite - phlogopite. Medium-grained quartz veins and segregations and sulphide stringers and segregations are abundant. Primary quartz and feldspar grains are still apparent and both show alteration. Minor amounts of andalusite and tourmaline are also present.

I - 18

This sample is similar to I - 16 but the alteration is less intense and biotite and phlogopite is less abundant. Chlorite is the dominant mineral together with minor amounts of andalusite. Primary quartz and feldspar grains are visible.

A - 122

Highly weathered material from the sulphide horizon. The sample contains approximately 60% sulphides and abundant fuchsite. Note the base metal, barium and precious metal values.

A - 124

Psammitic gneiss similar to I - 5.

A -125

Pelitic schist sample from within the ferruginous zone (see figure 14).

A - 126

Weathered sample from the sulphide horizon at the upper waterfall. The rock contains approximately 50% sulphides and abundant fuchsite.

A - 128

Similar to I - 16.

A - 129

Garnet - rich pelitic schist.

A - 130

Psammitic gneiss similar to I - 5.

A - 131

Pelitic schist.

NKUNZANA MINE

NK - 6

Sericite - Quartz Schist.

The shear zone material from Nkunzana Mine consists almost entirely of sericite and quartz. Rare plagioclase porphyroblasts also occur. (see Plate 19).

NK - 7

Quartz - Biotite - Chlorite - Sericite Schist.

This sample is typical of the alteration zone adjacent to the shear zone and is characterized by the presence of biotite and chlorite.

NK - 8

Quartz - Sericite Schist.

The unaltered host rock at Nkunzana consists mainly of quartz and sericite, with quartz being dominant. Minor amounts of biotite are also present.

STUDY AREA D

R - 1

Metagabbro.

This sample is typical of the metagabbro host at Rebellion Reef Mine. It consists of a fine-grained matrix of sericitzed feldspar, and medium-grained hornblende.

Anthophyllite and biotite are common, and biotite appears to be replacing hornblende. Aggregates of fine-grained fresh quartz and feldspar also occur. Minor amounts of zircon are present.

R - 3

Sheared Metagabbro.

The shear zone material at Rebellion Reef Mine consists of randomly orientated shattered quartz fragments showing intense undulose extinction. The quartz fragments are set in a very fine-grained unrecognizable matrix, possibly sericite. Fine-grained muscovite flakes are also present. Epidote and pyrite are rare. (see Plate 20)

C - 3

Sheared Metagabbro.

Float sample from dump at Coopers Shaft Mine. The sample contains abundant disseminated pyrite.